

Studies on development of process related issues in aqueous reprocessing of fast reactor spent fuels

By
SATYABRATA MISHRA
(CHEM 02200704008)

Indira Gandhi Centre for Atomic Research,
Kalpakkam, India

*A thesis submitted to the
Board of Studies in Chemical Sciences*

*In partial fulfillment of requirements
for the Degree of*

**Doctor of Philosophy
of
Homi Bhabha National Institute (HBNI)**



August, 2013

Homi Bhabha National Institute

Recommendations of the Viva Voce Committee

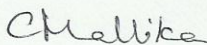
As members of the Viva Voce Committee, we certify that we have read the dissertation prepared by **Satyabrata Mishra** entitled “**Studies on development of process related issues in aqueous reprocessing of fast reactor spent fuels**” and recommend that it may be accepted as fulfilling the thesis requirement for the award of Degree of Doctor of Philosophy.

Chairman – **Dr. T. Gnanasekaran**



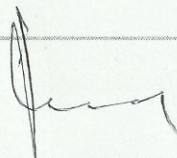
Date: 21/3/14

Guide / Convener – **Dr. C. Mallika**



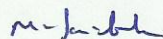
Date: 21.03.14

External Examiner- **Dr. M. Lakshmi pathy Reddy**



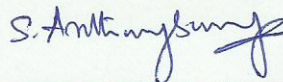
Date: 21/3/14

Doctoral Committee Member 1 - **Dr. M. Sai Baba**



Date: 21-03-14

Doctoral Committee Member 2 - **Dr. S. Anthonysamy**



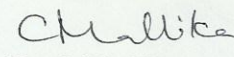
Date: 21/3/14

Final approval and acceptance of this thesis is contingent upon the candidate's submission of the final copies of the thesis to HBNI.

~~I~~We hereby certify that ~~I~~We have read this thesis prepared under my/our direction and recommend that it may be accepted as fulfilling the thesis requirement.

Date: 21.03.14

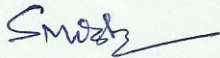
Place: Kalpakkam


Dr.C.Mallika
Guide

STATEMENT BY THE AUTHOR

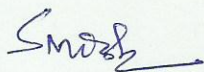
This dissertation has been submitted in partial fulfillment of requirements for an advanced degree at Homi Bhabha National Institute (HBNI) and is deposited in the Library to be made available to borrowers under rules of the HBNI.

Brief quotations from this dissertation are allowable without special permission, provided that accurate acknowledgement of source is made. Requests for permission for extended quotation from or reproduction of this manuscript in whole or in part may be granted by the Competent Authority of HBNI when in his or her judgment the proposed use of the material is in the interests of scholarship. In all other instances, however, permission must be obtained from the author.


(Satyabrata Mishra)

DECLARATION

I, hereby declare that the investigation presented in the thesis has been carried out by me. The work is original and has not been submitted earlier as a whole or in part for a degree/diploma at this or any other Institution/University


(Satyabrata Mishra)

List of publications arising from the thesis

Journals

1. "Development of a continuous homogeneous process for denitration by treatment with formaldehyde" **Satyabrata Mishra**, Falix Lawrence, R. Srinivasan, N.K. Pandey, C. Mallika, S.B. Koganti and U. KamachiMudali, *J. Radioanal. Nucl.Chem.* 2010, 285, 687- 695.
2. "Development and characterization of porous silicon nitride tubes" **Satyabrata Mishra**, C. Mallika, P.K. Das, U. KamachiMudali and R. Natarajan, *Trans.Ind.Ceram. Soc.* **2013**, 72, 52-55.
3. "Thermodynamics of solubility of tri-n-butyl phosphate in nitric acid solutions" **Satyabrata Mishra**, S. Ganesh, P. Velavendan, N.K. Pandey, C. Mallika, U.K. Mudali and R. Natarajan, *Adv. Chem.Engg.Research*, **2013**, 2, 55-60.
4. "Effect of temperature, concentration of acid and metal ions on the solubility of TBP in aqueous phase" **Satyabrata Mishra**, S. Ganesh, P. Velavendan, N.K. Pandey, C. Mallika, U.K. Mudali and R. Natarajan, *J. Radioanal. Nucl. Chem.* (Communicated).
5. "Effect of metal ions and organics on chemical denitration of HLLW" SanatKarmakar, **Satyabrata Mishra**, C. Mallika, U. KamachiMudali and R. Natarajan, *J. Chem. Engg. Sci.* (Communicated).
6. "Electrochemical divided cell design for radioactive environment" **Satyabrata Mishra**, Falix Lawrence, N.K. Pandey, C. Mallika, U. KamachiMudali and R. Natarajan, *J. Applied Electrochem.* (Manuscript under preparation).
7. "A comparative study on the evolution of physiochemical properties and metal retention behaviour of thermally degraded TBP-Dodecane-HNO₃/TBP-NPH-HNO₃ systems" **Satyabrata Mishra**, S.Joshi, N.K. Pandey, C. Mallika, U.K. Mudali and R. Natarajan, *Sep.Sci.Technol* (Manuscript under preparation).
8. "A systematic study on the effect of radiolysis in alteration of physiochemical and metal retention properties of TBP-Dodecane-HNO₃and TBP-NPH-HNO₃ systems" **Satyabrata Mishra**, S.Joshi, N.K. Pandey, C. Mallika, U.K. Mudali and R. Natarajan, *Sep.Sci.Technol* (Manuscript under preparation).

Conferences

1. **Satyabrata Mishra**, Falix Lawrence, R. Srinivasan, N.K. Pandey, C. Mallika and S.B. Koganti, "Influence of surface area of anodes in electrochemical reduction processes and performance evaluation of an electroplated Ti anode", Proc. Discussion Meet on Electroanalytical Techniques and Their Applications (DM-ELANTE-2008), Munnar, Feb. 2008, Paper No. 15.
2. **Satyabrata Mishra**, Falix Lawrence, C. Mallika, S.B. Koganti and U. KamachiMudali, "Characterisation of reaction bonded silicon nitride tubes", 20th Annual Conf. of Indian Nuclear Society (INSAC – 2009), organized by INS, IGCAR and BHAVINI, Chennai, Jan. (2010), p. 124.
3. **Satyabrata Mishra**, Falix Lawrence, R. Srinivasan, N.K. Pandey, C. Mallika, U. KamachiMudali and S.B. Koganti, "Pilot plant scale denitration by treatment with formaldehyde", Proc. DAE-BRNS Biennial Internatl. Symp.on Emerging Trends in Separation Science and Technology (SESTEC-2010), Kalpakkam, March (2010), pp. 297, 298
4. **Satyabrata Mishra**, C. Mallika, U. Kamachi Mudali, R. Natarajan and P.K. Das, "Development and characterization of porous silicon nitride tubes" Natl. Symp. on 'Materials and Processing (MAP-2012)', BARC, Mumbai, Oct . (2012).
5. **Satyabrata Mishra**, S. Ganesh, P. Velavendan, N.K. Pandey, C. Mallika, U.K. Mudali and R. Natarajan, "Effect of temperature, acidity and metal ions on the solubility of TBP in aqueous phase", The Eleventh Biennial Symp. on 'Nuclear and Radiochemistry (NUCAR-2013)', Jabalpur, Feb. (2013).
6. **Satyabrata Mishra**, S. Joshi, C. Mallika, N.K. Pandey, U. Kamachi Mudali and R. Natarajan, "Physiochemical properties and metal retention behaviour of thermally degraded TBP-Dodecane-HNO₃ and TBP-NPH-HNO₃ systems", 66th Annual Session of IChE (CHEMCON 2013), ICT, Mumbai, Dec. (2013)
7. **Satyabrata Mishra**, C. Mallika, U. Kamachi Mudali and R. Natarajan, "A systematic study on the alteration in physiochemical and metal retention properties of radiolytically degraded TBP-Dodecane-HNO₃ and TBP-NPH-HNO₃ systems", The Sixth Biennial Symp. on "Emerging Trends in Separation Science and Technology (SESTEC-2014)", BARC, Feb (2014)

DEDICATED
TO
MY BELOVED PARENTS

ACKNOWLEDGEMENTS

I would like to express my sincere respect and gratitude to **Dr. C. Mallika**, Head, PC&MS, RR&DD, Reprocessing Group, IGCAR for her wholehearted support, encouragement and guidance during the whole research work. Thanks are due to her constant inspiration, insightful guidance and excellent support all the way leading to completion of my PhD work. I am deeply obliged to her constructive suggestions, meticulous planning, and effective approach towards research related problems.

It is my great privilege to acknowledge **Dr. R. Natarajan**, Director, RpG, for providing all the required facilities and his keen interest in all the research activities being pursued in this thesis. His motivating words, kind advices and helpful suggestions on several occasions have been a source strength and inspiration for me.

I thank **Dr. Baldev Raj, Shri. S. C. Chetal** the former Directors and **Dr. P.R. Vasudeva Rao** present Director of IGCAR for permitting me to pursue research at this premier centre. I would like to express my sincere thanks to **Dr. S.B. Koganti**, former Head, RR&DD, for his valuable suggestions, help in all his possible ways and lively technical discussion when and where required.

I gratefully thank **Dr. U. Kamachi Mudali**, Head, RR&DD, for his consistent encouragement and support.

Special thanks to **Mr. N.K. Pandey**, RR&DD, for his whole hearted support and valuable discussions whenever required, without whom the thesis would not have completed. I would also

like to thank **Dr. Falix Lawrence** and **Dr. R.Srinivasan**, RR&DD, Reprocessing Group, for their support during the experimental work.

My sincere thanks to the doctoral committee Chairman **Dr. T. Gnanasekaran** and doctoral committee members **Dr. M. Sai Baba** and **Dr. S. Anthony**samy for their constant encouragement and valuable suggestions throughout this thesis work.

I want to register my thanks to **Dr. S. Ganesh** and **Mr. P. Velavendan** for analyzing numbers of samples using gas chromatography. Also sincere thanks to **Mr. Sailesh Joshi**, RSD for recording IR spectra of various degraded samples.

I am very much thankful to the lab mates **Sanat, Ramakrishna, Rahul and pravati** for keeping the lab atmosphere cheerful to carry out the research work. I am also thankful to **U.Veeramani and T.Selvan** for their assistance in carrying out the experiments. I am very much indebted to all the RR&DD members for creating a frank and lively environment which helped me a lot.

Special thanks to some of my friends **Anirudha, Biswabhanu, Manoj and Biranchi** whose help and support helped me to reach at this level of my life.

Words fail to express my indebtedness to some of my teachers **Mr. Biswanath Sahoo, Mr. Sudhakar Panda, Mr. Aditya Kumar Swain and Dr. Lingaraj Behera** whose special ways of teaching, care and guidance showed me the path to move forward.

Nothing is going to be completed without saying thanks to my parents (**Shri Rasananda Mishra and Smt. Sabita Mishra**), brothers (**Priyabrata Mishra and Debabrata Mishra**), uncles (**Santosh Kumar Hota and Saroj Kumar Hota**) and grandmother (**Premalata Hota**) for their everloving affection, patience, wish and prayers throughout my life. I thank the Almighty for providing me such a nice family.

Last but not least, I thank my wife **Dr. Sini Krishnan**, for her wholehearted support, care and co-operation during the entire course of my Ph.D work.

CONTENTS

	Page No.
Synopsis	I
List of Figures	XVII
List of Tables	XXI
List of Abbreviation	XXVI
 Chapter 1 INTRODUCTION	
1. 1. Nuclear Energy	1
1. 2. Indian Nuclear Power Programme	2
1. 2.1. Nuclear Fuel Cycle	3
1.2.2. Reprocessing	5
1.2.3. PUREX Process	6
1.2.4. Improvements in PUREX process	12
1.3. Challenges in Reprocessing	13
1.4. Scope of the Present Investigation	13
<i>References</i>	15
 Chapter 2 LITERATURE REVIEW	
2.1. Reduction of Nitrate Ions in Aqueous Solutions	16
2.1.1. Introduction	16
2.1.2. Denitration Processes	17
2.1.2.1. Nitrate to ammonia and ceramic (NAC) process	17

2.1.2.2.	Biological denitration	18
2.1.2.3.	Electrochemical method	19
2.1.2.4.	Thermal denitration	23
2.1.2.5.	Chemical denitration	24
1	Active metals	24
2	Hydrazine and hydroxylamine	24
3	Ammonia	24
4	Formic acid	25
5	Formaldehyde	26
5.1	Chemistry of denitration by HCHO	27
2.2.	Degradation of Solvent Used in Nuclear Fuel Reprocessing	28
2.2.1.	Introduction	28
2.2.2.	Irradiation Tools	29
2.2.3.	Degradation of Extractant-diluent System	29
2.2.3.1.	Degradation products from the diluent (Compounds A and B)	31
2.2.3.2.	Degradation products from TBP (Compounds I, II, III, IV and V)	31
2.2.3.3.	Mixed degradation products (Compounds AII and BIII)	31
2.2.4.	Diluent Degradation Mechanism	32
2.2.5.	Factors Influencing the Degradation of the Solvent System	33
2.2.5.1.	Nature of the irradiation Source	33
2.2.5.2.	Irradiation dose and dose rate	35
2.2.5.3.	Nature of the diluents	35
2.2.5.4.	Nitric acid concentration	36
2.2.6.	Complexing Ability of the Degradation Products of TBP	37
2.2.7.	Complexing Ability of Diluent Degradation Products	38
2.2.8.	Physiochemical Properties of Degradation Products	38
2.2.9.	Removal of Degradation Products from Spent Solvents	39
2.3.	Solubility of Tri Butyl Phosphate in Aqueous Phase	40
2.3.1.	Introduction	40
2.3.2.	Solubility of TBP in Water and Acid	40
2.3.3.	Estimation of TBP	42

2.4.	Conclusions	43
	<i>References</i>	44

Chapter 3 EXPERIMENTAL

3.1.	Materials and Chemicals	51
3.1.1.	Chemicals	51
3.1.2.	Materials	52
3.2.	Instrumentation and Facilities	52
3.2.1.	Gamma Chamber	52
3.2.2.	Electrochemical System	52
3.2.3.	UV-Visible Spectrophotometer	53
3.2.4.	FT-IR Spectrometer	55
3.2.5.	Gas Chromatography	58
3.2.6.	Densitometer	59
3.2.7.	Viscometer	60
3.2.8.	Surface Tension Analyzer	60
3.2.8.1.	Static methods	61
3.2.8.2.	Du Nouy ring method	61
3.2.9.	Buchi Rotavapour	62
3.2.10.	Incubator Shaker	62
3.2.11.	Titroprocessor	62
3.2.11.1.	Analysis of a mixture of two acids	63
3.2.12.	pH Meter	64
3.2.13.	ICP-OES Method	64
3.2.14.	XRD Analysis	64
3.2.15.	Electronic Single Pan Balance	64
3.3.	Preparation of Stock Solutions, Standard Solutions and Reagents	65
3.3.1.	Nitric Acid Solution	65
3.3.2.	TBP Solutions	65
3.3.3.	Phenolphthalein Solution	65

3.3.4.	Arsenazo(III) Solution	65
3.3.5.	Uranium, Ruthenium and Zirconium Nitrate Solutions	65

Chapter 4 PARAMETRIC STUDIES ON ELECTROCHEMICAL DESTRUCTION OF NITRIC ACID

4.1.	Introduction	66
4.2.	Mechanism of electrolytic acid killing	67
4.3.	Scope of the work	69
4.3.1.	Potentiostatic Studies	70
4.3.1.1.	Cyclic voltammogram of HNO ₃ system	70
4.3.1.2.	Estimation of kinetic parameters for the reduction of nitric acid	72
4.3.2.	Electro-reduction of 4 M HNO ₃ in Batch Mode	75
4.3.2.1.	Constant current experiments	76
4.3.2.2.	Experiments with constant cell potential	79
4.3.2.3.	Development of platinum electroplated titanium anodes	81
4.3.2.4.	Influence of surface area of anodes in acid killing	82
4.3.3.	Electro-reduction of Nitric Acid in Continuous Mode	88
4.3.3.1.	Life prediction of PET anodes	89
4.3.4.	Development and Characterization of Porous Silicon Nitride Tubes	91
4.3.4.1.	Preparation of porous Si ₃ N ₄ discs	92
4.3.4.2.	Fabrication of RBSN tubes	93
4.3.4.3.	Characterization of silicon nitride discs	94
4.3.4.4.	Performance of the sintered Si ₃ N ₄ disc	95
4.3.4.5.	Performance evaluation of RBSN tubes in acid killing	96
4.4.	Conclusions	99
	<i>References</i>	100

Chapter 5 DEVELOPMENT OF A CONTINUOUS HOMOGENEOUS PROCESS FOR DENITRATION BY TREATMENT WITH FORMALDEHYDE.

5.1.	Introduction	102
------	--------------	-----

5.2.	Scope of the work	103
5.3.	Mechanism of denitration using HCHO	103
5.4.	Lab scale experiments	104
5.4.1.	Batch Mode Denitration	104
5.4.2.	Continuous Mode Denitration with Pure Nitric Acid and Simulated Waste Solution	107
5.4.3.	Estimation of HNO ₃ , HCOOH and HCHO	109
5.4.3.1.	Analysis of a mixture of nitric and formic acids	109
5.4.3.2.	Analysis of formaldehyde	109
5.4.4.	Optimization of Feed Rate of HCHO	110
5.4.5.	Effect of Refluxing on the Destruction of Residual HCHO	113
5.4.6.	Denitration of Simulated Waste, With and Without Dissolved Organics	114
5.5.	Pilot plant scale denitration studies	118
5.5.1.	Results of Experiments with 3 and 6 L/h as the Feed Rates of Acid	120
5.5.2.	Recovery of Nitric Acid	125
5.6.	Conclusions	125
	<i>References</i>	126

Chapter 6 EVOLUTIONS OF PHYSIOCHEMICAL PROPERTIES AND METAL RETENTION BEHAVIOUR OF THERMALLY AND RADIOLYTICALLY DEGRADED TBP-DD/NPH SYSTEMS IN NITRIC ACID MEDIUM

6.1.	Introduction	127
6.2.	Scope of the work	128
6.3.	Experimental details	128
6.3.1.	Thermal Degradation	128
6.3.2.	Radiolytic Degradation	129
6.3.3.	Viscosity, Density and Surface Tension Measurements	129
6.3.4.	Phase Disengagement Time	130
6.3.5.	Estimation of Zr in the Aqueous Phase by Spectrophotometry Using Arsenazo(III)	130

6.3.6.	Zirconium Retention Test	131
6.4.	Results of thermal degradation studies	132
6.4.1.	Variation in Physical Properties (Density, Viscosity and Surface Tension)	132
6.4.2.	Zirconium Retention	138
6.4.3.	IR Analysis of the Thermally Degraded Samples	142
6.5.	Results of radiolytic degradation studies	145
6.5.1.	Variation in Physical Properties (Density, Viscosity and Surface Tension)	145
6.5.2.	Zirconium Retention	147
6.5.3.	IR analysis of the radiolytically degraded samples	148
6.6.	Conclusions	154
	<i>References</i>	155

Chapter 7 EFFECTS OF TEMPERATURE, ACIDITY AND ELECTROLYTES ON THE SOLUBILITY OF TBP IN AQUEOUS PHASE

7.1.	Introduction	156
7.2.	Scope of the work	157
7.3.	Solubility measurements	158
7.3.1.	Calibration Procedure	158
7.3.2.	Equilibration with Aqueous Phase	159
7.3.3.	Estimation of TBP in Aqueous Phase	159
7.4.	Influence of temperature, acid concentration and metal ions on the solubility of tbp	159
7.4.1.	Effect of Temperature and Nitric Acid Concentration	159
7.4.2.	Effect of Individual Metal Ions as a Function of Acidity and Temperature	161
7.4.3.	Effect of Metal Ions Together as a Function of Acidity and Temperature	163
7.5.	Thermodynamic modeling of the experimental data	163
7.5.1.	Effect of Nitric Acid Concentration	167
7.5.2.	Effect of Temperature	168
7.5.3.	Effect of Individual Metal Ions	170
7.5.4.	Effect of TBP Concentration	171

7.6.	Conclusions	173
	<i>References</i>	174

Chapter 8 SUMMARY AND SCOPE FOR FUTURE WORK

8.1.	Summary	175
8.1.1.	Parametric Studies on the Electrochemical Destruction of Nitric Acid	175
8.1.2.	Development of a Continuous Homogeneous Process for denitration by Treatment with Formaldehyde	176
8.1.3.	A Study on the Evolution of Physiochemical Properties and Metal Retention Behaviour of Thermally and Radiolytically Degraded TBP-DD/NPH Systems in Nitric Acid Medium	177
8.1.4.	Effect of Temperature, Acidity and Electrolytes on the Solubility of TBP in Aqueous Phase	177
8.2.	Scope for future work	178
	JOURNAL PUBLICATIONS AND CONFERENCE PROCEEDINGS	180

SYNOPSIS

1. Introduction

The demand for energy is steadily increasing with ever increasing population and rapid industrialization all over the world. Huge consumption of natural energy resources such as oil and gas, and the uncertainty in the development of renewable resources, make the option of nuclear energy inevitable for the future energy demand. Nuclear reactors employ natural or enriched uranium as the fuel [1]. The spent fuel discharged from the nuclear reactors comprises fissile elements such as plutonium and depleted uranium and several other elements (fission products) formed by the fission reaction.

The aim of reprocessing is to recover the fissile elements uranium and plutonium which form the bulk of the spent fuel for recycling in nuclear reactors and to compact the fission products waste in a form suitable for long term storage [2]. PUREX (Plutonium URanium EXtraction) process is widely employed for the aqueous reprocessing of spent nuclear fuels containing plutonium and uranium. The basic steps of PUREX process are the head end treatment involving chemical or mechanical decladding followed by the dissolution of fuel in nitric acid, feed clarification and adjustment of chemical conditions of the solution amenable for solvent extraction. In the solvent extraction step, uranium (U(VI)) and plutonium (Pu(IV)) are co-extracted using 30% Tributyl phosphate (TBP) in pure n-Dodecane (DD) or n- paraffin hydrocarbon (NPH) followed by scrubbing of organic stream with nitric acid, to back wash fission products co-extracted with uranium and plutonium. In the next step, partitioning of uranium and plutonium is achieved by selective reduction of Pu(IV) in the organic phase using suitable reducing agents to less extractable Pu (III) which goes to the aqueous phase and back extraction of U(VI) with dilute nitric acid.

The aqueous phase resulting from the solvent extraction step in the fuel reprocessing of Fast Breeder Reactor (FBR) contains non-volatile fission product elements and corrosion products in about 4 M nitric acid. This aqueous phase constitutes the bulk of the high level liquid waste (HLLW) and is one of the major concerns as the amount of the waste generated during the reprocessing of spent nuclear fuels is very substantial [3, 4]. Owing to the high radioactivity as well as corrosiveness of the HLLW, it can be neither exposed nor stored for a longer period. Removal of nitric acid from the HLLW is warranted for the reduction of volume, minimization of corrosion in waste tanks during subsequent storage of concentrated waste solution as well as to simplify the procedure for waste fixing.

Various denitration processes have been proposed in the literature for the disposal of highly radioactive waste solutions, among which electrochemical [5, 6], chemical [7] and biological denitration method [8] have been used worldwide. Electrochemical treatment is the most widely used technology for the destruction of nitrates, nitrites, organic complexants and compounds and also for the removal of radionuclides and hazardous metals from the waste solutions. The reduction of nitrate in an electrochemical cell can be carried out under acidic, neutral and basic conditions. Nitrates and nitrites in acidic solutions are reduced to nitrogen-containing gases such as NO_2 , NO , N_2O , N_2 and NH_3 . The main advantage of this method is that, it offers an easily controlled and safe mode of destruction of nitrate ions without the requirement of external chemical addition [9, 10]; however, energy consumption, maintenance and fabrication related issues restrict the implementation of electrochemical destruction of nitrate ions in plant scale process. Simple, efficient and faster reduction of nitric acid is achieved in chemical method by means of a homogeneous reaction with formaldehyde [11, 12] or formic acid [13]. The main advantage of using HCHO / HCOOH is that, it leaves no residual chemical and the gaseous

products NO_2 , NO and CO_2 are removed automatically. Denitration using formaldehyde offers the advantage of low chemical cost, easy recoverability of nitric acid, and in the case of waste treatment the production of a solution relatively low in inert salt concentration suitable for fission product recovery or ultimate disposal. The reaction of HNO_3 with HCHO is fast but is initiated after a certain induction period during which period, the auto catalytic generation of HNO_2 takes place, beyond which the reaction proceeds rapidly. The delay in induction period leads to uncontrollable process conditions due to pressurization of the system, which demands safety precautions. Literature survey reveals that the induction period is dependent on the concentration of nitric acid, nitrite content and temperature and can be considerably minimized or suppressed either by passing gaseous NO_2 through the acid prior to the addition of HCHO [12] or by carrying out the reaction at a temperature above 98°C . Presence of cations like ferric and uranyl ions and the nitrite anion are reported to increase the rate of reaction, thereby decreasing the induction period [12].

Liquid-liquid extraction process remains the most favoured route for recycling (individual or by families) of nuclear materials during reprocessing of the spent fuel. Solvent extraction adopts 30% TBP in NPH or DD as the extractant for the separation of plutonium and uranium from nitric acid solution containing a large number of fission products. During the extraction stage, nitric acid also gets extracted to the solvent [14]. Owing to high dose of radiation, the solvent as well as the diluent employed in the extraction process undergo chemical, thermal and especially radiolytic degradation resulting in a number of degraded products with varying physicochemical properties. This multiplicity is reinforced by the biphasic nature of the chemical system and the presence of numerous solutes, be it in aqueous or organic phase. Radiolysis of such a system thus, leads to the formation of a multitude of radicals and ionized species (including the reactive

species H^\bullet , OH^\bullet , solvated electrons, H_2 or H_2O_2), which recombine to form molecular products and shared between the two phases. The degraded products of 30% TBP-n-dodecane- HNO_3 can be broadly placed in two major categories: Those of extractant TBP (HDBP, H_2MBP , butanol, high molecular weight organo-phosphates and also oligomers of TBP (detectable only at higher absorbed doses) and those of hydrocarbon diluents i.e., mixture of hydrocarbons and a number of nitroparaffins and subsequent derivatives. The species mainly responsible for the solvent deterioration are products of radiation-chemical degradation of hydrocarbon diluents, among which the most harmful are nitration and oxidation products and also mixed products of reaction with TBP. The acidic degradation products of TBP can be removed by alkaline treatment before recycling; however, the solvent wash becomes ineffective in successive recycling of the solvent due to incomplete removal of nitric acid-induced degradation products of the diluent, which are relatively more hydrophobic and constitute the major impurities fraction in the radiolytically degraded solvent. The accumulation of the degradation products in the solvent can lead to different types of damage that disrupt the PUREX process like decreasing the decontamination performance of uranium and plutonium for fission products (mainly ruthenium, zirconium, cerium and niobium) [15,16], increase in product (uranium and plutonium) loss in aqueous raffinate [17], formation of emulsions, suspensions, and cruds at the liquid-liquid interface which disturb the continuous extraction process [18] and the evolution of physiochemical properties of the phases, mainly viscosity, interfacial tension, etc. [19].

During extraction, the solubility of TBP represents a balance between the highly polar oxygen atoms which favour miscibility with aqueous phase and the alkyl groups which are hydrophobic in nature and hence, show affinity towards the organic phase [20]. Owing to its mutual solubility in nitric acid, the aqueous stream leaving the extraction cycle contains a small amount of TBP,

which is potentially hydrolysable to non-volatile species. When the aqueous solutions are concentrated at high temperatures in evaporators, exothermic reactions occur due to the decomposition of TBP-associated compounds. Removal of the dissolved TBP is thus, desirable for the safe operation of the reprocessing plant. Several accidents which occurred during the heating of nitric acid solutions containing TBP have been reported in literature [21-23]. Hence, it is informative to know the solubility of TBP in the actual solutions of the process as well as the effect of temperature, concentrations of nitric acid and other electrolytes on the solubility of TBP in aqueous phase. The solubility of pure TBP in water is about 0.4 g/l at 25°C [20] and in the aqueous solution of 3 M HNO₃ it is around 0.27 g/l [24]. When TBP is diluted with an inert substance insoluble in water, the solubility of TBP decreases. Solubility of 30 % TBP diluted with n-dodecane in 3 M HNO₃ is reported to be 0.225 g/l. Presence of salts in the aqueous phase decreases the solubility markedly. In 2 M UO₂(NO₃)₂ solution, the solubility is only 1/20 of that in pure water [20].

The scope of the present investigation is in the process development and addressing issues relevant to the back end of nuclear fuel cycle in aqueous reprocessing. The study includes development of a continuous homogeneous process for denitration of HLLW by treatment with formaldehyde and comparing its efficiency with denitration by electrochemical method. An exhaustive study has been carried out to compare the evolution in physiochemical properties as well as metal retention behaviour of thermally as well as radiolytically degraded TBP-DD and TBP-NPH systems with and without nitric acid as the aqueous phase. The effect of temperature, concentration of acid and metal ions on the solubility of TBP in aqueous phase was also studied and the thermodynamic parameters relevant to the solubility of TBP in nitric acid have been derived.

2. Organization of the thesis

The thesis is divided into eight Chapters. The first Chapter deals with a brief introduction to nuclear energy, Indian nuclear power programme, reprocessing of spent nuclear fuel and the various issues encountered in aqueous reprocessing. The scope of the present study is also discussed in this Chapter. Chapter 2 describes in detail the available literature relevant to the present study. Chapter 3 encompasses the equipment, facilities, the details of instrumentation and analytical procedure employed for the thesis work. Chapter 4 deals with the electrochemical destruction of nitric acid and studies pertaining to the development of materials for the electrochemical process. The demonstration of a continuous homogeneous process for the denitration of simulated HLLW by treatment with formaldehyde and comparison of the performance of formaldehyde with denitration by electrochemical method have been dealt with in Chapter 5. Chapter 6 gives the results of a comparative study on the physiochemical properties of thermally and radiolytically degraded TBP-DD and TBP-NPH systems with and without aqueous phase. The factors influencing the solubility of TBP in aqueous phase and the estimation of thermodynamic parameters relevant to the solubility are discussed in Chapter 7. The conclusions derived from the present work and the scope for future work constitutes Chapter 8. A brief summary of each Chapter is as follows:

Chapter 1

This Chapter gives a glimpse of the present energy scenario of our country, the need for nuclear energy and also how vital is its role in our future economic growth. The three stages of Indian nuclear power programme are described in detail in this Chapter. The need for reprocessing of spent nuclear fuel and the challenges in aqueous reprocessing are also documented. This Chapter concludes with the scope of the present investigation.

Chapter 2

Chapter 2 presents an exhaustive literature survey on the merits and demerits of various methods reported in the literature for the destruction of nitrates. In NAC (Nitrate to Ammonia & Ceramic) process, a majority of the nitrate content from sodium nitrate based nuclear wastes is removed by using metallic aluminum. Waste waters containing nitrates get reduced to gaseous nitrogen by various classes of bacteria in Biological Denitration method. Electrochemical treatment is the inherently safe method for the destruction of nitrates, nitrites, organic complexants and compounds, as well as the removal of radionuclides and hazardous metals from the waste solutions. Thermal denitration involves heating solid nitrates in an inert atmosphere at high temperature to produce nitrogen oxides. Chemical denitration can be achieved by using different classes of compounds such as active metals (Cd, Al, and Zn) and reducing agents (NH_3 , N_2H_4 , NH_2OH , HCHO , HCOOH , urea, sugar, ethanol etc.). A review of the literature reports on the problems encountered owing to solvent-diluent degradation during the reprocessing of spent nuclear fuels from FBRs is also presented. The review encompasses a brief account of head-end and back-end processes, radiolytic degradation of extractant as well as diluent, degradation mechanism and influence of diluent or aqueous nitric acid phase in altering the hydrodynamic properties due to degradation.

This Chapter also discusses the mutual solubility of TBP between aqueous and organic phases. Various analytical techniques for quantification of TBP in aqueous phase have also been highlighted. Effect of metal nitrates such as uranyl nitrate and plutonium nitrate on the solubility of TBP in nitric acid is mentioned.

Chapter 3

This Chapter describes briefly the equipment, facilities and analytical techniques used for the thesis work. Redox behaviour of nitric acid at different working electrodes was investigated using cyclic voltammetry. Inductively Coupled Plasma Optical Emission Spectroscopy (ICP-OES) was used for determining the concentration of metal ions in simulated HLLW. Powder X-ray diffraction (XRD) technique was used for phase identification of sintered ceramic pellet. Characterization of degraded solvent was accomplished with the aid of Fourier transform infrared spectroscopy (FTIR). UV-Visible spectroscopy was used for determining the zirconium concentration during the estimation of zirconium retention by degraded solvent. Instruments such as Densitometer, Viscometer and Surface Tension Analyzer were used in the measurement of density, viscosity and surface tension respectively, of the raw samples as well as thermally and radiolytically degraded samples. Concentration of dissolved TBP in aqueous nitric acid phase was estimated by Gas Chromatography.

Chapter 4

Reduction behaviour of 4 M HNO_3 was investigated at different working electrodes using cyclic voltammetry. For the purpose of optimizing the process conditions for acid killing in the plant by electrolytic method, destruction of nitric acid was carried out in batch as well as continuous modes using Pt plated Ti mesh anodes and Ti cylinder as the cathode. In the batch process, experiments were done with 4 M nitric acid using different cathodic current densities in the range 40 to 60 mA/cm^2 . From the destruction rates, the feed rate required for the destruction of 4 M acid to about 1 M in continuous mode was arrived to be approximately 0.4 lph. Subsequently, continuous experiments were carried out with this feed rate, at the cathodic current density of 40 mA/cm^2 . Experiments were conducted with two anodes of surface area 1750 and 780 cm^2 . The

corresponding area of the Ti vessels (cathode) was 3250 and 2000 cm² respectively. The experimental results facilitated deriving the kinetic parameters and the design of the cell for scaling up of the process.

The role of the surface area of anodes in the electrochemical reduction process was investigated and the performance of Pt electroplated Ti (PET) anode in acid killing was evaluated. PET electrode with platinum coating thickness as 5 micron showed good performance up to 75 h, when it was tested at the anodic current density of 110 mA/cm². The efficiency of the electrode declined due to the formation of a passive film in nitric acid medium. Subsequent cleaning etching of the electrode made it to perform well up to 778 h with the anodic current density as 110 mA/cm². The PET electrode with the coating thickness of 10 µm worked up to 860 h at the anodic current density of 165 mA/cm². Diffusion annealing of the PET anodes enabled to extend the service life of the electrode by another 350 h. The anolytes after testing the PET anodes in acid killing experiments were analysed by ICP-OES technique to determine the elemental composition which got leached out from the electrode.

As the porous aluminous porcelain diaphragm tubes in the electrolytic cells, employed in the aqueous reprocessing of spent nuclear fuels, undergo leaching in concentrated nitric acid, corrosion resistant and porous, one end closed silicon nitride tubes of length 600 mm were fabricated indigenously by reaction bonding of pre-formed silicon green tubes in nitrogen atmosphere. The process parameters for the fabrication were optimized to produce tubes with density, porosity and liquid permeability in the range 2.2-2.5 kg.dm⁻³, 20-25% and 10⁻⁵-10⁻⁶ cm.s⁻¹ respectively, since these parametric values were identified to be optimum for serving as an efficient diaphragm tube. The performance of the fabricated tubes was evaluated by using them as the diaphragm tubes in the electrolytic destruction of 4 M nitric acid and the efficiency of the

process was compared with that for a cell in which an imported, commercially available silicon nitride tube was used as the diaphragm material. Though performance of both the tubes was comparable, the resistance offered by the indigenous tube to the flow of current through it was much lower than that of the other tube. Development of materials and parametric study to determine optimum conditions for electrolytic acid killing constitute Chapter 4 of the thesis.

Chapter 5

This Chapter describes the development of a continuous homogeneous process for denitration by treatment with formaldehyde. For the purpose of demonstrating the reduction of nitric acid by formaldehyde in a safe and continuous mode, a pyrex reaction vessel with 5 necked lid and flanges was fabricated and batch experiments were conducted to determine the temperature at which the reaction starts instantaneously. At the boiling temperature of formaldehyde (98°C), the induction time (which is the time required to produce sufficient quantity of nitrous acid to initiate the reaction) was found to be negligible. Subsequent experiments were carried out in continuous mode with a fixed flow rate of nitric acid as 1.2 lph and with various flow rates of formaldehyde from 0.06 to 0.3 lph, to determine the ratio of nitric acid to HCHO for efficient reduction. The experiments were stopped when the total acidity was below 2 M. When the concentration of nitric acid reduces to about 2 M, a sizeable amount of the intermediate compound, formic acid gets accumulated in the reaction mixture, as the rate of formation of formic acid is higher than its rate of oxidation at low concentrations of nitric acid. Refluxing the contents of the reaction vessel for 2 to 3 h (after stopping the feed) favoured the oxidation of formic acid, thereby reducing the total acidity to below 1 M. Continuous experiments were also carried out with a simulated HLLW solution to find out the effect of metal ions on the destruction of nitric acid by formaldehyde. It was observed that the rate of destruction was marginally reduced with

simulated solution because of the precipitation of metal ions as formates. Based on the results of lab scale continuous denitration experiments, a pilot plant set up comprising a glass reactor vessel of 6 litre capacity along with its accessories such as packed tower, absorber, condenser and receiver flask was designed and fabricated for the purpose of demonstrating the safe and continuous destruction of 4 M nitric acid by formaldehyde, with 50% capacity required for the Plant. Experiments were conducted with the feed rates of 0.5, 3 and 4.5 lph of 4 M nitric acid and 0.12, 0.72 and 1.14 lph of formaldehyde respectively (in each experiment the mole ratio of nitric acid to formaldehyde was maintained as 4:3 for better process safety as well as efficiency). The steady state concentration of nitric acid for the above three flow rates was determined to be 2.2 M in 4 h, 1.6 M in 3 h and 1.7 M in 2.5 h respectively. During these experiments, samples were analysed for acidity, unreacted formaldehyde and formic acid concentrations. In the continuous destruction of simulated HLLW using formaldehyde, severe foaming could be observed in the reactor as soon as the reaction started. To investigate the effect of organics and metal ions on foaming, lab scale continuous denitration experiments were conducted at 100°C with 4 M nitric acid equilibrated with 220 ppm of pure TBP (220 ppm is the solubility of TBP in 4 M HNO₃ at 25°C). Experiments were carried out after the equilibration periods of one h, one day and seven days. Feed rates of nitric acid and formaldehyde to the reactor vessel were maintained as 5 & 4 ml/min respectively. The induction period before the starting of slow reaction as well as vigorous reaction were recorded. With a simulated solution of fission product metal ions after equilibrating with 220 ppm of pure TBP, heavy frothing was observed and the rate of denitration was marginally lower than for the solution without fission product elements. Attempts were made to minimize the residual formaldehyde and formic acid in the reactor vessel by stopping the feed solutions when acidity got reduced to ~ 2 M and refluxing the reaction

mixture at 100°C for 2 to 3 h. Attempts were also made to identify the fission product elements responsible for foaming and to control the extent of foaming with the aid of anti-foaming agents.

Chapter 6

The thermal and radiolytic degraded products of solvent-diluent-aqueous nitric acid systems were characterized after effecting degradation by simulated and accelerated experiments and the results are discussed in Chapter 6. Thermal degradation of different sets of solutions consisting of pure TBP, TBP + 4M HNO₃ (v/v), 30% TBP-DD, 30% TBP-DD + 4M HNO₃ (v/v), DD + 4M HNO₃ (v/v), NPH + 4M HNO₃ (v/v), 30% TBP-NPH and 30% TBP-NPH + 4M HNO₃ (v/v) at 40°C for 800 h and at 60°C for 400 h was carried out. The solutions were mixed continuously during thermal treatment at 400 rpm speed using an incubator shaker. Samples at intervals of 100 h were analysed. The physical properties (density, viscosity, surface tension and phase disengagement time) of the samples before and after degradation were measured. For the estimation of zirconium retention by the degraded samples, equal volumes of degraded organic and Zr stock solution were equilibrated for 45 min using a test tube rotator. The Zr concentration in the aqueous solution was measured by spectrophotometry. Subsequently, the loaded organic was stripped using 0.01 M HNO₃ and the Zr concentration in the aqueous solution was estimated. The difference gives the retention. For solvent wash, equal volumes of degraded organic and 0.5 M Na₂CO₃ were equilibrated for 45 min. Zr retention after solvent wash was measured as per the above procedure. The Zr retention of the raw samples as well as the degraded samples before and after solvent wash with 0.5 M Na₂CO₃ was measured. The IR spectra of the raw samples were compared with that of the degraded samples to find out the functional groups generated during degradation; the IR signatures were observed to be identical, indicating that different classes of compounds were not formed.

Radiolytic degradation of various sets of samples such as DD, NPH, 30% TBP-DD and 30% TBP-NPH in the presence of 4 M HNO₃ as the aqueous phase was carried out using ⁶⁰Co gamma source up to 100 MRad as the absorbed dose. The physical properties (density, viscosity, surface tension and phase disengagement time) of the degraded samples were measured as a function of dose rate. The Zr retention by the degraded samples before and after solvent wash was estimated. The degraded samples were subjected to IR analysis which indicated the formation of new functional groups such as carbonyl, hydroxyl, nitro and amine based compounds.

Chapter 7

The widely used solvent, TBP undergoes hydrolysis to non-volatile species, which have adverse effects on process operation. Hence, it is desirable to determine the solubility of TBP in the actual solutions of the process as well as the effect of temperature, concentrations of nitric acid and other electrolytes on TBP solubility in aqueous phase. For determining the solubility of TBP at various temperatures as a function of acidity (0 – 14 M) using Gas Chromatography, 2 ml of pure TBP was added to 25 ml of aqueous solution in a centrifuge tube and was shaken thoroughly for 45 minutes. Solubility was measured at 25, 40 and 60°C. The desired temperature was maintained by using an incubator shaker. After mixing, the aqueous phase was separated and to extract the dissolved TBP in aqueous phase, 10 ml of the aqueous phase was contacted with 2 ml of fresh n-dodecane and was shaken thoroughly for 15 minutes. The resulting organic phase was injected to GC and TBP concentration was measured. The concentrations of TBP dissolved in aqueous phase, both free and bound to the acid due to the formation of TBP complexes with nitric acid have been calculated. A classical thermodynamic approach has been used to determine the formation constants of TBP-nitric acid complexes. As the fission product metal ions namely Zr and Ru interfere in the extraction of U and Pu by TBP, their influence in the solubility of TBP

with and without uranium ions was also investigated. Chapter 7 deals with the solubility of TBP in aqueous phase in the presence of interfering metal ions.

Chapter 8

This Chapter provides the summary and conclusions of all the studies reported in the thesis and puts forward recommendations for future work, which includes a detailed investigation towards the cause as well as mechanism of frothing resulted during chemical denitration of HLLW, suitable anti frothing agent to suppress the extent of frothing. Complete characterization of the degraded products resulted during radiolysis of TBP-DD/NPH-HNO₃ system is demanded to find out the species responsible for holding Pu.

References

1. Olander, D., *J. Nucl. Mat.* **389** (2009) 1-22.
2. Swanson, J. L., "PUREX Process Flow sheets", In: Science and Technology of Tributyl Phosphate, Eds. W.W. Schulz, L.L. Burger, J.D. Navratil, K.P. Bender, CRC Press Inc. Boca Raton, p 55, 1984.
3. Kim, K.W., Kim, S.H., Lee, E.H., *J. Radioanal. Nucl. Chem.* **260** (2004) 99.
4. Baumgartner, F., Schmieder, H., *Radiochim. Acta* **25** (1978) 191.
5. Rutten, O.W., Sandwizk, j.S., Weert, A.V., *J. Appl. Electrochem.* **29** (1999) 87.
6. Mallika, C., Keerthika, B., Kamachi Mudali, U., *Electrochim. Acta* **52** (2007) 6656.
7. Bray, L.A., (1963) Report HW-76973.
8. Mimori, T., Miyajima, K., Nemoto, K., Nakano, T., Masui, H., Mori, T., Takahashi, T., (1995) US Patent 5476989.
9. Schmieder, H., Kroebel, R., (1977) US Patent 4056482.
10. Suzuki, Y., Shimizu, H., Inoue, M., Fujiso, M., Shibuya, M., Iwamoto, F., Outou, Y., Ochi, E., Tsuyuki, T., (1998) Proceedings of the 5th international conference on recycling, conditioning and disposal, (RECOD 98), France, Vol **3**, 838.
11. Evans, T. F., (1959) Report HW-58587.
12. Healy, T.V., *J. Appl. Chem.* **8** (1958) 553.
13. Kim, K.W., Kim, S.H., Lee, E.H., *J. Nucl. Sci. Tech.* **41** (2004) 473.
14. Hesford, E., Mc Kay, H. A. C., *J. Inorg. Nucl. Chem.* **13** (1960) 156.
15. Nowak, Z., Nowak, M., Seydel, A., *Radiochem. Radioanal. Lett.* **38** (1979) 343.
16. Neace, J. C., *Sep. Sci. Technol.* **18** (1983) 1581.
17. Hardy, C. J., Scargill, D., *J. Inorg. Nucl. Chem.* **17** (1961) 337.
18. Smith, D.N., Edwards, H. G. M., Hugues, M. A., Courtney, B., *Sep. Sci. Technol.* **32** (1997) 2821.
19. Tripathi, S. C., Ramanujam, A., *Sep. Sci. Technol.* **38** (2003) 2307.
20. Burger, L.L., Forsman, R. C., (1951) Report HW-20936.
21. Sege, G., (1953) Report HW-28690.
22. Biplab, D., Mondal, P., Shekhar Kumar, *J. Radioanal. Nucl. Chem.* **288**(2011) 641.

23. Dicholkar, D. D., Patil, L. K., Gaikar, V. G., Shekhar Kumar, Kamachi Mudali, U., Natarajan, R., *J. Radioanal. Nucl. Chem.* **289** (2011) 545.
24. Leroy (1967) Report ORNL-TR-4344.

LIST OF FIGURES AND TABLES

Figure No.	Title of the Figure	Page No.
I.1.	Three stages of Indian Nuclear Power Programme	3
I.2.	Nuclear Fuel Cycle	7
I.3.	Schematic Process flow sheet for reprocessing of fast reactor fuels	4
II.1.	Degradation scheme of solvent-diluent system	30
II.2.	Possible mechanism for the formation of diluents degradation products	34
III.1.	Block diagram of a conventional UV-VIS Spectrophotometer	53
III.2.	Layout of a simple IR spectrometer	56
III.3.	Block diagram of a gas chromatograph	58
III.4.	Schematic of titration curve during analysis of mixture of two acids	63
IV.1.	Electrolytic cell set up for potentiostatic studies	70
IV.2.	Cyclic voltammogram of 4 M HNO ₃ recorded with Pt electrode at 298	71
IV.3.	Cyclic voltammograms of 4 M HNO ₃ recorded with and without NaNO ₃ using Pt electrode at 298 K	71
IV.4.	Cyclic voltammograms of 4 M HNO ₃ recorded at Pt electrode with different scan rates at 298K	73
IV.5.	Schematic of the electrolytic cell setup for acid killing	75
IV.6.	Plot of concentration against time for the electrochemical reduction of HNO ₃ under constant potential conditions; Symbols: experimentally determined values; Model predicted results are shown as trend lines	80
IV.7.	Time vs current during electrolysis	81
IV.8.	Schematic representation of anodes	83
IV.9.	Concentration of acid vs time during reduction with different anodes	87
IV.10.	Dependence of temperature on the surface area of anodes	87
IV.11.	Schematic representation of the electrolytic cell set up for continuous acid killing	89
IV.12.	Performance of PET anode (SA: 780 cm ²) during continuous flow experimental runs	90

IV.13.	Cross sectional view of the sintered disc by SEM	95
IV.14.	XRD pattern of sintered pellet	95
IV.15.	Comparison of the performance of RBSN tubes as diaphragm in electrolytic acid killing.	97
IV.16.	Comparison of cell voltage during electrolysis	98
V.1.	Schematic diagram of lab scale experimental set up	105
V.2.	Visualization of induction period	106
V.3.	Variation of reaction temperature with time for initial 10 min. during denitration of Solution-A: pure 4 M HNO ₃ ; Solution-B: Simulated HLLW and Solution-C: Simulated HLLW with organics (Feed rate of formaldehyde : 0.24 L/h; Feed rate of nitric acid: 1.2 L/h)	114
V.4.	Vessel outlet concentration of HNO ₃ with time (data points: experimental results; lines: computed results)	116
V.5.	Borosilicate apparatus for pilot plant scale denitration and NO _x absorption	119
V.6.	Continuous destruction of 4 M nitric acid in pilot plant scale set up; Feed rates of HNO ₃ and HCHO: 6 and 1.5 L/h	121
V.7.	Picture showing frothing in the denitration experiment conducted with Solution B	123
VI.1.	Calibration graph for Zr estimation in aqueous phase	130
VI.2.	Mechanism for the formation of interacting molecules	142
VI.3.	Comparison of IR spectra of thermally degraded 30 % TBP-DD system at 40°C	142
VI.4.	Comparison of IR spectra of thermally degraded 30 % TBP-DD-HNO ₃ system at 40°C	143
VI.5.	Comparison of IR spectra of thermally degraded 30 % TBP-NPH system at 40°C	143
VI.6.	Comparison of IR spectra of thermally degraded 30 % TBP-NPH-HNO ₃ system at 40°C	143
VI.7.	Comparison of IR spectra of thermally degraded 30 % TBP-DD-HNO ₃ system at 60°C	144

VI.8.	IR spectra of thermally degraded 30% TBP-NPH-HNO ₃ system at 60°C	144
VI.9.	Comparison of IR spectra of radiolytically degraded 30 % TBP-DD w.r.to absorbed dose	149
VI.10.	Comparison of IR spectra of radiolytically degraded 30 % TBP-DD-HNO ₃ system w.r.to absorbed dose	150
VI.11.	Comparison of IR spectra of radiolytically degraded 30 % TBP-NPH w.r.to absorbed dose	151
VI.12.	Comparison of IR spectra of radiolytically degraded 30 % TBP-NPH-HNO ₃ w.r.t absorbed dose	152
VI.13.	IR spectra of radiolytically degraded 30 % TBP-DD-HNO ₃ after irradiating to 100 MRad	153
VI.14.	IR spectra of the fractions collected during the distillation of radiolytically degraded 30 % TBP-DD-HNO ₃ system after 100 MRad	153
VII.1.	Calibration graph for dissolved TBP (2 to 200 ppm)	158
VII.2.	Solubility of pure TBP in aqueous phase as a function of temperature and acidity	160
VII.3.	Solubility of pure TBP in aqueous phase as a function of temperature and acidity in the presence of Ru.	161
VII.4.	Solubility of TBP in aqueous phase as a function of temperature and acidity in the presence of Zr	162
VII.5.	Solubility of pure TBP in aqueous phase in the presence of U	162
VII.6.	Solubility of TBP in aqueous phase as a function of temperature and acidity in the presence of U, Ru and Zr	163
VII.7.	Aqueous solubility of TBP as a function of nitric acid concentration at 25°C	167
VII.8.	(a) Concentration of bound TBP and free TBP vs acidity; (b) Concentration of different species of TBP vs acidity	168
VII.9.	Solubility of pure TBP in aqueous phase as a function of temperature and acidity	169
VII.10.	Effect of temperature on equilibrium constants	170

VII.11.	Effect of Zr and Ru ions on the solubility of TBP at different nitric acid Concentrations	171
VII.12.	Effect of volume percent of TBP on its solubility at different nitric acid Concentrations	172
VII.13.	Variation of equilibrium constants and salting out coefficient with TBP Concentration	173

Table No.	Title of the Tables	Page No.
II.1.	Radiolytic and chemical stability of pure hydrocarbons	34
II.2.	Solubility of TBP in nitric acid at 298 K	41
II. 3.	Dependence of solubility of TBP (g/L) in aqueous phase on temperature and metal ion concentration	42
II.4.	Working conditions and range for the estimation of TBP by different analytical procedures	43
IV.1.	Peak parameters obtained for 4 M HNO ₃ from the voltammograms recorded with Pt	73
IV.2.	Results of the electro-reduction experiment at the cathodic current density of 40 mA/cm ²	77
IV.3.	Experimental parameters and acid strength during electro-reduction with <i>J</i> as 50 mA/cm ²	77
IV.4.	Trend in temperature, cell potential and acid strength during electro reduction with cathodic <i>J</i> as 60 mA/cm ²	78
IV.5.	Constant current electrolysis at 50 mA/cm ² as cathodic <i>J</i> and without diaphragm	79
IV.6.	Rate constant and efficiency for the electro-reduction of 4 M nitric acid under constant potential conditions	80
IV.7.	Electro-reduction of nitric acid using anode A, at cathodic <i>J</i> = 40 mA/cm ²	83
IV.8.	Electro-reduction using anode A, at the cathodic current density 50 mA/cm ²	83
IV.9.	Reduction of HNO ₃ using anode B at the cathodic current density 40 mA/cm ²	84
IV.10.	Electro-reduction using anode B at cathodic <i>J</i> , 50 mA/cm ²	84
IV.11.	Destruction of 4 M nitric acid using anode C (cathodic current density: 40 mA/cm ²)	85
IV.12.	Electro reduction using anode C, at the cathodic current density 50 mA/cm ²	85
IV.13.	Reduction of nitric acid using anode D, at cathodic current density 40 mA/cm ²	86
IV.14.	Destruction of nitric acid using anode D, at cathodic current density 50 mA/cm ²	86

IV.15.	Temperature, rate constant and efficiency for the electro-reduction process with different anodes	88
IV.16.	Density and porosity of sintered silicon nitride discs with different sintering aids	94
IV.17.	Comparison of the performance of RBSN tubes in electrolytic acid killing	98
V.1.	Dependence of temperature on the initiation of reaction	105
V.2.	Chemical composition of fission and corrosion product elements used for simulated waste solution	107
V.3.	Process conditions and concentrations of acid and HCHO in the product solution during and after terminating a denitration experiment, Feed rates of (a) HCHO: 0.06 L/h and (b) HNO ₃ : 1.2 L/h	110
V.4.	Concentrations of acid and HCHO in the product solution during and after terminating a denitration experiment; Feed rates of (a) HCHO: 0.12 L/h and (b) HNO ₃ : 1.2 L/h	111
V.5.	Results of the denitration experiment with feed rates of (a) HCHO: 0.18 L/h and (b) HNO ₃ : 1.2 L/h	111
V.6.	Process conditions and analytical results from the product solution during and after terminating a denitration experiment; Feed rates of (a) HCHO: 0.24 L/h and (b) HNO ₃ : 1.2 L/h	112
V.7.	Results of acid killing experiment with the feed rates as (a) HCHO: 0.30 L/h and (b) HNO ₃ : 1.2 L/h	112
V.8.	Concentrations of HNO ₃ , HCHO and HCOOH in the product solution during refluxing	113
V.9.	Results of denitration experiment using simulated HLLW solution in 4 M HNO ₃ ; Feed rates of (a) HCHO: 0.24 L/h and (b) HNO ₃ : 1.2 L/h	115
V.10.	Concentrations of acid and HCHO in the product solution during denitration of a simulated HLLW solution with dissolved TBP; Feed rates of (a) HCHO: 0.24 L/h and (b) HNO ₃ : 1.2 L/h	115
V.11.	Comparison of concentrations of HNO ₃ , HCHO and HCOOH in the product solution with different stock solutions	117

V.12.	Concentrations of intermediate products during and after denitration experiment with feed rates of (a) HCHO: 0.72 L/h and (b) HNO ₃ : 3 L/h	120
V.13.	Results of denitration experiment with feed rates of (a) HCHO: 1.12 L/h and (b) HNO ₃ : 4.5 L/h	120
V.14.	Denitration experiment with feed rates of (a) HCHO: 1.5 L/h and (b) HNO ₃ : 6.0 L/h	121
V.15.	Results of the denitration experiment with simulated HLLW; feed rates of (a) HCHO: 1.5 L/h and (b) HNO ₃ : 6.0 L/h	122
V.16.	Concentration of intermediate products in the denitration experiment with simulated HLLW containing dissolved TBP; Feed rates of HCHO: 1.5 L/h and (b) HNO ₃ : 6.0 L/h	123
V.17.	Concentrations of HNO ₃ , HCHO and HCOOH in the collection tank after terminating the addition of reactants in pilot plant as well as full-scale capacity experiments	124
VI.1.	Densities (g/cc, at 25°C) of different systems thermally degraded at 40°C	132
VI.2.	Densities at 25°C (g/cc) for various systems thermally degraded at 60°C	132
VI.3.	Densities (g/cc) at 25°C, for thermally degraded systems w.r.to aqueous phase acidity at 40°C	133
VI.4.	Densities (g/cc) at 25°C, for various systems thermally degraded w.r.to aqueous Phase acidity at 60°C	134
VI.5.	Viscosity (mPa.S) at 25°C, for various systems thermally degraded at 40°C	135
VI.6.	Viscosity (mPa.S) of different systems at 25°C, after thermal degradation at 60°C	135
VI.7.	Viscosity (mPa.S) for various systems thermally degraded w.r.to aqueous phase acidity at 40°C	135
VI.8.	Viscosity (mPa.S) at 25°C, for various systems thermally degraded w.r.t aqueous phase acidity at 60°C	136
VI.9.	Surface tension (dyne/cm) at 25°C, for various systems thermally degraded w.r.t aqueous phase acidity at 40°C	136

VI.10.	Surface tension (dyne/cm) at 25°C, for thermally degraded system w.r.t aqueous phase acidity at 60°C	137
VI.11.	PDT (s) of various systems thermally degraded at 40°C	137
VI.12.	PDT (s) of various systems thermally degraded at 60°C	138
VI.13.	Zirconium retention (ppm) by raw samples; stock Zr: 1170 ppm	138
VI.14.	Zirconium retention (ppm) by thermally degraded samples at 40°C for 200 h; stock Zr: 1170 ppm	139
VI.15.	Zirconium retention (ppm) by thermally degraded samples at 40°C for 400 h; stock Zr: 1170 ppm	139
VI.16.	Zirconium retention (ppm) by thermally degraded samples at 40°C for 600 h; stock Zr: 1170 ppm	140
VI.17.	Zirconium retention (ppm) by thermally degraded samples at 40°C for 800 h; stock Zr: 1170 ppm	140
VI.18.	Zirconium retention (ppm) by thermally degraded samples at 60°C for 100 h; stock Zr: 1170 ppm	141
VI.19.	Zirconium retention (ppm) by thermally degraded samples at 60°C for 200 h; stock Zr: 1170 ppm	141
VI.20.	Densities (g/cc) at 25°C, for the radiolytically degraded systems as a function of absorbed dose	145
VI.21.	Viscosity (mPa.s) at 25°C, for various radiolytically degraded systems as a function of absorbed dose	145
VI.22.	Surface tension (dyne/cm) at 25°C, for various radiolytically degraded systems as function of absorbed dose	146
VI.23.	Phase Disengagement Time (s) of various radiolytically degraded systems as a function of absorbed dose	146
VI.24.	Zirconium retention (ppm) by radiolytically degraded samples after the absorbed dose of 5 MRad; Stock Zr: 1490 ppm	147
VI.25.	Zirconium retention (ppm) by radiolytically degraded samples after 10MRad; Stock Zr: 1490 ppm	147

VI.26.	Zirconium retention (ppm) by radiolytically degraded samples after 15MRad; Stock Zr: 1490 ppm	147
VI.27.	Zirconium retention (ppm) by radiolytically degraded samples after 20MRad; Stock Zr: 1490 ppm	148
VII.1.	Equilibrium constants and salting out coefficient values at 25°C	167
VII.2.	Values of thermodynamic parameters	170

ABBREVIATIONS

PUREX: Plutonium URanium Extraction.

TBP: Tri Butyl Phosphate.

FBR: Fast Breeder Reactor

FBTR: Fast Breeder Test Reactor

HAN: Hydroxyl Ammonium Nitrate

MEO: Mediated Electrochemical Oxidation

DEO: Direct Electrochemical Oxidation

MWD: Mega Watt Day

D: Distribution ratio

K_d: Distribution Coefficient

HLLW: High Level Liquid Waste

ICP-OES: Inductively Coupled Plasma – Optical Emission Spectroscopy

XRD: X-Ray Photoelectron Spectroscopy

FTIR: Fourier Transform Infrared Spectroscopy

CV: Cyclic Voltammetry

NPH: Normal Paraffin Hydrocarbon

mA: milli Ampere

V: Volts

Fig.: Figure

T: Temperature in Kelvin

E_{p,c}: Cathodic Peak Potential, in V

I_{p,c}: Cathodic Peak Current, in mA/A

E_{p,a}: Anodic Peak Potential, in V

I_{p,a}: Anodic Peak Current, in mA/A

a : Activity

C: Molar concentration

ΔG: Free energy change

ΔH: Enthalpy change of reaction

F: Vol % TBP

K: Equilibrium constant

k_s : Salting out coefficient

R: Universal gas constant

ΔS : Entropy change

α : Dissociation constant

γ : Activity coefficient

1. INTRODUCTION

1. 1. Nuclear Energy

Energy is the forefront of major political issues in all countries. The economic growth of any country depends on the availability and consumption of electricity. At present, fossil fuels (coal, lignite, oil and natural gas) are the major contributors to electricity generation, accounting for nearly 80 % of the electricity produced annually. Though, they contribute the major fraction of electric power, they are the major source for increasing the concentration of greenhouse gases in the atmosphere. Renewable sources like solar thermal power, hydroelectric power, wind energy and biomass power contribute another 18 % to the total electricity produced. Nevertheless, the search for a carbon free and sustainable energy source continues worldwide. Because of the high demand for electricity and the need for a large base-load and its ability to generate clean electricity with less impact on the environment, nuclear energy remains as a viable alternative to fossil fuels.

In India, nuclear energy contributes only 2 to 3 % of the total energy being consumed. India will need around 3400 TWh (TeraWatt hour) of electricity annually by 2070 [1]. This amount will be required, despite setting a low bench-mark of 2000 kWh per capita per annum for the future. The estimated total potential of all renewable resources in India is 1229 TWh [1], which when completely realized will account for only 36.1 % of the total estimated demand of 3400 TWh in 2070. Although India has reasonable resources of renewable energy, it is not so well endowed that its future electricity requirement can be fully met by renewable sources. Eventually, about 100 years later, the contribution from fossil fuels will also become negligible given the rate at which these are depleting due to their high consumption. Hence, the only sustainable energy

resource available in the long run is the nuclear energy. The Indian nuclear resources have been estimated to be about 60,000 ton of uranium and about 3, 60,000 ton of thorium [2]. Owing to the limited resources of naturally occurring fissile element ^{235}U , the sustainability of nuclear energy depends on the availability of the man made fissile elements like ^{239}Pu , ^{233}U etc. To meet the future energy demand in India, Department of Atomic Energy (DAE) has chalked out a three stage power programme [3, 4] in which reprocessing of the spent nuclear fuel is the vital link between the three steps.

1. 2. Indian Nuclear Power Programme

The three stage programme, schematically shown in Fig. I.1 and based on a closed nuclear fuel cycle had been envisaged and implemented in India by Dr. Homi J. Bhabha in early 50s for the effective utilization of the natural resources for the production of energy [5]. This is based on the limited uranium reserves and the availability of vast thorium resources (estimated to be around 3, 60,000 tonne which is about 32 % of the world's reserves) in India.

The first stage deals with the production of electrical energy through natural uranium fuelled pressurized heavy water reactors (PHWRs) and the allied fuel cycle facilities. Presently, two boiling water reactors (BWRs) and fifteen PHWRs built at various locations of India are in operation and producing a total of about 4120 MW electrical energy [6]. The second stage is based on the setting up of Fast Breeder Reactors (FBRs) which utilize the depleted uranium and plutonium recovered from the spent fuels of PHWRs as well as ^{233}U produced from ^{232}Th , which is used as a blanket material in FBRs. The 40 MW thermal Fast Breeder Test Reactor (FBTR) is in operation at Kalpakkam since 1985 [7]. A 500 MW electrical Prototype Fast Breeder Reactor (PFBR), which is in the advanced stage of construction at Kalpakkam will be commissioned soon. FBRs can breed more fuel than it consumes. The third stage of Indian nuclear power

programme is aimed at the exploitation of the plentiful resources of thorium in India and the reactors of third stage would use ^{232}Th - ^{233}U as the fuel. A 300 MWe Advanced Heavy Water Reactor (AHWR) [8], proposed to be constructed will use thorium-uranium and thorium-plutonium mixed oxides. The operation of this reactor will facilitate to gain experience in all aspects of technology related to thorium fuel cycle. Above all, with these long-term strategies, the nuclear industry is expected to undergo a paradigm shift from a mere electricity producer to being an indispensable part of India's energy policy.

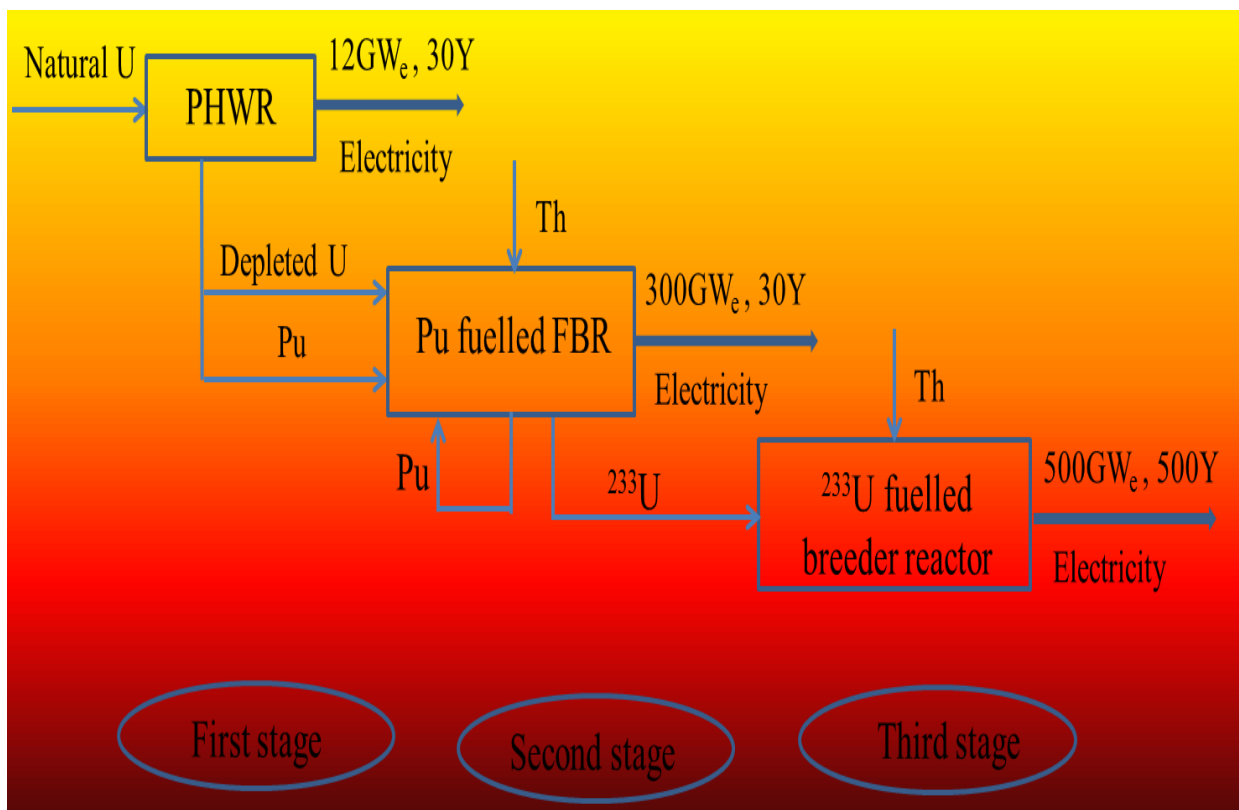


Fig. I.1. Three stages of Indian Nuclear Power Programme

1. 2.1 Nuclear Fuel Cycle

Nuclear fuel cycle encompasses uranium mining, uranium enrichment (if required), fuel fabrication, reactor operation, spent fuel reprocessing, vitrification and waste disposal. For long-term nuclear power production, there are two fuel cycle options that are of relevance and under

consideration at the present juncture, viz. the once through cycle with permanent disposal of spent fuel and the closed fuel cycle with reprocessing and recycling of uranium and plutonium. Both options require efficient and safe waste management strategies and are being practiced by different countries as per their priorities. While countries like US, Canada, Sweden and Spain have opted for once through fuel cycle, India has opted to closing the fuel cycle (as shown in Fig. I.2) for better utilization of the available limited resources.

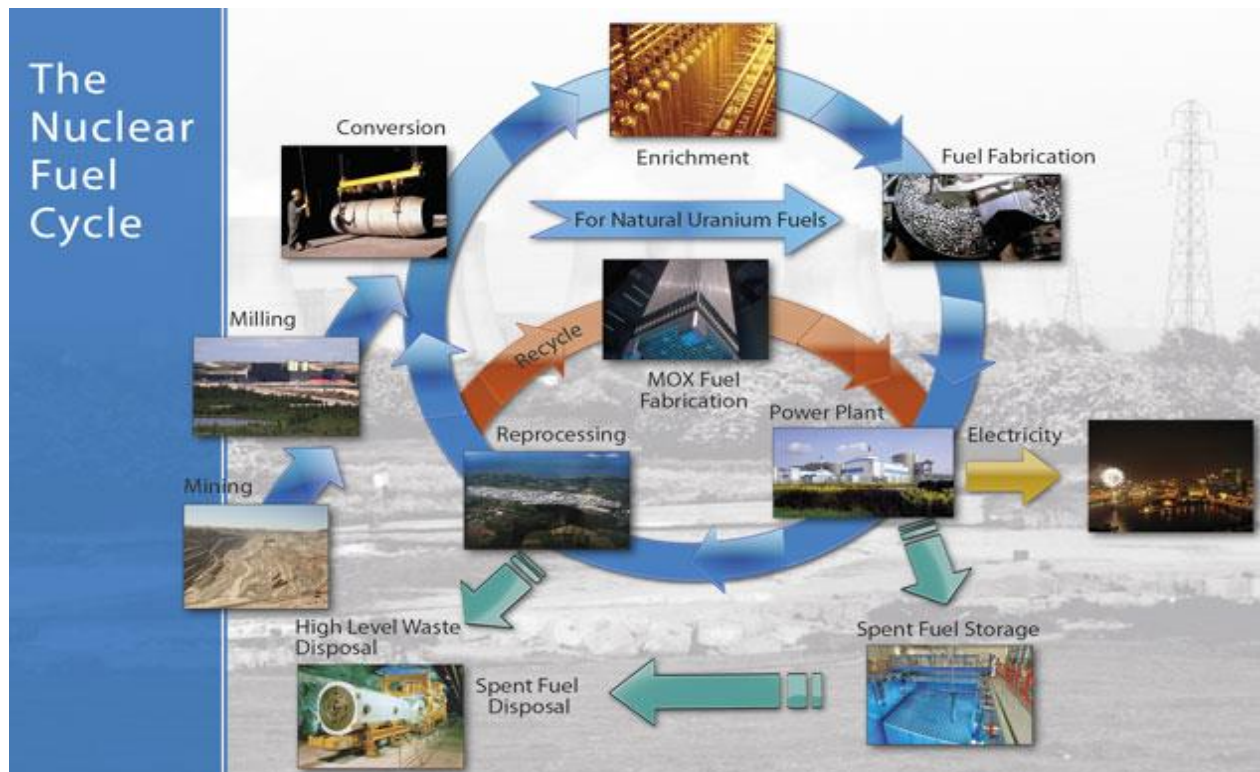


Fig. I.2. Nuclear Fuel Cycle (Courtesy: Web)

The sustainability of an advanced fuel cycle relies on the ability to maximize the usage of nuclear energy and on improving ways for long-term storage of waste forms. Removal of minor actinides (i.e. Np, Am, Cm and Cf) with U and Pu from the waste and their recycling in fast neutron reactors will significantly reduce the potential impact of the latter on the environment and simplify the procedure for the safe disposal of the highly active waste in a deep geological

repository. Therefore, separation of the trans uranium elements (TRUs) and their incineration in fast neutron devices (critical or sub-critical reactors) become a key feature of advanced fuel cycles.

1.2.2. Reprocessing

Reprocessing forms the vital link among the three stages of nuclear power programme and the success of the closed fuel cycle would depend on the efficient utilization of plutonium for power generation, as it can increase the quantum of energy derived from a given amount of uranium which varies depending on the reactor systems used. For India it is imperative that the three-stage nuclear power programme can sustain only with efficient reprocessing technology, the associated waste management programs and the development of re-fabrication technologies, essentially the closing of the back end of the fuel cycle. The prime objective of spent nuclear fuel reprocessing is to recover the plutonium, and unused uranium for contribution towards energy security as well as avoiding wastage of valuable energy resources. The recovered materials can effectively close the fuel cycle, thereby lowering to a large extent of the dependence on fossil fuel, and improving the energy security. The advantage in a once-through fuel cycle is that it would avoid the difficulties to be encountered in reprocessing; however, it can extract only about half a percent of energy content of mined uranium. Moreover, the recovered material from closed fuel cycle can directly be enriched, thereby reducing the demand of mining and milling of new uranium.

The initiative for nuclear fuel reprocessing has started in 1964 in India, as the known sources of uranium were inadequate to meet the long-term nuclear power programme [4]. By the time India entered into the domain of reprocessing, a certain level of understanding and maturity had already been achieved in this domain. The most popular aqueous route for the separation of

unspent uranium and fission produced plutonium from the waste fission products is known as PUREX (Plutonium URanium EXtraction) process. In this process, the major solvent extraction step employing 30 % n-tributyl phosphate (TBP) in an inert diluent, n-paraffin hydrocarbon (NPH with 12-14 carbon atoms) or pure n-dodecane is totally amenable for automation and remote handling. At present India has three operating plants for the reprocessing of nuclear fuels discharged from thermal reactors; one at Trombay has the reprocessing capacity of 60 tonne per year, the second and third plants are located at Tarapur and Kalpakkam respectively, with the capacity of 100 tonne of fuel processing per year. The compact facility for the reprocessing of advanced mixed carbide/oxide spent fuels of FBTR is also located at Kalpakkam. The demonstration fuel reprocessing plant (DFRP) with the capacity of 100Kg and 500 Kg per year for the processing of FBTR and PFBR fuels respectively is in the advanced stage of fabrication. From the safety point of view, the reprocessing technology has made vast improvement by complying with the national and international safety regulatory requirements and its annual radioactivity release through various forms of effluents have steadily decreased over the years. At present, these releases are very small in comparison to the environmental burden of plutonium and other radioactive elements released into atmosphere through testing of nuclear weapons and nuclear accidents.

1.2.3. PUREX Process

PUREX process has been the workhorse of fuel reprocessing for the separation and purification of plutonium and uranium from spent nuclear fuels in the last few decades and no other process developed before or after can claim its versatility [9]. This process is a solvent extraction process in which plutonium and uranium are selectively and almost completely extracted by TBP with fission product decontamination factors in the range 10^6 - 10^8 [8]. PUREX process has undergone

many modifications since its introduction and the flow sheets employed vary depending on the practitioners. The typical flow sheet for the reprocessing of spent fuels discharged from FBRs (Fast Breeder Reactors) is shown in Fig. I. 3 [4].

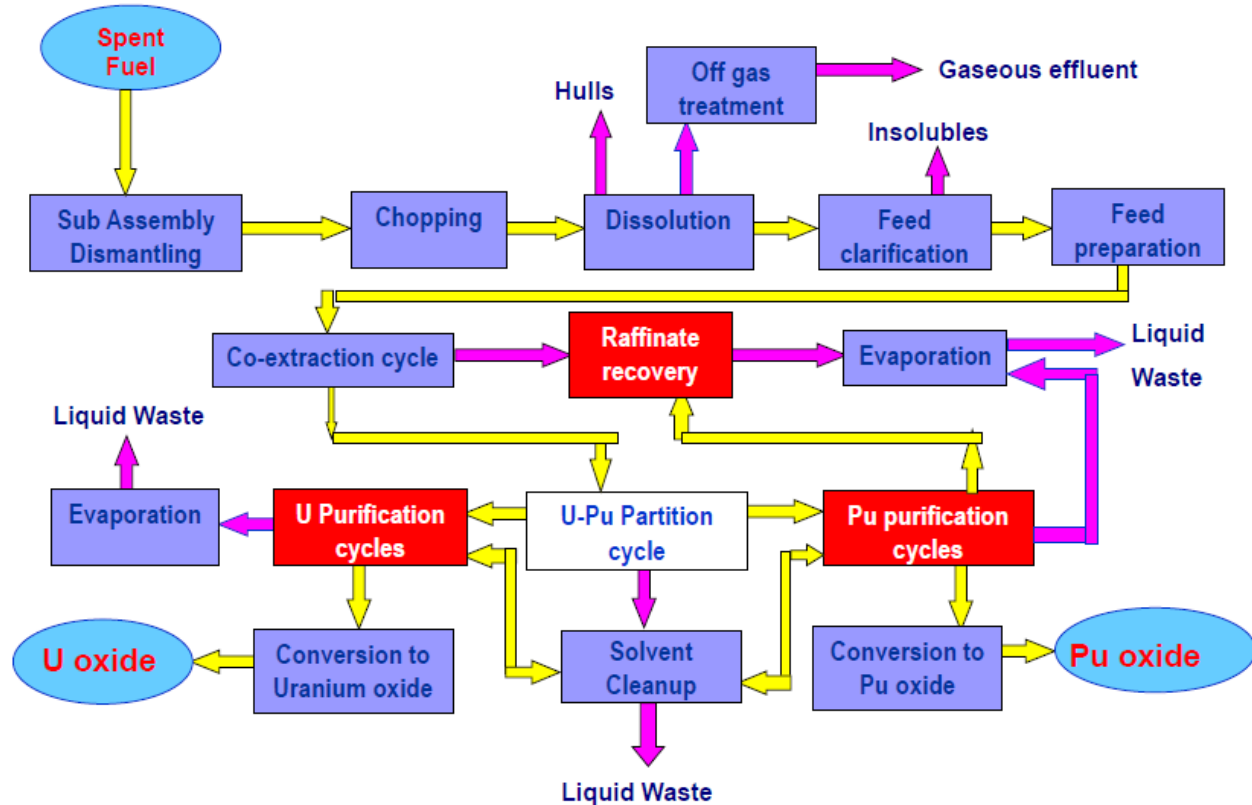
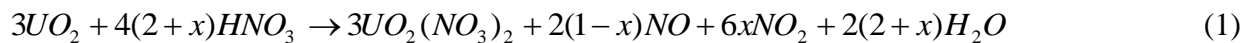


Fig. I.3. Schematic Process flow sheet for reprocessing of fast reactor fuels.

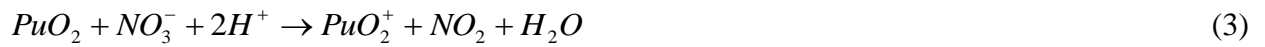
The irradiated MOX (Mixed Oxide) fuel pins are initially chopped into smaller pieces. The dissolution is typically carried out at elevated temperature, 70-110 °C, to allow dissolution on a short timescale. During dissolution in nitric acid the uranium is oxidised to uranyl and nitrogen oxides (Equation 1 below) where x depends on the nitric acid concentration.



(Where $0 < x < 1$)

Unlike uranium dioxide, plutonium dioxide does not dissolve in nitric acid to an appreciable degree. Thermodynamic calculations have shown that the dissolution of plutonium dioxide either

by reaction with acid (Equation 2) or by oxidation (Equations 3 and 4) are thermodynamically unfavorable. Despite this, in MOX fuel, when the microscopic plutonium concentration is a small fraction of the uranium, the plutonium does dissolve in nitric acid.



Air is sparged during dissolution to reduce the evolution of NO/NO₂ gas and to have a fumeless dissolution. Almost all fuel constituents are dissolved during this process leaving behind the stainless steel clad. The acidity of dissolver solution is then adjusted to 4M. The bulk of plutonium is present as Pu(IV), and a small amount present as Pu(VI) is subsequently adjusted to Pu(IV). For this adjustment, earlier plants employed NaNO₂ followed by digestion at around 50°C, but of late, many plants use N₂O₄ gas or hydroxyl amine nitrate as they do not add any salt content to the high level liquid waste [10]. The following equations describe the conversion of Pu(VI) to Pu(IV) [11];



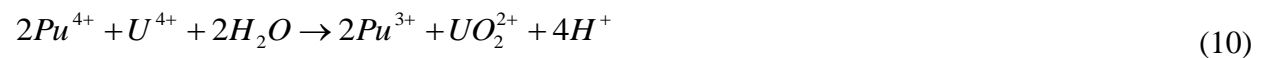
The conditioned solution is subjected to solvent extraction with 30% TBP (Tributyl phosphate (TBP) mixed with heavy normal paraffin (HNP)). Uranium and plutonium from nitric acid medium is selectively extracted into the organic phase and bulk of the fission product activity remains in the aqueous phase and this is known as the raffinate. Uranium and plutonium present organic phase is contacted with dilute nitric acid to strip out uranium and plutonium by a process

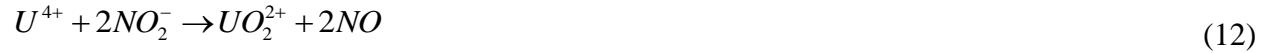
known as stripping. The organic phase obtained after removal of uranium and stripping and plutonium is known as lean organic phase. The process of co extraction and stripping of uranium and plutonium is known as co-decontamination cycle.



The aqueous phase constitutes the bulk of the high level liquid waste (HLLW). Owing to the high radioactivity as well as corrosiveness of the HLLW, it can be neither exposed nor stored for a longer period. Removal of nitric acid from the HLLW is warranted for the reduction of volume, minimization of corrosion in waste tanks during subsequent storage of concentrated waste solution as well as to simplify the procedure for waste fixing. Denitration is achieved either by electrolytic method or by a chemical method using suitable reductants.

The process solution after co-decontamination is sent to a partitioning contactor, where the U & Pu gets separated from each other. Partitioning of uranium and plutonium is carried out by the selective reduction of Pu(IV) to Pu(III) in the organic phase, which then comes back to the aqueous phase of lower acidity. This reduction is generally carried out by using ferrous sulphamate, uranous nitrate stabilized with hydrazine or hydroxylamine nitrate stabilized with hydrazine [10]. The commonly used reductant is uranous nitrate stabilized with hydrazine, as it does not introduce any additional metal ion into the system and thus, does not increase the amount of high level solid waste. Hydrazine also helps in stabilizing U(IV) in nitric acid medium by scavenging the nitrite ions. The reduction of Pu(IV) to Pu(III) takes place as follows [10]:





Hydrazine destroys nitrous acid by the following reactions:



After separation, the 'Pu' solution will be in nitric acid (aqueous) medium and Uranium will be in TBP (Organic) medium. The Uranium stream is stripped with dilute nitric acid and is sent for purification cycles.

The partitioned 'Pu' solution after valency adjustment in a conditioning step is subjected to two cycles of purification (i.e. two solvent extraction cycles) using 20% TBP as the solvent to get the required separation from the fission products and then is sent for its conversion to solid Pu Oxide. In reconversion step, Pu feed solution gets conditioned and precipitated as its oxalate using oxalic acid as the precipitating agent. The precipitated slurry is filtered, dried and calcined in a furnace to convert it to solid Pu oxide. The supernatant stream after oxalate precipitation containing U and traces of Pu is treated for oxalate destruction, concentrated by evaporation and the evaporate concentrate is sent to 'U' purification cycle for the recovery of 'U'.

The 'U' process solution obtained after partitioning is taken for valency adjustment in a conditioning step and is subjected to two cycles of purification by solvent extraction using 30% TBP as the solvent primarily to decontaminate it from the residual Pu present in it and also to reduce the radioactivity in the process solution. The purified 'U' solution is then sent for conversion of all U to its Oxide, where Uranyl nitrate product solution from the purification cycles is precipitated as ammonium diuranate (ADU). The precipitated ADU slurry is filtered, dried and calcined in a furnace for conversion to solid U-oxide.

The raffinate waste from the Co- decontamination, Pu purification and U purification cycles are sent to Pu and U recovery cycles for the recovery of Pu and U by solvent extraction using 15% TBP as the solvent. The raffinate obtained after recovery of Pu and U in the recovery cycle is evaporated for waste volume reduction. The recovered U and Pu solution from the recovery cycle is sent to appropriate streams of the main process.

During the extraction stage owing to high dose of radiation, the solvent as well as the diluent employed in the extraction process undergo chemical, thermal and especially radiolytic degradation resulting in a number of degraded products with varying physiochemical properties. Regeneration of solvent demands the elimination of acidic degradation products like mono butyl phosphoric acid (H₂MBP) and dibutyl phosphoric acid (HDBP), for which the solvent is generally given a Na₂CO₃ wash. In this context, commonly used Na₂CO₃ contributes significantly toward the generation of large salt volumes. Electrolytic methods are becoming increasingly popular to restrict the waste volumes in the first two steps, whereas, hydrazine carbonate is a potential candidate to replace Na₂CO₃ for solvent treatment.

Reprocessing of fast reactor fuel differs from that of thermal reactor fuel in the following aspects:

1. The fissile material content in fast reactor fuel is high compared to that in thermal reactors, thus making criticality an issue during reprocessing right from the dissolution stage. Also, with such high plutonium content, the risk of third phase formation and plutonium hydrolysis will be high.
2. The burn-up is high in fast reactors and will be typically of the order of 50 to 100 GWD/tonne as compared to 1000-12000 MWD/tonne in thermal reactors. Hence, the fission product content and their activity will be much higher in the spent fuel from fast reactor in comparison to thermal

reactor. This will lead to higher solvent degradation during reprocessing of fast reactor spent fuel.

3. Spent fuel from sodium cooled fast reactors will have to be treated prior to chopping to remove the adhering sodium.

4. Fast reactor fuels will have higher amount of platinum group metal fission products which form insoluble intermetallic alloy residues; thus, affecting the overall fissile material recovery.

1.2.4. Improvements in PUREX process

As a part of the Advanced Fuel Cycle Initiative (AFCI), Argonne National Laboratory has developed the Uranium Extraction (UREX) Process, which consists of five solvent-extraction processes that separate the dissolved spent fuel into seven fractions [12]. The five solvent-extraction processes are: (i) UREX for the quantitative extraction of uranium and technetium; (ii) Chlorinated Cobalt Dicarbollide- Polyethylene Glycol (CCD-PEG) for the recovery of Cs and Sr; (iii) Neptunium Plutonium Extraction (NPEX) for the recovery of plutonium and neptunium; (iv) TRUEX to recover Am, Cm, and Rare Earth Element (REE) fission products and (v) Cyanex 301 for the separation of Am and Cm from REEs. The co-processing option appears particularly promising for the reprocessing of Pu-based fast reactor spent fuels. In this approach, the recycling of spent nuclear fuel will be done without separating out pure plutonium. This will aid in nuclear non-proliferation, recovery and reuse of fuel resources. The long-lived fission products such as ^{99}Tc and ^{129}I will be separated and immobilized before disposal in repositories. Short-lived fission products such as ^{137}Cs and ^{90}Sr will be allowed to decay until they meet the requirement for disposal as low-level waste. Transuranics such as Pu, Np, Am and Cm will be separated from the fission products, so that they could be fabricated into fuel for an Advanced Burner Reactor (ABR). Birk et al. [13] reviewed the recent developments in the PUREX process for nuclear-fuel reprocessing and have recommended U/Pu co-processing and Pu/Np co-

stripping. Aqueous soluble simple hydroxamic acids, for example, aceto-hydroxamic acids are effective in the separation of uranium from neptunium and plutonium [14, 15]. The strong interaction of hydroxamic acids has been quantified by determining the stability constants. Recently, straight chain N, N-dihexyloctanamide (DHOA) was evaluated for the co-processing of spent nuclear fuel [16].

1.3. Challenges in Reprocessing

Even though PUREX process is well entrenched to meet the present and near future challenges, it is associated with crucial problems due to radiological impacts such as presence of radioactivity, build-up of heavy isotopes and contaminated equipment. The selection of materials for reprocessing application is a major concern as identification of suitable materials depends on various factors such as cost, availability, mechanical properties, corrosion behaviour etc. All round development in the field of science and technology has its implications in PUREX process too. Minimization of losses to waste, improvements in solvent quality, solvent purification, development of alternate extractant, crystallization of uranyl nitrate, direct denitration of products to oxide, co-processing and co-conversion for fuel development, recovery of useful isotopes like ^{237}Np , ^{99}Tc , Pd, etc., separation of long-lived actinides and fission products under partitioning and transmutation option with a general reduction of waste volume are some of the challenging R&D tasks which are being pursued.

1.4. Scope of the Present Investigation

The scope of the present investigation encompasses some studies on process development and addressing issues relevant to the back end of nuclear fuel cycle in aqueous reprocessing. The study includes the development of a continuous and homogeneous process for the safe denitration of HLLW by treatment with formaldehyde and comparing its efficiency with

denitration by electrochemical method. An exhaustive study has been carried out to compare the evolution in physiochemical properties as well as metal retention behaviour of thermally as well as radiolytically degraded TBP-DD and TBP-NPH systems with and without nitric acid as the aqueous phase. The effect of temperature, concentration of acid and metal ions on the solubility of TBP in aqueous phase has also been studied and the thermodynamic parameters relevant to the solubility of TBP in nitric acid have been derived.

References

1. Sukhatme, S.P., *Current Sci.*, **101** (2011) 624
2. Natarajan, R., Proc. DAE-BRNS Theme meeting on emerging trends in separation science and technology (SESTEC-2004), BARC, Mumbai
3. Baldev Raj, Kamath, H.S., Natarajan, R., Vasudeva Rao, P.R., *Prog. Nucl Energy*, **47** (2005) 369
4. Dey, P.K., Bansal, N.K., *Nucl. Engg. Design*, **236** (2006) 723
5. Bhabha, H.J., Proc. Internatl. Conf. on the Peaceful uses of Atomic Energy, 1, Geneva, 1955, p-103
6. Nuclear Power Corporation of India Limited, Home page, <http://www.npcil.nic.in>
7. IGC Newsletter, **86** (2010 3); IGCAR, Kalpakkam, India
8. <http://www.dae.gov.in/gc/ahwr-leu-broc.pdf>, BARC, DAE, India;
<http://www.barc.ernet.in/publications/eb/golden/reactor/toc/chapter1/1.pdf>
9. Uriarte, A.L., Rainey, R.H., Report No. ORNL-3695 (1965)
10. Sood, D.D., Patil, S.K., *J. Radioanal. Nucl. Chem.*, **203** (1996) 547
11. Sini, K., Satyabrata, M., Mallika, C., Pandey, N.K., Falix, L., Kamachi Mudali, U., Natarajan, R., *J. Radioanal. Nucl. Chem.*, **295** (2013) 1505
12. Vandegrift, G.F., Regalbuto, M.C., Aase, S., Bakel, A., Battisti, T.J., Bowers, T., Byrnes, J.P., Clark, M.A., Emery, J.W., Falkenberg, J.R., Gelis, A.V., Pereira, C., Hafenrichter, L., Tsai, Y., Quigley, K.J., Vander Pol, M.H., Proc. Advances for Future Nuclear Fuel Cycles Internatl. Conf., ATLANTE 2004, France, June (2004)
13. Birkett, J.E., Carrott, M.J., Fox, O.D., Jones, C.J., Maher, C.J., Roubé, C.V., Raylor, R.J., Woodhead, D.A., *Chimia*, **59** (2005) 898
14. Carrott, M.J., Fox, O.D., LeGurun, G., Jones, C.J., Mason, C., Taylor, R.J., Andirieux, F.P.L., Boxall, C., *Radiochim. Acta*, **96** (2008) 333
15. Taylor, R.J., Sinkov, S.I., Choppin, G.R., May, I., *Solvent Extr. Ion Exch.* **26** (2008) 41
16. Pathak, P.N., Prabhu, D.R., Kanekar, A.S., Manchanda, V.K., Recent R&D studies related to spent nuclear fuel reprocessing, Plutonium Futures “The Science” 2008 Conf., Dijon, France, July (2008)

2. LITERATURE REVIEW

2.1. Reduction of Nitrate Ions in Aqueous Solutions

2.1. 1. Introduction

The basic steps involved in the reprocessing of nuclear spent fuels, adopting PUREX process are the head end steps involving chemical or mechanical decladding followed by the dissolution step in nitric acid, feed clarification and adjustment of chemical conditions for subsequent solvent extraction step. The solvent extraction step involves the separation of both uranium and plutonium from the fission products in aqueous solution in nitric acid medium, by extracting into organic solvent and back washing the small fraction of fission products extracted along with uranium and plutonium into aqueous stream. The loaded organic with U and Pu can be separated from each other using solvent extraction step again in the presence of uranous solution [U(IV)], which reduces Pu(IV) to Pu(III), thereby bringing the less extractable Pu(III) into the aqueous phase followed by solvent extraction purification cycles separately for uranium and plutonium.

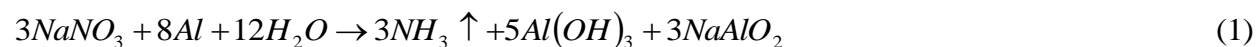
The aqueous phase resulting from the solvent extraction step of Fast Breeder Reactor's (FBR) fuel reprocessing containing non-volatile fission product elements and corrosion products constitutes the bulk of high level liquid waste (HLLW). The HLLW in about 4 M nitric acid is one of the major concerns in the waste treatment, as the amount of the waste generated during the aqueous reprocessing of spent nuclear fuels is substantial [1-3]. Owing to its high radioactivity as well as corrosive nature, it can neither be exposed nor can it be stored for a longer period. Removal of nitric acid from HLLW is warranted for reduction of volume, minimization of corrosion in waste tanks during subsequent storage of concentrated waste solution as well as to simplify the procedure for waste fixing. A series of denitration processes have been proposed in the literature for the purpose of reducing the waste volume as well as for

the safe disposal of highly radioactive waste solutions. The various denitration processes are briefly in the following Section:

2.1.2. Denitration Processes

2.1.2.1 Nitrate to ammonia and ceramic (NAC) process

The NAC process had been developed to remove a majority of the nitrate content from sodium nitrate based nuclear wastes [4, 5]. In this process, solid aluminium powder is added to a highly basic solution (pH: 11.5) which has a nitrate concentration of about 4 M at the temperature of 323 K. The process involves the chemical reduction of nitrate ions to ammonia by powdered aluminium. Aluminium is converted to aluminium hydroxide and sodium aluminite, as shown in the following stoichiometric reaction:



Small-scale batch tests with high-level waste in 3 to 6 M NO_3^- ions revealed that approximately twice the theoretical amount of aluminium is required to reduce essentially all the nitrate to ammonia [6]. Laboratory-scale tests have demonstrated that a smaller excess of stoichiometric aluminium is required to destroy the entire nitrate using a continuous-flow reactor [7, 8].

The Advantages of NAC process are

- Safe, economic and environmentally acceptable methodology for the reduction of nitrate-containing mixed wastes.
- Occurs at a relatively low temperature (323 K) and atmospheric pressure and provides environmentally acceptable waste form for the disposal of nitrate mixed waste.

However, this method of denitration has the following disadvantages:

- Since the process converts nitrate to ammonia rather than nitrogen gas, further off-gas treatment is required.

- The ammonia gas produced by the reaction is potentially explosive; consequently, inert atmosphere must be maintained in the system.
- As the process is highly exothermic, safety controls will be required to prevent a runaway reaction.

2.1.2.2. Biological denitration

The biological reduction of nitrate in waste water to gaseous nitrogen, accompanied by the oxidation of a nutrient carbon source to gaseous carbon dioxide, is an ecologically sound and cost-effective method of treating waste waters containing nitrates [9]. Biological denitrification exploits the ability of certain naturally-occurring bacteria to use nitrates for respiration under anoxic (absence of oxygen) conditions. The overall process is the reduction of nitrate to nitrogen gas and it proceeds as follows:



Denitrification can be achieved using both heterotrophic [10-12] and autotrophic [13, 14] bacteria. In heterotrophic denitrification an organic carbon substrate such as methanol, ethanol or acetic acid is required as a food source for the bacteria. In autotrophic denitrification an inorganic energy source such as sulphur, reduced sulphur species (e.g. thiosulphate) or hydrogen is required; the carbon needed for bacterial growth is obtained from bicarbonate in the water. Heterotrophic denitrification systems are applied more widely than autotrophic processes.

In biological denitration, the nitrate is converted to nitrogen gas at ambient temperature and pressure and the required equipment is simple and easily operated. The limitations of this process are that the bacteria can tolerate only a narrow pH and salt concentration range in addition to the slow denitrification rate, which dictates large bioreactors.

2.1.2.3. Electrochemical method

Electrochemical treatment is a proven and inherently safe technology for the destruction of nitrates, nitrites as well as the removal of radionuclides and hazardous metals from the waste solutions [15]. The reduction of nitrate in an electrochemical cell can be carried out under acidic, neutral and basic conditions. However, the reduction of nitrate in acidic solutions takes place at more positive potentials and hence, more favourable [16]. In this method, nitrate and nitrite are reduced to nitrogen-containing gases: nitrous oxide, nitrogen and ammonia [16, 17]. These gases escape from the solution and are released into the vapour phase, thus separating from the solution. The main advantage of this method is that, it offers an easily controlled and safe mode of the destruction of nitrate ions without the requirement of external chemical addition.

a. Mechanism of electrolytic acid killing

Electrochemical reduction of nitric acid occurs according to the following reactions taking place at the electrodes [18, 19]

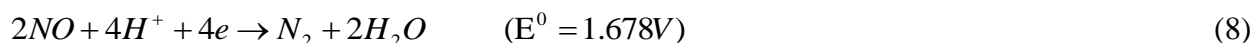
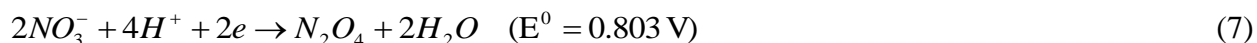
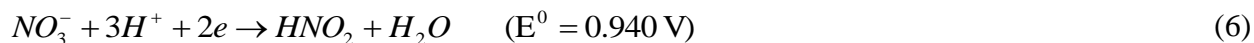
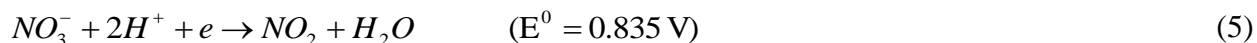
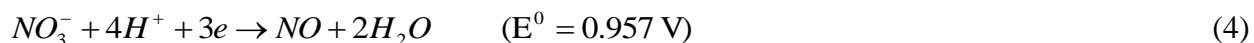
At anode:

Under the influence of an electrical potential, hydrogen ions are generated at the anode according to the reaction

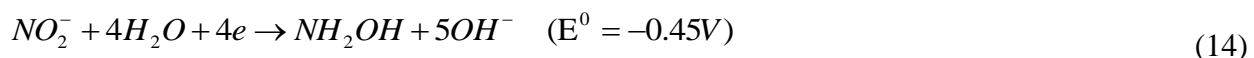
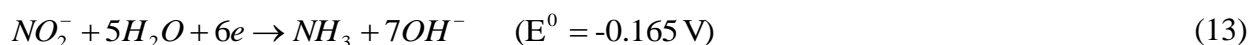
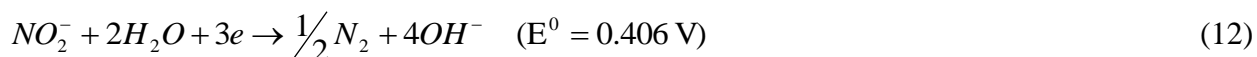
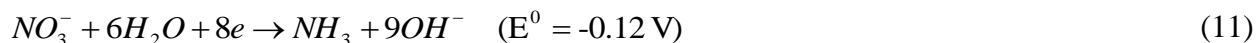
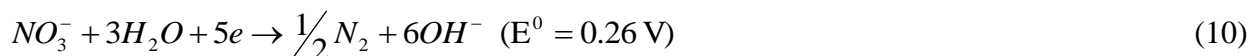
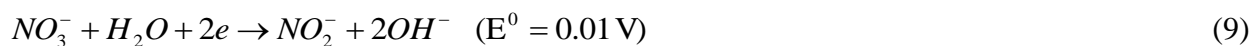


These hydrogen ions are transported with hydrated water to the cathodic compartment through the porous diaphragm. As a result, the concentration of the acid in the anodic compartment increases. The migrated H^+ ions from the anodic compartment react with NO_3^- at the cathode to produce H_2O and NO_x ; as a result, nitric acid concentration in the catholyte decreases. In addition to these reactions, other competing side reactions also occur at the cathode. In the cathode compartment, the electrochemical reduction of nitric acid occurs as follows:

At cathode:



In addition to the reactions (4) to (8), the following reactions may also proceed at cathode during electrolysis [20]:



Hydrogen evolution is the main parasitic cathodic reaction



Oxygen evolution is the main anodic reaction.



Some of the hydrogen ions set free at the cathode, reduce part of nitric acid in the vicinity of the electrode. During electrolysis in a cell with diaphragm, the concentration of the acid in the catholyte decreases not only by loss of hydrogen and migration of nitrate ions to the anolyte, but also by partial conversion of the acid to the oxides of nitrogen. The composition of the gas generated by electrolysis depends on the concentration of nitric acid and the cathode material [19]. When the concentration of nitric acid is more than 5 mol/l, more of NO_x get evolved and at concentrations below 5 mol/l, the main component is NO with traces of NO_2 . At very low acid concentrations, the liberated gases are a mixture of NO, N_2O , N_2 and an appreciable amount of H_2 . The current efficiency of the process decreases if the reductants diffuse to the anode and get re-oxidized. Such a reoxidation reaction in which NO getting oxidized to NO_2 by the O_2 gas released at the anode is prevented by the use of a separator (semi permeable ceramic diaphragm membrane) to isolate the anode from the cathode compartment.

Baumgartner and Schmieder [21] reported that there exists a nitric acid limiting concentration of 3.8 M, below which nitrate reduction takes place only by the addition of cations such as Cu, Fe, Mn and Na. However, Palamalai et al. [22] found out that the limiting concentration of nitric acid can be extended up to 1 M, without the presence of any metal ions. Electrochemical reduction of nitrates has been carried out using various metallic electrodes including Pt [23, 24], Rh [25], Pd [26], Cu [27] and graphite. Cattarin [28] reduced nitrate on Cu to nitrite at -1.1 V vs standard calomel electrode (SCE) and to ammonia at -1.4 V vs SCE with high yields, whereas Li et al. [29] used Ni, Pb, Zn and Fe cathodes and observed that all of them produced nitrite as the intermediate and ammonia as the final product. The controlled potential for lead was -2.0 V vs SCE, while for the others it was -1.5 V vs SCE. The Zn and Pb cathodes yielded over 90 % nitrate reduction after an electrolysis time of one hour. Kim et al. [30] studied the reduction

behaviour of nitric acid using a glassy carbon fiber column electrode system. Electrochemical reaction below 2 M nitric acid was not observed by them and above 2 M, reduction could be achieved with a slow rate. Kerkeni et al. [31] used platinized platinum catalysts modified by copper monolayers as the cathode material for nitrate reduction. This electrode was efficient in the reduction of nitrate than in the reduction of nitride to the corresponding products.

Dima et al. [32] made a comparative study to determine the reactivity of 0.1 M nitrate ions on seven different electrodes (Pt, Pd, Rh, Ir, Cu, Ag and Au) in acidic solution using cyclic voltammetry, which showed that the current densities for the nitrate reduction depend strongly on the nature of the electrode. Reduction of nitric acid from 4 to 0.5 M using Platinum Electroplated Titanium (PET) cathode could be achieved by Mallika et al. [33]. They reported that PET electrode with Pt plating thickness of 3 μm did not fail up to 110 h at the cathode current density of 60 mAcm^{-2} in 8 M HNO_3 medium. Huang et al. [34] studied the effect of pH (2 - 4.5) on nitrate reduction in iron-nitrate-water system and found that nitrate could be rapidly reduced to ammonium ion in this pH range. A kinetic model incorporating the effect of pH on nitrate reduction was also proposed.

Slow corrosion of a metal cathode is possible through long-term use, whereby some metal would be lost and contaminate the environment. Nickel based cathodes have less tendency to corrode. One way to avoid metal corrosion is to cover the electrode with an electro catalyst. This would also facilitate the shifting of potential to more positive values by lowering the over potential. Glassy carbon electrodes have been coated with several highly stable metal phthalocyanines (MPC) and nitrate reduction is carried out with them in basic solution [35].

Electrochemical method for the reduction of nitrate ions offers the following advantages:

- Easily controlled and safe mode of operation.
- No secondary waste generation since there is no addition of external chemicals.
- The process could be used on acidic or alkaline waste streams without pretreatment. For acidic solutions, the waste will be neutralized while the nitrate is being destroyed.

In spite of the advantages in the reduction of nitrates by electrochemical method, it is not considered for deployment in plants due to the disadvantages listed below:

- Electrolysis affects ions other than the nitrates that are intended to be destroyed.
- In some cases, the products plate-out on electrodes; however, this problem can be solved partially by proper selection of electrode and by reversing electrode currents.
- Release of the off-gases will require further evaluation.
- For plant scale application, fabrication of rugged electrodes of large surface area with high corrosion resistance and freedom from inactivation through poisoning is a challenge.
- The electro migration of ions in aqueous solutions is accompanied by electro-osmosis, a process in which water diffuses through the membrane. This leads to volume imbalance over long treatment periods. In addition, the electrolysis process consumes water and requires significant quantities of makeup water.

2.1.2.4. Thermal denitration

Heating a solid nitrate in an inert atmosphere eventually to produce nitrogen oxides is one of the first detailed thermal studies on the decomposition of NaNO_3 by Freeman [36].



Above 973 K, NaNO_2 decomposes to produce nitrogen oxides. NO_x is produced when nitrate-containing nuclear waste is heated to 673 K with H_3PO_4 in a 2:1 nitrate to phosphate ratio and

allowed to go to dryness [37]. Pilot scale tests using a plasma torch have demonstrated that a mixture of sodium and potassium nitrate can be converted to solid carbonates and nitrogen gas [38].

2.1.2.5. Chemical denitration

1. Active metals

Active metals have been used for many years to reduce nitrate in basic solutions to nitrite or ammonia. Metals that have been suggested for analytical purposes include Cd [39], Cd amalgam [40, 41], Al [42] and Zn [43]. At pH values less than 8, no nitrate reduction takes place when these metal powders are added, but at pH values greater than 11.5, nitrate is reduced to ammonia as the principal product with some nitrite and nitrogen gas.

2. Hydrazine and hydroxylamine

Hydrazine is used in several spectrophotometric analytical methods to reduce nitrate to nitrite. In most instances traces of a Cu(II) salt are added as a catalyst [44, 45]. A concentrated aqueous solution of hydroxylamine nitrate (HAN) mixed with alkyl ammonium nitrate salts burn very rapidly, partially reducing the nitrate present.

3. Ammonia

The reduction of nitrate with ammonia in basic or acidic solution to nitrogen and/or nitrous oxide is expected, based on the standard redox potentials. Such reactions do occur; but only at high temperatures and pressures. Such a reaction takes place when ammonium nitrate explodes at high temperature and pressure [46]. Heating of aqueous solutions of ammonium nitrite under atmospheric conditions produces nitrogen.



4. Formic acid and other organic species

Denitration by formic acid exhibits a complex behaviour. It occurs not through a direct reaction between nitric acid and formic acid, but through the mutual reactions of several intermediates generated from nitric acid and formic acid [47]. So, when both the concentrations of nitric acid and formic acid are not maintained properly during denitration, the decomposition rate of nitric acid becomes slow or the total acidity level in the solution gets high at the final stage. In the conventional denitration by formic acid, the lowest final total acidity could be achieved, only when the total mole ratio of formic acid to nitric acid was about 1.5 [48, 49]. When the mole ratio is higher than this value, much of the excess protons from formic acid remain in the solution, which causes the total acidity level to increase after the denitration, even though the concentration of nitric acid itself is low enough due to a high decomposition rate of nitric acid in the solution. On the other hand, when the mole ratio is lower than 1.5, the denitration rate and its yield are lower. Even at the mole ratio of 1.5, it takes a few h to accomplish a desired denitration. For example, with an initial nitric acid concentration of 2.0 M, it took about 2.5 and 5 h for the final total acidities to reach 0.5 and 0.25 M respectively [50, 51]. The long denitration time, limitation of the final acidity and the precipitation of metal ions during denitration make the conventional denitration by formic acid unavailable for a continuous operation in the wet partitioning process. Accordingly, denitration by formic acid is usually operated by batch mode. A number of simple organic compounds have been used, or attempts have been made to reduce nitrate in aqueous solutions. These include acetaldehyde, glucose, methane, methanol, oxalic acid, tributyl phosphate and urea. Glucose was possibly one of the best reducing agent to react with nitrate, especially at high temperature and pressure [47]. With glucose to nitrate ratio of 0.4, a temperature of 623 K, a pressure of 158 atm and the value of pH as 13, 48 % of the nitrate was

converted to N_2 and the pH decreased to 8.2 after 2 h. Under similar conditions, urea showed only 20 % conversion and methane 6 %.

5. Formaldehyde

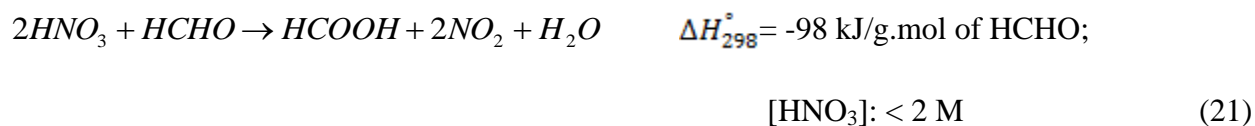
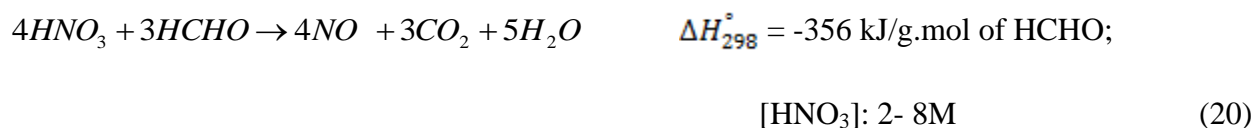
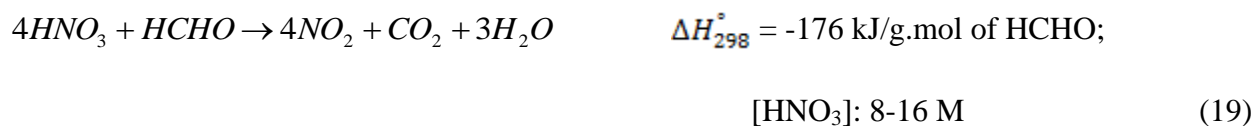
The denitration of high-level liquid waste by formaldehyde is used mainly to adjust the acidity and nitrate concentration prior to vitrification process, destroying the entire nitrate. There exists an induction period after formaldehyde is added to the HLW and before the reaction initiates. If excess amounts of formaldehyde get build up in the solution before the reaction starts, rapid reaction rates can produce high pressures in the reaction vessel. Several incidents of this type have occurred in the full scale facilities with minor consequences. The off-gas contains high concentrations of NO_x , demanding further treatment. The gas can be scrubbed, but this will produce large volumes of radioactively contaminated nitric acid or nitrate salts that will require further treatment for disposal. The preferred treatment for the off-gas would be catalytic reduction with ammonia, which will produce nitrogen gas.

The main advantage of denitration using HCHO is that, it leaves no residual chemical and the gaseous products NO_2 , NO and CO_2 are removed automatically. The homogeneous denitration with organic reductant HCHO is a complex chemical process which depends on factors such as temperature, acidity, reaction mixture composition, concentration of the reaction intermediates etc. The reaction of HNO_3 with HCHO is initiated after a certain induction period during which period, auto catalytic generation of HNO_2 takes place and the reaction proceeds rapidly. The delay owing to induction period leads to uncontrollable process conditions because of pressurization of the system, which demands safety precautions. Literature survey reveals that the induction period is dependent on the concentration of nitric acid, nitrite content and temperature and can be considerably minimized or suppressed either by passing gaseous NO_2

through the acid prior to the addition of HCHO [52] or by carrying out the reaction at a temperature above 373 K. At 373 K and at acid concentrations above 3 M, the reaction is instantaneous. At marginally lower temperatures, the induction period can be shortened by adopting a heterogeneous catalysed denitration using catalysts like Pt/SiO₂, Pd–Cu, heavy metal ions such as V, Cr, Fe, U and activated carbon. Nevertheless, the amount of solids introduced during denitration increases the burden in waste fixing. Denitration using formaldehyde possesses the advantage of low chemical cost, easy recoverability of nitric acid and in the case of waste treatment, the production of a solution relatively low in inert salt concentration suitable for fission product recovery or ultimate disposal.

5.1. Chemistry of denitration by HCHO

Denitration with HCHO is influenced by the concentration of nitric acid reacting [52, 53].



At nitric acid concentrations below 2 M, appreciable amount of the intermediate compound, formic acid is produced and the reaction mechanism is dictated by reaction (21). Further addition of HCHO to dilute nitric acid causes the buildup of formic acid as the rate of formation of HCOOH exceeds the rate of destruction of HNO₃. Formic acid produced in reaction (21) also

destroys nitric acid as per reaction (22). However, the destruction rate for reaction (22) is only moderate in homogeneous denitration.

The process of denitration of acidic HLW by HCHO has been in use for many years in full-scale facilities. It leaves no residual chemicals and the gaseous products NO_2 , NO and CO_2 are removed automatically. However, this process is also not free from disadvantages. Because the nitrate is converted to nitrogen oxides rather than nitrogen gas, further off-gas treatment would be required. This process is potentially unstable; therefore, safety controls will be required to prevent a runaway reaction. Acid killing by HCHO process is not normally capable of destroying the entire nitrate; consequently, substantial concentrations of nitrate would still be present in the waste after treatment.

2.2. Degradation of Solvent Used in Nuclear Fuel Reprocessing

2.2.1. Introduction

Liquid-liquid extraction process remains the most favoured route for recycling of nuclear materials during reprocessing of the spent fuel. Solvent extraction adopts 30% TBP in NPH (n-paraffin hydrocarbon) or DD (Dodecane) as the extractant for the separation of plutonium and uranium from nitric acid solution containing a large number of fission products. During the extraction stage, a small amount of nitric acid also gets extracted to the solvent [54]. Owing to high dose of radiation, the solvent as well as the diluent employed in the extraction process undergo chemical, thermal and especially radiolytic degradation resulting in a number of degradation products with varying physiochemical properties. The accumulation of the degradation products in the solvent can lead to different types of damage that disrupt the PUREX process, such as a decrease in the decontamination performance of uranium and plutonium for fission products (mainly ruthenium, zirconium, cerium, and niobium) [55, 56], an increase of

product loss namely, uranium and plutonium in aqueous raffinate [57], formation of emulsions, suspensions and cruds at the liquid-liquid interface, which disturb the continuous extraction process [58] and the evolution of physiochemical properties of the phases, mainly viscosity and interfacial tension [59].

2.2.2. Irradiation Tools

In most of the studies, the solvent samples were exposed to γ -irradiation with a ^{60}Co source [60-63]. Some studies were carried out with α -rays also, either with an external beam from a cyclotron [64] or by direct introduction of α -emitters such as ^{239}Pu [65], ^{241}Am [66, 67] and ^{244}Cm [68] in the solutions. Few experiments were performed with β -radiation using a ^{90}Sr source [69]. Wilkinson and Williams [70] investigated radiolysis with electron accelerators. Irradiation experiments can be performed with monophasic systems (in the absence of an aqueous phase) or under extraction conditions in the presence of an aqueous phase, in static or dynamic conditions [71].

2. 2. 3. Degradation of Extractant-diluent System

Tri-n-butyl phosphate (TBP) in hydrocarbon diluents is the work-horse in the aqueous reprocessing by PUREX process for the extraction of uranium and plutonium from the spent nuclear fuels [72]. Davis in 1984 [73] identified the degradation products and the specific role of diluents. In 1995, Tahraoui and Morris [74] reviewed the literature on the decomposition of solvent extraction media during nuclear reprocessing with respect to the mechanisms involved in the chemical and radiolytic degradation of TBP and diluents. Tallent and Mailen [75, 76] have proposed the mechanism for the formation of different degradation products particularly from diluents. The hypothesis put forward by Lane [77] also explains the mechanism for the formation of different degradation products of solvent as well as diluents. With the development of

advanced mass-spectrometric techniques (GC-MS, gas chromatography and tandem mass spectrometry, ESI-MS, electro-spray ionization and tandem mass spectrometry), the structures of minor degradation products (isomeric dimers of TBP, their oxidation products and their lower homologues) could be established [78-80]. The behaviour of the rich fractions of high molecular-weight compounds has been investigated by Tripathi et al. [81, 82]. The two most important types of reactions studied extensively are hydrolysis and radiolysis of the solvent but other known reactions include oxidation, nitrolysis and pyrolysis. The possible decomposition reactions of solvent-diluent are presented in Fig. II.1.

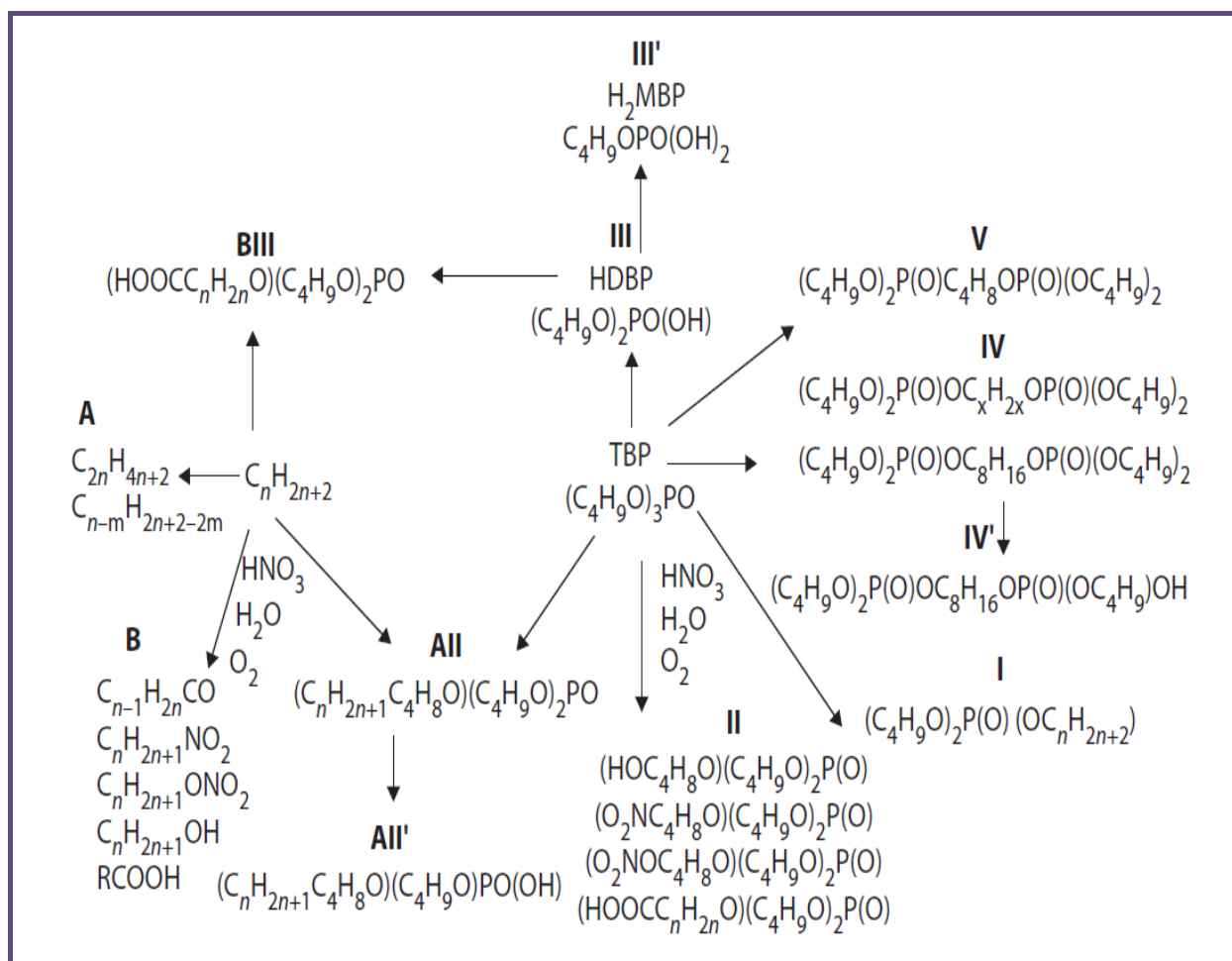


Fig. II.1. Degradation scheme of solvent-diluent system

The degraded products can be separated into three distinct groups:

2.2.3.1. Degradation products from the diluent (Compounds A and B)

The Compounds A in Fig. II.1 include alkane dimers and fragments of dodecane. Compounds B result from nitration and oxidation of the diluent. These nitration and oxidation reactions arise from the reactions of HNO_3 , O_2 , H_2O and their radiolytic products with organic components.

2.2.3.2. Degradation products from TBP (Compounds I, II, III, IV and V)

Compounds of type I are formed by the homolytic breaking of the C-C bond on the butyl chain. Compounds II correspond to the isomers resulting from nitration and oxidation of TBP. Hydrolysis of TBP (breaking of the C-O bond) results in the formation of Compound III (HDBP), which in turn undergoes further hydrolysis to form III' (H_2MBP). Compounds IV correspond to isomers of di phosphates. The central alkyl chain is produced by the combination of two radicals and can therefore, be linear or branched on different positions. These compounds can undergo hydrolysis to form IV' compounds. Compounds V correspond to isomers of phosphate-phosphonates. The isomers differ from one another based on the position of the new P-C bond along the C_4H_8 radical.

2.2.3.3. Mixed degradation products (Compounds AII and BIII)

Compounds AII result from the recombination of alkyl and TBP radicals, which then undergo further hydrolysis to form AII'. Compounds BIII are long-chain carboxylic acids, produced from HDBP secondary reactions.

Numerous gaseous products such as H_2 , CH_4 , CO , CO_2 , $\text{C}_1\text{-C}_4$ hydrocarbons and several nitrogen-containing compounds (HNO_3 , N_2 , NO , N_2O and NO_2) are also released [82-84]. In the gas phase, the highest yield measured was always for H_2 . But gaseous compounds containing nitrogen are generated when the radiolysis is performed in the presence of HNO_3 .

The principal degradation reaction is the hydrolysis of TBP to form HDBP and butanol [57, 84]. HDBP can undergo further hydrolysis and butanol can undergo nitrolysis (producing butyl nitrate) or oxidation (producing carboxylic acids). All of the degradation products can undergo thermal pyrolysis leading to the generation of gases. Butyl nitrate has been found as a liquid product, and in the gas phase. Along with butyl nitrate, the other non-phosphate products are mainly butanol and trace amounts of carboxylic acids as reported by Tashiro et al. [85]. These authors have also reported that the amount of non-phosphate degradation products is equal to the amount of phosphate degradation products. The liquid products can either stay in the organic solvent phase or can be transferred into the aqueous nitric acid phase. The HDBP is soluble in the organic phase and it has been shown that over 90 % of the HDBP formed stays in the solvent [86, 87]. Butanol moves into the aqueous phase, while butyl nitrate was found to be present in both the aqueous and organic phases and also in the gaseous phase [88].

2.2. 4. Diluent Degradation Mechanism

The chemical degradation of the diluent, NPH both in the pure state and in 30 % TBP solution was investigated in a series of experiments by Tallent and Mailen [76]. Based on the various degraded products formed and the information obtained from literature, they proposed a mechanism for diluent's degradation. The experimental results indicated that the degradation of NPH in TBP-NPH-HNO₃ system is consistent with the active chemical agent, which is a radical-like nitrogen dioxide (NO₂) molecule, rather than HNO₃, as such.

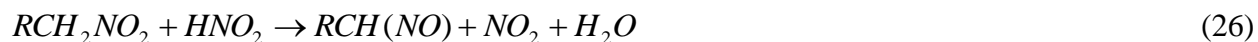


The hydrocarbon radical (R[•]CH₂) reacts with a molecule of NO₂ to give a nitro or nitrite compound.





The nitro compound (RCH_2NO_2) reacts with nitrous acid (HNO_2) to form a nitroso compound.



The nitro compounds can undergo hydrolysis to form carboxylic acids ($RCOOH$). The nitrite (RCH_2-ONO) compounds formed in the reaction may also hydrolyze to a considerable extent to form an alcohol.



Lane [77] has provided evidence for the species responsible for the retention of zirconium in degraded solvents, and their formation from nitro paraffins during the course of diluent's degradation is also outlined. The mechanism for their formation is shown in Fig.II.2.

2.2. 5. Factors Influencing the Degradation of the Solvent System

2.2.5.1. Nature of the irradiation Source

The nature of the radiation (γ , β , α or accelerator radiation) does not have any qualitative influence on the degradation of TBP-diluent system in contact with an aqueous phase. Moreover, the yield of the decomposition products of TBP [89] was almost identical, irrespective of the nature of radiations. After radiolysis of TBP in n-dodecane without aqueous solution, the yield of H_2MBP was substantially lower under α -irradiation than under γ -irradiation [$G\alpha(H_2MBP) = 0.158$ and $G\gamma(H_2MBP) = 0.443$] [89]. G-value represents the number of molecule changes for each 100 eV of energy absorbed

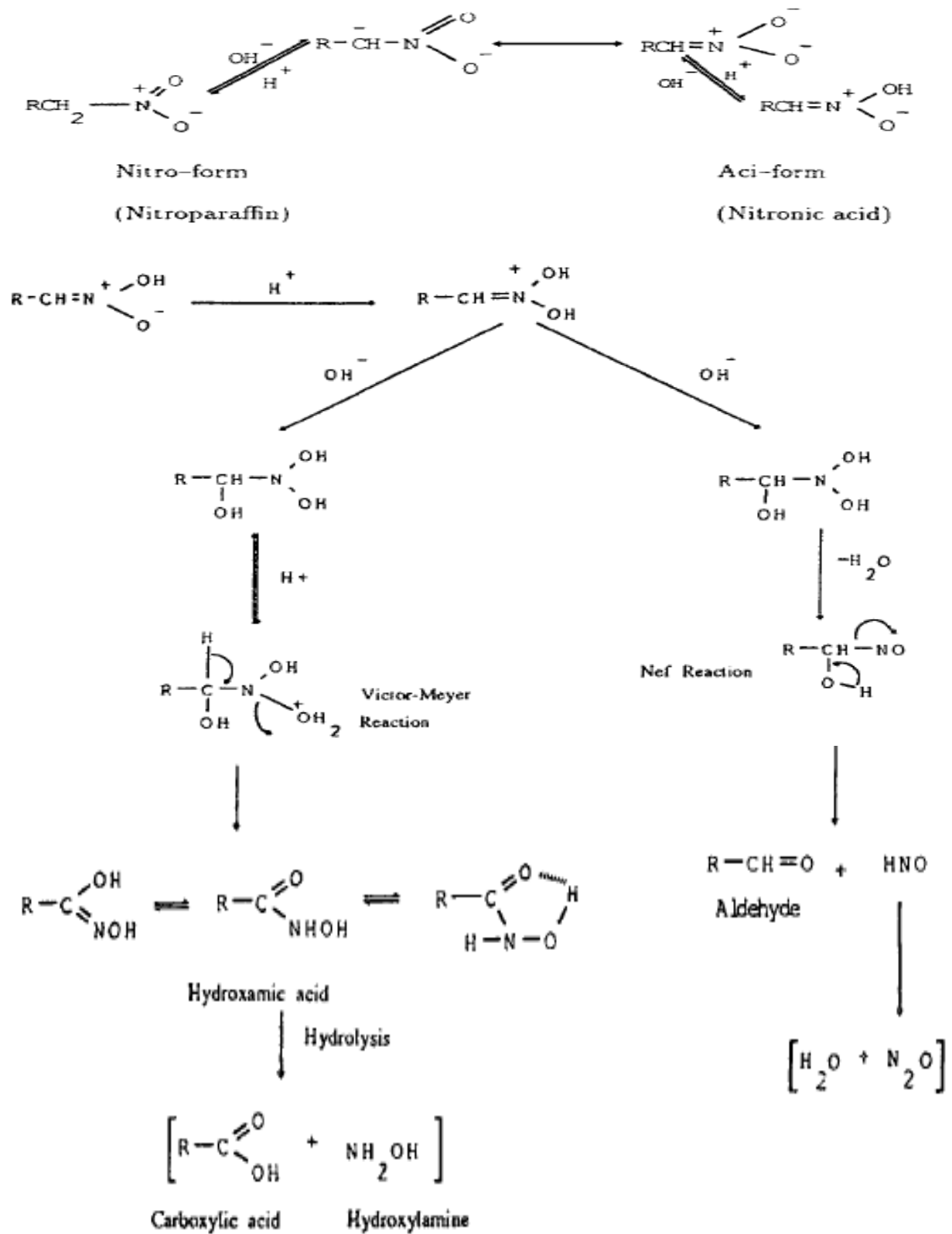


Fig.II.2. Possible mechanism for the formation of diluents degradation products.

2.2.5.2. Irradiation dose and dose rate

In most of the cases, an increase of the dose led to an increase in the degradation products. For a radiation dose lower than 0.1 MGy, the yield of the TBP decomposition products was independent of the irradiation dose and $G(\text{HDBP}) > G(\text{H2MBP})$ [90]. Above 0.2 MGy, the value of G for the majority of identified phosphorus products decreased with increasing absorbed dose [84, 91]. Further, for doses higher than 1 MGy, the HDBP concentration increase rate slowed down and was correlated with a build-up in the concentration of H2MBP [90, 92]. The dose rate appears to have no significant influence on $G(\text{HDBP})$ and $G(\text{H2MBP})$ [93], and on the yield of RNO and RNO₂ compounds [55].

2.2.5.3. Nature of the diluents

Diluents can inhibit or sensitize TBP radiolysis. The effect of various diluents (aliphatic hydrocarbons, aromatic and halo-carbons) on TBP degradation products was examined over a wide range of nitric acid concentrations [94]. Diluent like CCl₄ sensitizes TBP degradation [95]; in contrast, aromatic diluent inhibits its degradation due to protective effect [84, 94, 96-99]. The use of aliphatic hydrocarbons as diluents led to an intermediate yield of degradation products. Canva and Pages [100] confirmed that some saturated aliphatic hydrocarbons (hexane, cyclohexane and dodecane) sensitize or increase the decomposition of TBP. Though Egorov et al. [101] observed an increase in the radiolytic and chemical stability of TBP with the carbon chain length of the diluent (n-octane < n-dodecane < mixture n-C14/n-C15), Adamov et al. [102] did not notice any change in the composition of the radiolysed TBP-alkane solution when n-undecane was replaced by higher hydrocarbons (up to C17). The length of 12–14 carbons was considered as optimal to avoid difficulties in removing the high-molecular-weight products in the regeneration stage. Though the chemical and radioactive stability of branched aliphatic

hydrocarbons and olefins seemed to be lower than for linear hydrocarbons [103], the radiation resistance of TBP solutions in iso- and n-paraffins was almost the same [104]. Despite their protective effect with respect to degradation, the use of aromatic diluents has been avoided because of their low flash point. The classical diluents selected for PUREX process operations were hydrocarbons, either pure compounds (i.e. n-dodecane) or mixtures of different products (i.e. hydrogenated polypropylene tetramer, odourless kerosene, etc.) [103]. Halo-carbon diluents have two major drawbacks linked to their radiolytic behaviour: sensitization of TBP degradation and the production of extremely corrosive halide ions [63, 99]. The relative chemical as well as radiolytic stabilities of 21 different diluents and pure hydrocarbons based on "Z test" were investigated by Dennis [105]. The results are summarized in Table.II.1.

2.2.5.4. Nitric acid concentration

In the presence of nitric acid, radiation-induced decomposition of TBP solutions increases significantly [106]. For a given dose, the yield of acidic TBP degradation products (HDBP and H2MBP) increased marginally with the concentration of nitric acid in dodecane [55, 82, 94, 107, 108], but the influence was considerable in the system containing CCl_4 [94, 109]. For the TBP-alkane system, the global yields of oxidation products (hydroxy, nitro and carbonyl compounds) increased markedly with increasing concentrations of nitric acid (from 0.5 to 3 mol L⁻¹) [55, 107]. In the presence of nitric acid, the radiolysis of TBP leads to new degradation products, named as "modified phosphates" corresponding to type II compounds (viz. Fig. II.1).

Table II.1. Radiolytic and chemical stability of pure hydrocarbons

Class of compounds		Radiolytic stability			Chemical stability		
		A	B	C	A	B	C
Normal paraffin	n-Dodecane	*			*		
	n-Dodecane ^e	*			*		
Iso paraffins	Penta methyl heptane	*			*		
	Tri methyl heptane	*			*		
	Tri methyl hexane	*			*		
Cyclo paraffin	n- Butyl cyclohexane	*			*		
	cyclohexane	*			*		
Olefins	1-Undecene			*			*
	1-Dodecene			*			*
	1-Hexadecene			*			*
	Dimethyl hexene			*			*
Aromatic hydrocarbons	Iso butyl benzene	*			*		
	sec-Butyl benzene				*		
	1,2-Diethyl benzene		*			*	
	5% Naphthalene in n-Dodecane		*			*	
Aromatic Cycloparaffins	Tetrahydro naphthalene		*				*
	Indane			*			*

* Chemical degradation with 4 M HNO₃ - 0.1 M HNO₂ for 7 days at 343 K

* Radiolytic degradation using irradiated fuel element 8.4 Wh/l for 4 h at 333 K

* "Z" number is the number of moles of Zr retained per billion litre of solvent

* Stability = x ("Z" No. of pure compound / "Z" No. of n-dodecane)

* x < 2 (Stable-A), 2 < x < 8 (moderately unstable-B), x > 8 (highly unstable-C)

* e: olefin free

2.2.6. Complexing Ability of the Degradation Products of TBP

DBP is partially soluble in aqueous phase, depending on the composition of the two phases. It can form strong complexes with Pu(IV), Th(IV), Zr(IV), U(VI), Np(VI) and other cations, causing modification of An(IV) and An(VI) distributions [99, 110] and various problems in the PUREX process [80, 99]. The complexes formed with Zr(IV) can lead to the formation of stable

emulsions, called cruds [80, 99], and are present at the aqueous-organic interface and stabilized by micro solid particles. Complexes between DBP and Ln^{+3} have also been observed, but their low solubility leads to third phase which could be observed at low acidity (containing several species with different chemical forms) [111]. MBP has comparable complexing ability for metallic cations; however, because of its low formation yield and its high aqueous solubility, the damage is effectively more limited than for DBP.

2.2.7. Complexing Ability of Diluent Degradation Products

Removal of the diluent degradation products is difficult by aqueous alkaline treatments and they slowly accumulate and reduce the solvent's performance. The nitro alkanes are the most complexing in nature and nitro paraffins in the enol form lead to a synergistic extraction of Zr in the presence of TBP [96]. In the presence of nitric acid, nitro paraffins turn into hydroxamic acids. Experiments with the addition of hydroxamic acids in the range 10^{-4} - 10^{-3} M in $\text{HNO}_3/\text{TBP}/\text{OK}$ validated the strong correlation between the Zr retention in solvent and the presence of hydroxamic acid [112]. Ru-retention, which increases with hydroxamic acid concentration and ageing time of loaded organic phase [113] has been explained by a slow reaction between hydroxamic acid in the organic phase and RuNO species. This species can be extracted easily by TBP, thus causing Ru retention. Nevertheless, the presence and the amount of hydroxamic acid are controversial (concentrations between 10^{-8} and 4×10^{-4} M have been measured) [113, 114]. Carboxylic acids formed by the hydrolysis of nitro compounds have been identified to be complexing U(VI) [115].

2.2.8. Physiochemical Properties of Degradation Products

Degradation products can modify the physical properties of the chemical system and thereby disturb the hydrodynamic behaviour. Density and viscosity of the solvent (TBP-diluent-aqueous

phase) change insignificantly after irradiation, irrespective of the nature of the diluent (dodecane, mesitylene or CCl_4) [59, 94, 116]. For example, in 30 % TBP-n-dodecane- $0.56 \text{ mol L}^{-1} \text{ HNO}_3$ system, the density varied from 0.837 to 0.847 gm/cc after irradiation at 0.5 MGy and the viscosity changed from 1.96 to 2.38 mN s m^{-2} [59]. The effect of the aqueous phase on the interfacial tension of irradiated TBP-diluent/nitric acid systems was measured [116]. For neutral and acidic aqueous phases, the interfacial tension was similar to those of fresh and irradiated systems, but in contact with $0.6 \text{ mol L}^{-1} \text{ NaOH}$ solution (which is representative of alkaline treatment), a decrease in interfacial tension was observed. An increase in radiation dose resulted in the lowering of flash point and fire point of PUREX solvent [117]. For example, after an absorbed dose of 300 W h L^{-1} , the flash point of 30 % TBP-dodecane was about 16 K lower than that of fresh solvent.

2.2.9. Removal of Degradation Products From Spent Solvents

Several methods of regeneration such as chemical scrubbing treatment and regeneration of solvent by distillation have been employed to maintain the quality of PUREX process solvent [118]. Chemical methods are used to solubilize the degradation products in aqueous phase. Alkaline solutions remove acidic products (HDBP, H2MBP and long-chain carboxylic acids) from the solvent [99, 119-121]. A regular solvent scrubbing appears to be beneficial for long-term use of PUREX solvent, because it limits the increase of high molecular-weight phosphates (82). Distillation under reduced pressure allowed the separation of the TBP-diluent mixture components into three fractions: diluent, 60 % TBP and distillation residue. The first two fractions could be reused in the process, but the residue contained high molecular-weight degradation products, which were not eliminated by alkaline scrubbing. Distillation removed the degradation products that were responsible for poor hydrodynamic behaviour and for the

retention of radioactive products such as plutonium, zirconium and ruthenium [118]. Some researchers have studied the effect of treatment with solid sorbents. Activated alumina was found to be effective for secondary cleanup after alkaline scrubbing to remove the compounds responsible for the decrease of interfacial tension and the complexing of plutonium. Drying of the solvent was found to improve the capacity of activated alumina [56, 122, and 123].

2.3. Solubility of Tri Butyl Phosphate in Aqueous Phase

2.3.1. Introduction

In the PUREX process for the extraction of uranium and plutonium from the spent nuclear fuels [72], the solubility of TBP represents a balance between the highly polar oxygen atoms which favour miscibility with aqueous phase and the alkyl groups which are hydrophobic in nature and hence, show affinity towards the organic phase [124]. Owing to its mutual solubility in nitric acid, the aqueous stream leaving the extraction cycle contains a small amount of TBP, which is potentially hydrolysable to non-volatile species. When the aqueous solutions are concentrated at high temperatures in evaporators, exothermic reactions occur due to the decomposition of TBP-associated compounds. Removal of the dissolved TBP is thus, desirable in reprocessing plants for the safe operation of the plant. Several accidents which occurred during the heating of nitric acid solutions containing TBP have been reported in literature [125-127].

2.3.2. Solubility of TBP in Water and Acid

The solubility of pure TBP in water is about 0.4 g/l at 298 K [124] and in the aqueous solution of 3 M HNO₃ it is around 0.27 g/l [128]. When TBP is diluted with an inert matrix insoluble in water, the solubility of TBP decreases. Solubility of 30 % TBP diluted with n-dodecane in 3 M HNO₃ is reported to be 0.225 g/l. Baldwin et al. [129] had measured the solubility of TBP in water at temperatures from 276.4 to and reported that the solubility of TBP in water drops from

0.004 M at 276.4 K to 0.0011 at 323 K, with a value of 0.0016 M at 298 K. Presence of salts in the aqueous phase decreases the solubility markedly. In 2 M $\text{UO}_2(\text{NO}_3)_2$ solution, the solubility is only 1/20 of that in pure water [124]. Solubility of TBP and its decomposition products in HNO_3 system containing uranyl nitrate in the concentration range 200-1200 g/l at 298-401 K was studied by Usachev and Markov [130]. The solubility of TBP in aqueous solutions of plutonium nitrate ($\text{Pu}(\text{NO}_3)_2$) and in the highly radioactive liquid waste (HRLW) of PUREX process was investigated by Kuno et al. [131] and an empirical formulation was derived for the solubility of TBP in plutonium nitrate solutions in the concentration range of 0-0.1 M Pu and 1-8 M HNO_3 . Velavendan et al. [132] had investigated the effect of uranium and various fission product metal ions on the solubility of TBP in different concentrations of nitric acid (0–15.7 M) at room temperature. Studies on TBP solubility in H_2O and HNO_3 showed that solubility is low at room temperature (typical values reported were between 200–300 mg/L) and decreased with diluent to TBP ratio [124, 132]. It had also been shown that TBP solubility decreased with $[\text{HNO}_3]$ until 8–9 M, after which there was an increasing trend [124, 133]. Table II.2 provides some data on the solubility of TBP and TBP-diluent in water and HNO_3 at room temperature. The data in the Table indicates the effect of $[\text{HNO}_3]$ to be more pronounced than the effect of diluent.

Table. II.2. Solubility of TBP in nitric acid at 298 K

$[\text{HNO}_3]$	100 % TBP	30 %TBP	Reference
0 (H_2O)	0.45 g/L	0.30 g/L	137, 133
2 M	0.30 g/L	0.30 g/L	137
3 M	0.20 g/L	-	138

Baldwin et al. [129] reported that the solubility of TBP in the aqueous phase decreases with temperature, but other investigators observed that temperature increases the solubility of TBP [130, 131, and 134]. Studies on the solubility of TBP in aqueous solutions of uranyl or plutonium

nitrate showed that solubility decreases with metal ion concentration [124, 131, 135]. The solubility data of TBP in aqueous solutions of concentrated $\text{UO}_2(\text{NO}_3)_2$ and in 3 M HNO_3 listed in Table II.3 reveals that the solubility increases with temperature and decreases in the presence of metal ions, except at very high concentrations. A review article on the solubility of TBP-water by Usachev and Markov [130] confirmed the non-availability of reliable data above 333 K. A mathematical model was developed to correlate the solubility of TBP in the aqueous phase of TBP-dodecane- HNO_3 biphasic system with $[\text{HNO}_3]$ and $[\text{TBP}]$, but could not be applied to temperature because of lack of data [136].

Table II. 3. Dependence of solubility of TBP (g/L) in aqueous phase on temperature and metal ion concentration

T (K)	3 M HNO_3	0.7 M HNO_3 / 600g/L $\text{UO}_2(\text{NO}_3)_2$	1200 g/L $\text{UO}_2(\text{NO}_3)_2$	Reference
298	0.2	-	-	139
313	-	0.092	-	130
333	-	0.136	0.44	130
373	-	0.221	1.70	130
378	0.4	-	-	139
393	-	-	3.65	130

2.3.3. Estimation of TBP

Several analytical procedures have been reported in the literature for the quantitative determination of TBP in aqueous solutions. The availability of TBP containing ^{32}P (a convenient beta emitter) permits accurate analytical determinations. Titrimetry [140] and Complexo-gravimetry [141] are the methods best suited for the quantitative determination of TBP at higher concentrations, whereas advanced analytical techniques such as Spectrophotometry [142], Radiometry [143], AAS [144], ESI-MS [142], HPLC with RI [127], IC [145, 146] and GC [147, 148] have been used for the quantitative estimation of trace levels of TBP in aqueous solutions. Among these, spectrophotometry involving ammonium molybdate is the most commonly used method. Solvent extraction of ^{95}Zr , followed by radiometry was adopted to quantify TBP up to

100 ppm level with 10 % error [143]. Generally, dissolved TBP is determined by gas chromatography-flame ionization detector with the detection limit of 5 $\mu\text{g}/\text{ml}$ of TBP, after its extraction into an organic phase [147, 148]. It also shows good linearity up to 5 $\mu\text{g}/\text{ml}$ in n-dodecane, but below 5 $\mu\text{g}/\text{ml}$ reproducibility of the results was not very good due to thermal instability of TBP and the error was found to be varying between 5 and 30 %. The analytical techniques employed for the estimation of dissolved TBP, with working conditions and range of detection for trace amount of TBP in aqueous phase have been well documented by Ganesh et al. [149] and the details are reproduced in Table.II.4.

Table II.4. Working conditions and range for the estimation of TBP by different analytical procedures

Method	Sample pretreatment	Analytical conditions	Working range (ppm)	Error (%)
ESI-MS	1/10,000 dilution	Negative ionization mode	1000	1
Titrimetry	Pre-treatment with alcohol	Titration with alkali	mg	5-10
HPLC	Alkali treatment	Refractive index detector	2	13
IC	Organic phosphate to inorganic by digestion	Suppressed conductivity	1-10	2.6
GC	Extraction with organic solvent	FID detector	5-100	5-30
Extraction of ^{95}Zr	Extraction of ^{95}Zr	Radiometry	5-100	10
Spectrophotometry	Organic phosphate to inorganic by digestion	Spectrophotometer	0.1-1	2

2.4. Conclusions

Though enough literatures are available on the processes discussed above, still there are gap areas which have to be addressed and sometimes the reported literature by different authors are contradictory also. Hence some systematic studies were carried out, to be discussed in further chapters that add to literature already reported and have direct application in the reprocessing plant.

References

1. Kim, K.W., Kim, S.H., Lee, E.H., *J. Radioanal. Nucl. Chem.*, **260** (2004) 99
2. Orebough, E.G., Report-DP 1417 (1976)
3. Lawrence, F., Srinivasan, R., Mathews, T., Mallika, C., Palamalai, A., Koganti, S.B., Proc. DAE-BRNS Symp. Nuclear and Radiochemistry (NUCAR), Amritsar, India, March (2005)
4. Mattus, A.J., Lee, D.D., Dillow, T.T., Farr, L.L., Loghry, S.L., Pitt, W.W., Gibson, M.R., ORNL/TM-12245, 1993
5. Mattus, A.J., Walker, J.F., Youngblood, E.L., Farr, L.L., Lee, D.D., Dillow, T.T., Tieg, T.N., ORNL/TM-12631, 1994
6. Caime, W.J., Hoefner, S.L., Environmental technology development through industry partnership, Morgantown, WV, DOE/MC/32113--96/CO633, Oct. (1995)
7. Muguercia, I., Solomon, S., Ebadian, M.A., Proc. Internatl. Topical Meeting on Nuclear and Hazardous Waste Management (SPECTRM '96), **3** (1996) 2363
8. Taylor, P.A., Kurath, D.E., Guenther, R., ORNL Document -DOE/MWIP-10, 1993
9. Rogalla, F., Ravarini, P., Larminat, G.De., Coutelle, E., *J. Inst. Water Environ. Managem.*, **4** (1990) 319
10. Richard, Y., *J. Inst. Water Environ. Managem.*, **3** (1989) 154
11. Hirata, A., Meutia, A.A., *Water Sci. Technol.*, **34** (1996) 339
12. Vander Hoek, J.P., Hijnen, W.A.M., Van Bennekom, C.A., Mijnaerends, B.J., *Aqua* **41**(1992) 209
13. Clark, F.E., Francis, C.W., Stmhecker, J.W., Y/DA-1990, Union Carbide-Nuclear Division, Oak Ridge Y-12 Plant, Oak Ridge, Tenn., Nov. 1975
14. Clark, F.E., Napier, J.E., Bustamante, R.B., Y/DA-6967, Union Carbide-Nuclear Division, Oak Ridge Y-12 Plant, Oak Ridge, Tenn., April 1977
15. Schmieder, H., Kroebel, R., US Patent 4056482 (1977)
16. Suzuki, Y., Shimizu, H., Inoue, M., Fujiso, M., Shibuya, M., Iwamoto, F., Outou, Y., Ochi, E., Tsuyuki, T., Proc. 5th Internatl. Conf. Recycling, Conditioning and Disposal (RECOD-98) **3** (1998) 838
17. Satyabrata, M., Falix, L., Srinivasan, R., Mallika, C., Pandey, N.K., Koganti, S.B., 2nd ISEAC Triennial Internatl. Conf. on Electroanalytical Chemistry and Allied Topics (*ELAC-2007*), Shimla, March (2007) p. 483

18. Epstein, J.A., Levin, I., Raviv, S., *Electrochim. Acta*, **9** (1964) 1665
19. Shibuya, S., Suzuki, Y., and Fujiso, F., Proc. Internatl. Conf. Technol.Expo. on Future Nuclear Systems: Emerging Fuel Cycles and Waste Disposal Options (GLOBAL '93), Seattle, Washington, September (1993), p. 1315
20. Plieth, W.J., in 'Encyclopaedia of Electrochemistry of the Elements', Vol. 8, Bard, A.J. (Ed.), Marcel Dekker, New York (1978), Chapter 5
21. Baumgartner, F., Schmieder, H., *Radiochim.Acta*, **25** (1978) 191.
22. Palamali, A., Singh, N.S.B., Sampath, S., Srinivasan, R., Koganti, S.B., Proc. Nuclear and Radiochemistry Symposium (NUCAR-2003), BARC, Mumbai, 2003, p.191
23. DeGrott, M.T., Koper, M.T.M., *J. Electroanal. Chem.* **562** (2004) 81
24. Safonova, T.Y., Petrii, O.A., *J. Electroanal. Chem.* **448** (1998) 211
25. Pletcher, D., Poorabedi, Z., *Electrochim. Acta*, **40** (1995) 615
26. Li, H.L., Robertson, D.H., Chambers, J.Q., Hobbs, D.T., *J. Electrochem. Soc.*, **135** (1988) 1154
27. Bockis, J.O.M., Kim, J., *J. Appl. Electrochem.*, **27** (1997) 623
28. Cattarin, S., *J. Appl. Electrochem.*, **22** (1992) 1077
29. Li, H.L., Chambers, J.Q., Hobbs, D.T., *J. Appl. Electrochem.*, **18** (1988) 454
30. Kim, K.W., Lee, E.H., Choi, I.K., Yoo, J.H., Park, H.S., *J. Radioanal. Nucl. Chem.*, **245** (2000) 301
31. Kerkeni, S., Pitara, E.L., Barbier, J., *Catalysis Today*, **554** (2002) 35
32. Dima, G.E., De Vooy, A.C.A., Koper, M.T.M., *J. Electroanal. Chem.*, **562** (2003) 15
33. Mallika, C., Keerthika, B., Kamachi Mudali, U., *Electrochim. Acta*, **52** (2007) 6656
34. Huang, Y.H., Zhang, T.C., *Water Research*, **38** (2004) 2631
35. Chebotareva, N., Nyokong, T., *J. Appl. Electrochem.*, **27** (1997) 975
36. Freeman, E.S., *J. Phys. Chem.*, **60** (1956) 1487
37. Kadner, M., Halwachs, W., Heiduk, J., DE 3,238,961 (G21F009-08), *Chem. Abstr.* **101** (1985) 139531
38. Johnson, A.J., Arnold, P.M., RFP-3899, Rockwell International, Golden, Colorado, 1986
39. Jones, M.N., *Water Res.*, **18** (1984) 643
40. Gaugush, R.F., Heath, R.T., *Water Res.*, **18** (1984) 449
41. Morris, A.W., Riley, J.P., *Anal. Chim. Acta*, **29** (1963) 272

42. Vogel, A.I., A Textbook of Quantitative Inorganic Analysis, 3rd ed., Longmans, 1961
43. Chow, T.J., Johnstone, M.S., *Anal. Chim. Acta*, **27** (1962) 441
44. Hendriksen, A., *Analyst*, **90** (1965) 83
45. Mullin, J.B., Riley, J.P., *Anal. Chim. Acta*, **12** (1955) 464
46. Linder, V., Kirk-Othmer's Encyclopedia of Chemical Technology, 4th ed., **10** (1991) 48
47. Kondo, Y., Kubota, M., *J. Nucl. Sci. Technol.*, **29** (1992) 140
48. Kim, K.W., Kim, S.H., Lee, E.H., *J. Radioanal. Nucl. Chem.*, **260** (2004) 99
49. Raw, C.J.G., Friedrich, J., Perrino, F., Jex, G., *J. Phys. Chem.*, **82** (1978) 1952
50. Lee, E.H., Hwang, D.S., Kim, K.W., Kwon, S.G., Yoo, Y.H., *J. Korean Ind. Eng. Chem.*, **8** (1997) 132
51. Lee, E.H., Hwang, D.S., Kim, K.W., Shin, Y.J., Yoo, j.H., *J. Korean Ind. Eng. Chem.*, **6** (1995) 882
52. Healy, T.V., *J. Appl. Chem.*, **8** (1958) 553
53. Kumar, S.V., Nadkarni, M.N., Mayankutty, P.C., Pillai, N.S., Shinde, S.S., Report BARC-781, 1974
54. Hesford, E., Mc Kay, H.A.C., *J. Inorg. Nucl. Chem.*, **13** (1960) 156
55. Nowak, Z., Nowak, M., Seydel, A., *Radiochem. Radioanal. Lett.*, **38** (1979) 343
56. Neace, J.C., *Sep. Sci. Technol.*, **18** (1983) 1581
57. Hardy, C.J., Scargill, D. *J. Inorg. Nucl. Chem.*, **17** (1961) 337
58. Smith, D.N., Edwards, H.G., Hugues, M.A., Courtney, B., *Sep. Sci. Technol.*, **32** (1997) 2821
59. Tripathi, S.C., Ramanujam, A., *Sep. Sci. Technol.*, **38** (2003) 2307
60. Tripathi, S.C., Bindu, P., Ramanujam, A., *Sep. Sci. Technol.*, **36** (2001) 1463
61. Moore, J.G., Crouse, D.J., ORNL-4618, Nov. 1970
62. Charles, A., Blake, Jr., Schmitt, J.M., ORNL, CONF-650918-5, 1965
63. Egorov, G.F., Afanas'ev, O.P., Zilberman, B.Y., Mikhailov, V., *Radiochem.* **44** (2002) 151
64. Ladrielle, T., Wanet, P., Lemaire, D., Apers, D.J., *Radiochem. Radioanal. Lett.*, **59** (1983) 355
65. Lloyd, N.H., Fellows, R.L., ORNL/ TM-9565, June 1985
66. Buchholz, B.A., Nunez, L., Vandergrift, G.F., *Sep. Sci. Technol.*, **31** (1996) 2231
67. Buchholz, B.A., Nunez, L., Vandergrift, G.F., ANL/CMT/CP-82400 (1994)
68. Bibler, N.E., *Inorg. Nucl. Chem.*, **34** (1972) 1417

69. Huggard, A.J., Warner, B.F., *Nucl. Sci. Eng.*, **17** (1963) 638
70. Wilkinson, R.W., Williams, T.F., *J. Chem. Soc.*, (1961) 4098
71. Chiariza, R., Horwitz, E.P., *Solvent. Extr. Ion Exch.*, **8** (1990) 907
72. Schulz, W.W., Navratil, J.D., *Science and Technology of Tributyl Phosphate*, Vol. 1, CRS Press Inc., Boca Raton (1984) Chapter 7
73. Davis, W. Jr., Radiolytic behavior, in *Science and Technology of Tributyl Phosphate, Vol I, Synthesis, Properties, and Analysis*; Schulz, W.W., Navratil, J.D., Talbot, A.E.(Eds.); CRC Press: Boca Raton, FL (1984) 221
74. Tahraoui, A., Morris, J.H., *Sep. Sci. Technol.*, **30** (1995) 2603
75. Tallent, O.K., Mailen, J.C., Pannell, K.D., ORNL /TM - 8814, Feb. (1984)
76. Tallent, O.K., Mailen, J.C., CONF-21056-8, ORNL, (1993)
77. Lane, E.S., *Nucl. Sci. Eng.*, **17** (1963) 620
78. Lesage, D., Virelizier, H., Jankowski, C.K., Tabet, J.C., *Spectroscopy*, **13** (1997) 275
79. Lamouroux, C., Virelizier, H., Moulin, C., Jankowski, C.K., *J. Chromatogr.* **91**(2001)261
80. Lesage, D., Virelizier, H., Tabet, J.C., Jankowski, C.K., *Rapid Commun. Mass Spectrom.*, **15** (2001) 1947
81. Tripathi, S.C., Ramanujam, A., Gupta, K.K., Bindu, P., *Sep. Sci. Technol.*, **36** (2001) 2863
82. Tripathi, S.C., Sumathi, S., Ramanujam, A., *Sep. Sci. Technol.*, **34** (1999) 2887
83. Burr, J.G., *Radiat. Res.*, **8** (1958) 214
84. Burger, L.L., McClanahan, E.D., *Ind. Eng. Chem.*, **50** (1958) 153
85. Tashiro, Y., Kodama, R., Sugai, H., *Nucl. Technol.*, **129** (2000) 93
86. Greenfield, B.F., Hardy, C.J. J., *Inorg. Nucl. Chem.*, **21**(1961) 359
87. Brodda, B.G., Heinen, D., *Nucl. Technol*, **34** (1977) 428
88. Kuno, Y., Sato, S., Masui, J., Kashimura, T., Shimizu, Koyama, K., PNC Report, PNC TN8410 95-061 (1995)
89. Ladrielle, T., Wanet, P., Lemaire, D., Apers, D., *J. Radiochem. Radioanal. Lett.*, **59** (1983) 355
90. Kulikov, I.A., Kermanova, N.V., Vladimirova, M.V., *Soviet Radiochem.*, **27** (1985) 58
91. Adamov, V.M., Andreev, V.I., Belyaev, B.N., Markov, G.S., Polyakov, M.S., Ritori, A.E., Yu Shil'nikov, A.Y., *Kernteknik*, **55** (1990) 133
92. Barelko, E.V., Solyanina, I.P., Babakina, G.S., *Soviet Radiochem.*, **18** (1976) 573

93. Barelko, E.V., Solyanina, I.P., *Atomic Energy*, **38** (1975) 25
94. Nowak, Z., *Nukleonika*, **22** (1977) 155
95. Hromadova, M., C̣ech, R., Rajec, P., *J. Radioanal. Nucl. Chem.*, **163** (1992) 99
96. Blake, C.A., Davis, W., Schmitt, J.M., *Nucl. Sci. Eng.*, **17** (1963) 626
97. Bellido, A.V., Rubenich, M.N., *Radiochim. Acta*, **36** (1984) 61
98. Barelko, E.V., Solyanina, I.P., Tsvetkova, Z.I. *Atomic Energy* **21**(1966) 946
99. Burger, L.L., *Progre. in Nuclear Energy Series III*, **2** (1958) 307
100. Canva, J., Pages, M., *Radiochim. Acta*, **4** (1965) 88
101. Egorov, G.F., Ilozhev, A.P., Nikiforov, A.S., Smelov, V.S., Shevchenko, V.B., Schmidt, V.S., *Soviet Atomic Energy*, **47** (1979) 591
102. Adamov, V.M., Andreev, V.I., Belyaev, B.N., Lyubtsev, R.I., Markov, G.S., Polyakov, M.S., Ritori, A.E., Yu Shil'nikov, A., *Soviet Radiochem.*, **29** (1987) 775
103. Vandegrift, G.F., Diluent for TBP extraction systems, in *Science and Technology of Tributyl Phosphate, Vol. I, Synthesis, Properties, and Analysis*; Schulz, W.W., Navratil, J.D., Talbot, A.E. (Eds.); CRC Press: Boca Raton, FL (1984) pp.69–136
104. Renard, E.V., Pyatibratov, Y.P., Neumoev, N.V., Vhizhov, A.A., Kulikov, I.A., Gol'dfarb, Y.Y., Sirotkina, I.G., Semenova, T.I., *Soviet Radiochem.*, **30** (1988) 734
105. Burton P. Dennis, Report DP-577, April 1961
106. Krishnamurthy, M.V., Sampathkumar, R., *J. Radioanal. Nucl. Chem. Lett.*, **166** (1992) 421
107. Adamov, V.M., Andreev, V.I., Belyaev, B.N., Markov, G.S., Polyakov, M.S., Ritori, A.E., Yu Shil'nikov, A.Y. *Soviet Radiochem.*, **34** (1992) 150
108. Nowak, Z., Nowak, M., *Radiochem. Radioanal. Lett.*, **14** (1973) 161
109. Kurtekov, M.M., Pushlenkov, M.F., Zil'berman, B.Y., Gryaznova, A.S., Efremova, T.I., *Soviet Radiochem.*, **9** (1967) 32
110. May, I., Taylor, R.J., Wallwork, A.J., Hasting, J.J., Fedorov, Y.S., Zilberman, B.Y., Mishin, E.N., Arkhipov, S.A., Blazheva, I.V., Poverkova, L.Y., Livens, F.R., Charnock, J.M., *Radiochim. Acta*, **88** (2000) 283
111. Zhang, P., Kimura, T., *Solvent Extr. Ion Exch.*, **24** (2006) 149
112. Healy, T.V., Pilbeam, A., Proc. Internatl. Solvent Extraction Conference ISEC'74, Lyon, France, Sept.(1974), Vol. 1, 459–467
113. Huang, H.X., Zhu, G.H., Hou, S.B., *Radiochim. Acta*, **46** (1989) 159

114. Di Furia, F., Modena, G., Scrimin, P., Gasparini, G.M., Grossi, G., *Sep. Sci. Technol.* **17** (1982) 1451
115. Ishihara, T., Ohwada, K., *J. Nucl. Sci. Technol.*, **3** (1966) 20
116. Nowak, Z., Nowak, M., *Nukleonika*, **26** (1981) 19
117. Ikeda, H., *J. Nucl. Sci. Technol.*, **41** (2004) 534
118. Ginisty, C., Guillaume, B., *Sep. Sci. Technol.*, 25 (1990) 1941
119. Sugai, H., *J. Nucl. Sci. Technol.*, **29** (1992) 445
120. Sugai, H., Munakata, K., *Nucl. Technol.*, **99** (1992) 235
121. Araujo, B.F., Matsuda, H.T., Kuada, T.A., Araujo, J.A., *J. Radioanal. Nucl. Chem. Lett.*, **166** (1992) 75
122. Mailen, J.C., *Nucl. Technol.*, **83** (1988) 182
123. Reif, D.J., *Nucl. Technol.*, **83** (1988) 190
124. Burger, L.L., Forsman, R.C., Report HW 20936 (1951)
125. Sege, G., Report HW-28690 (1953)
126. Biplab, D., Mondal, P., Kumar Shekhar, *J. Radioanal. Nucl. Chem.*, **288** (2011) 641
127. Dicholkar, D.D., Patil, L.K., Gaikar, V.G., Shekhar, K., Kamachi Mudali, U., Natarajan, R., *J. Radioanal. Nucl. Chem.*, **289** (2011) 545
128. Leroy, L., ORNL-TR-4344 (1967)
129. Baldwin, W.H., Higgins, C.E., Soldano, B.A., *J. Phys. Chem.*, **63** (1959) 113
130. Usachev, V.N., Markov, G.S., *Radiokhimiya*, **46** (2004) 471
131. Kuno, Y., Hina, T., Akiyama, T., Matsui, J., *J. Nucl. Sci. Tech.*, **30** (1993) 567
132. Velavendan P., Ganesh S., Pandey N.K., Geetha, R., Ahmed, M.K., Kamachi Mudali, U., Natarajan, R., *J. Radioanal. Nucl. Chem.*, (2012); DOI 10.1007/s10967-012-1945-1
133. Kumar, S.; Koganti, S.B., *Nucl. Technol.*, **129** (2000) 279
134. Usachev, V.N.; Markov, G.S., *Radiochem.*, **45** (2003)1
135. Harmon, H.D.; Hyder, M.L.; Tiffany, B.; Gray, L.W.; Soltys, P.A., SRL Report, DP-1418 (1976)
136. Kumar, S.; Koganti, S.B., *Ind. J. Chem. Technol.*, **6** (1999) 90
137. Ochsenfeld, W., Schon, J., Smits, D., Tullius, E., *J. Nucl. Engrs. Scientists*, **18** (1976) 258
138. Davis, W., Mrochek, J., Judkins, R.R., *J. Inorg. Nucl. Chem.*, **32** (1970) 1689
139. Davis, W.J., Kibbey, A.H., Report, ORNL-TM- 3062 (1970)

140. Krishnamurthy, M.V., Sampathkumar, R., *J. Radioanal. Nucl. Chem.*, **166** (1992) 421
141. Mamadal, S., Kundu, D., *J. Ind. Chem. Soc.*, **82** (2005) 1030
142. Lamouroux, C., Virelizier, H., Moulin, C., Tabet, J.C., Jankowski, C.K., *Anal. Chem.*, **72** (2000) 1186
143. Ishimori, T., Veno, K., *Talanta*, **16** (1969) 613
144. Christian, G.D., Feldman, F., *Anal. Chem. Acta*, **40** (1968) 173
145. Ruiz-Calero, V., Galceran, M.T., *Talanta*, **66** (2005) 376
146. Leo, M.L., Nollet, Handbook of water analysis (2007), p 284
147. Ali, M.A., Al-Ani, A.M., *Analyst*, **116** (1991) 1067
148. Kuno, Y., Hina, T., Akiyama, T., Matsui, M., *J. Chromatog.*, **537** (1991) 489
149. Ganesh, S., Velavendan, P., Pandey, N.K., Ahmed, M.K., Kamachi Mudali, U., Natarajan, R., *J. Radioanal. Nucl. Chem.*, **293** (2012) 529

5. DEVELOPMENT OF A CONTINUOUS HOMOGENEOUS PROCESS FOR DENITRATION BY TREATMENT WITH FORMALDEHYDE

5.1. Introduction

Removal of nitric acid from the high level liquid waste (HLLW) of nuclear fuel reprocessing plants is warranted for simplifying the procedure for waste fixing [1]. Nitric acid reduction to gaseous products is an attractive way to accomplish denitration. Chemical denitration using citric acid, tartaric acid and EDTA are reported [2] to be effective in the presence of radiation. Simple, efficient and rapid reduction of nitric acid is achieved in the chemical method by means of a homogeneous reaction with formaldehyde [3-8] or formic acid [1, 9-13]. The main advantage of denitration using HCHO/HCOOH is that, it leaves no residual chemicals and the gaseous products NO_2 , NO and CO_2 are removed automatically. Formic acid reacts with nitric acid in a way similar to that of the reaction of HCHO with HNO_3 , but proceeds with a slower rate. The denitration by formic acid shows a complex nature. It occurs not through a direct reaction between nitric acid and formic acid, but through the mutual reactions of several intermediates generated from nitric acid and formic acid [1]. It is known that when both the concentrations of nitric acid and formic acid are not sustained properly during denitration, the decomposition rate of nitric acid becomes slow or the total acidity level in the solution gets high at the final stage. Denitration using formaldehyde possess the advantage of low chemical cost, easy recoverability of nitric acid and in case of waste treatment, the production of a solution relatively low salt concentration suitable for fission product recovery or ultimate disposal. Though the reaction of HNO_3 with HCHO is fast, it is initiated after a certain induction period during which the auto catalytic generation of HNO_2 takes place, beyond which the reaction proceeds rapidly. The delay

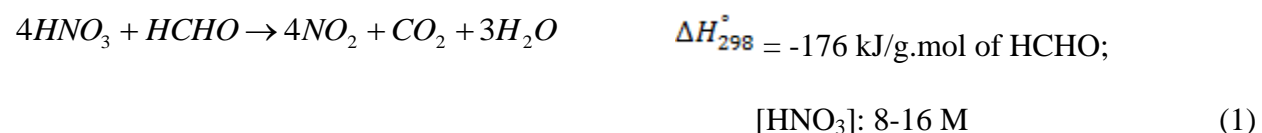
in induction period leads to uncontrollable process conditions due to pressurization of the system, which demands safety precautions. Literature survey reveals that the induction period is dependent on the concentration of nitric acid, nitrite content and temperature. It can be considerably minimized or suppressed either by passing gaseous NO_2 through the acid prior to the addition of HCHO [4] or by carrying out the reaction at a temperature above 98°C (boiling temperature of HCHO). Presence of cations such as ferric and uranyl ions increases the rate of reaction thereby decreasing the induction period [3].

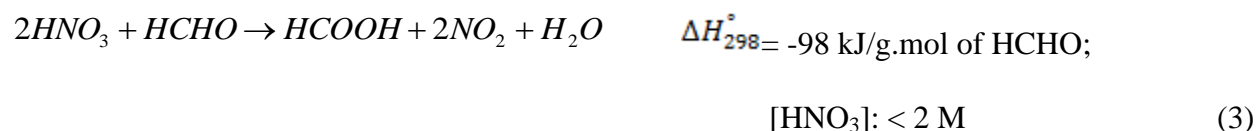
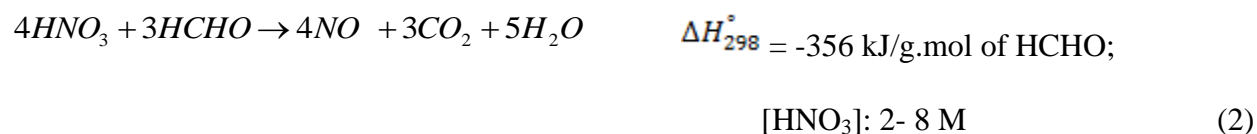
5.2. Scope of the work

In the present work, a homogeneous denitration process in continuous mode with formaldehyde, which offers safety and is governed by controlled kinetics has been demonstrated on a laboratory scale. The induction period before commencement of the reaction was eliminated by maintaining the reaction mixture at the pre-determined temperature of 98°C . Based on the results accrued from lab scale experiments, the equipment for pilot plant scale operation was designed, the reaction efficiency for continuous denitration was determined and the investigation of nitric acid destruction was extended to full-scale plant capacity. The role of organics in the waste in foaming up of the reaction mixture was also studied using a synthetic waste solution. The effect of reflux time on destroying residual formaldehyde and formic acid in the reaction mixture after reaching the acidity of 2 M during denitration was also investigated.

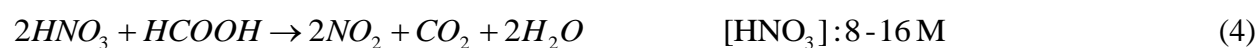
5.3. Mechanism of denitration using HCHO

The reaction between HNO_3 and HCHO has been studied extensively, which is mainly influenced by the concentration of nitric acid [4, 6].





Formic acid produced in reaction (3), will also react with nitric acid in a manner similar to Eqs. (1) and (2).



Equations (1), (2), (4) and (5) are interlinked by the reaction



At nitric acid concentrations below 2 M, appreciable amount of the intermediate compound, formic acid is produced and the rate of reaction is governed by reaction (3). Further addition of HCHO to dilute nitric acid causes the buildup of formic acid as the rate of formation of HCOOH exceeds the rate of destruction of HNO₃. The formic acid produced in reaction (3) also destroys nitric acid as per reaction (4). However, the destruction rate for reaction (4) is only moderate in the homogeneous denitration.

5.4. Lab scale experiments

5.4.1. Batch Mode Denitration

Denitration experiments in batch mode were conducted on a laboratory scale initially using the experimental set up shown in Fig. V.1. A 2.5 litre five necked glass reactor vessel attached to a reflux water condenser was placed on an electric heating mantle and the accuracy of the temperature was maintained within $\pm 1^\circ\text{C}$ with the aid of a PID temperature controller.

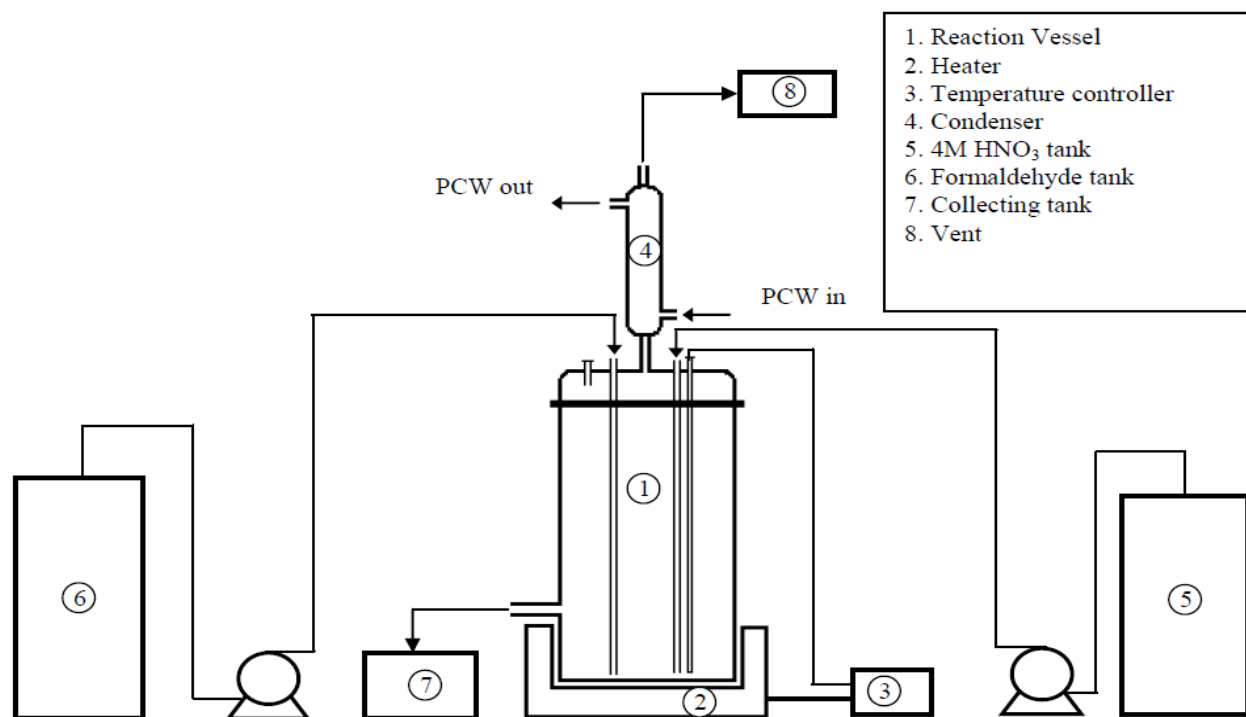


Fig. V.1. Schematic diagram of lab scale experimental set up

In the batch mode experiments, a fixed volume of 500 ml of 4 M nitric acid was taken in the reactor vessel. The temperature at which the reaction starts instantaneously was determined by heating the acid in the reactor vessel to different temperatures viz. 75, 85, 95 and 98°C and feeding methanol stabilized HCHO (37-41 % w/V; AR grade) by means of a fixed displacement pump after the corresponding temperature was attained, such that the induction period can be minimised. The results are given in Table V.1.

Table V.1. Dependence of temperature on the initiation of reaction

Commencement of reaction					
75°C	85°C	90°C	95°C	98°C	100°C
No reaction up to 1 h	No reaction up to 1 h	No reaction up to 1 h	Reaction after 20 min	Reaction after 1 min	Reaction after 40 sec

It is evident from the Table that commencement of denitration reaction is instantaneous above

98°C. Subsequently, all the batch and continuous experiments were carried out in the temperature range 98-100°C.

The induction period is characterized by some successive visual changes, as shown in Fig. V.2, prior to the starting of vigorous reaction. Initially, the reaction mixture turns to pale yellow in colour, especially at the top surface which gradually propagates to the liquid reaction mixture. Once a dark zone is formed, the temperature rises and simultaneously denitration starts vigorously liberating reddish brown fumes.

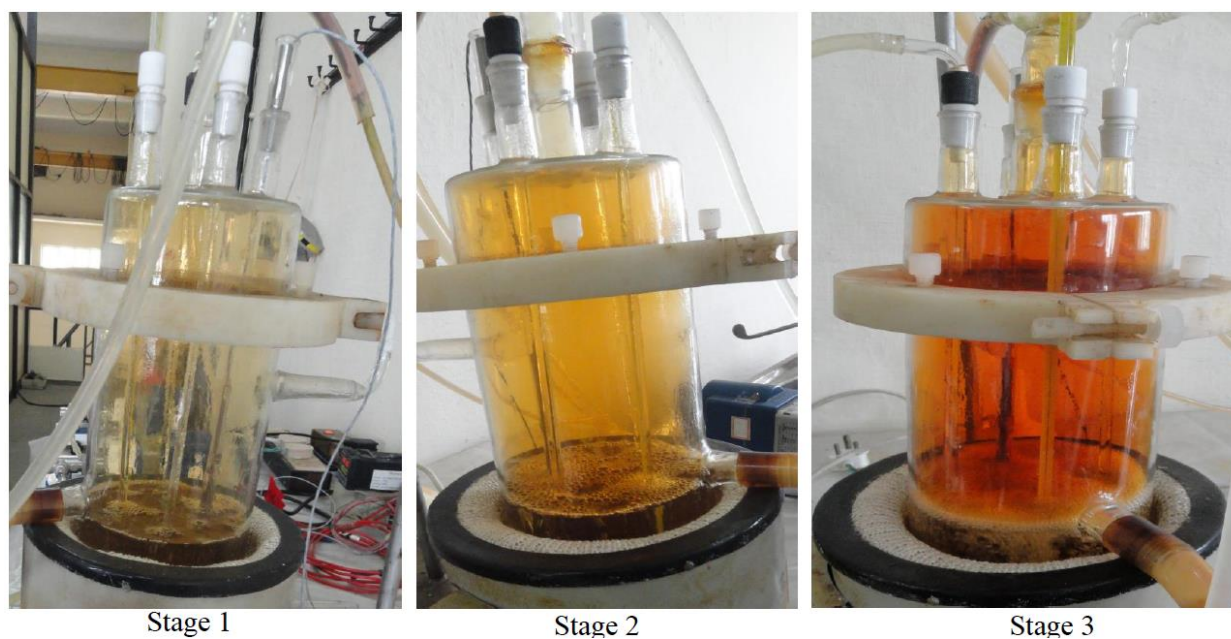


Fig. V.2. Visualization of induction period

The phenomena occurring in the reactor may be as follows:

Owing to the generation of NO_2 along with HNO_2 , the mixture turns yellow and due to the slight solubility of NO_2 , the yellow colour develops mainly at the upper part of the reactor. N_2O_3 may also get generated in the reaction mixture as per the following equation which is an exothermic reaction.



The heat generated during the above reaction accelerates the auto catalytic production of NO_2 and N_2O_3 , which are released from the reactor giving red fumes.

5.4.2. Continuous Mode Denitration with Pure Nitric Acid and Simulated Waste Solution

For the continuous experiments, a fixed volume of 1.2 L of 4 M nitric acid was taken in the reactor vessel. The reaction mixture of 4 M HNO_3 and HCHO were simultaneously dropped into the nitric acid placed in the reactor at 98°C . The feed rate of HNO_3 was kept constant as 0.12 L/h using a metering device. Formaldehyde was fed at flow rates in the range 0.06 - 0.30 L/h. Samples were periodically removed for estimating total acidity, concentration of nitric acid, residual formic acid and formaldehyde.

A 25 component (fission and corrosion product elements) – simulated HLLW envisaged in the reprocessed waste of FBR spent fuel with a burn-up of 150 GWd/ton and after a cooling period of 1 year was prepared in 4 M HNO_3 and its rate of denitration was computed in order to find out the effect of metal ions on acid killing. The chemical form of the elements used for the preparation and their concentration in the simulated waste solution are listed in Table V.2.

Table V.2. Chemical composition of fission and corrosion product elements used for simulated waste solution

Element	Concentration in the waste (g/L)	Chemical form of the element used	Quantity (g/L)
*Ag	0.097	AgNO_3	0.153
Ba	0.485	$\text{Ba}(\text{NO}_3)_2$	0.922
Cd	0.046	$\text{Cd}(\text{NO}_3)_2$	0.097
Ce	0.769	$\text{Ce}(\text{NO}_3)_3 \cdot 6\text{H}_2\text{O}$	2.383
Cs	1.405	CsNO_3	2.061
Eu	0.051	$\text{Eu}(\text{NO}_3)_3 \cdot 6\text{H}_2\text{O}$	0.151
Gd	0.032	$\text{Gd}(\text{NO}_3)_3 \cdot 6\text{H}_2\text{O}$	0.091
La	0.418	$\text{La}(\text{NO}_3)_3 \cdot 6\text{H}_2\text{O}$	1.300

Mo	1.115	$(\text{NH}_4)_2\text{MoO}_4 \cdot 4\text{H}_2\text{O}$	2.927
**Nd	1.186	$\text{Nd}(\text{NO}_3)_3 \cdot 6\text{H}_2\text{O}$	3.868
Pd	1.070	$\text{Pd}(\text{NO}_3)_3$	2.317
Pr	0.410	$\text{Pr}(\text{NO}_3)_3$	0.951
Rb	0.070	Rb_2CO_3	0.181
Rh	0.350	$\text{Rh}(\text{NO}_3)_3 \cdot 2\text{H}_2\text{O}$	1.105
Ru	1.086	$\text{RuCl}_3 \cdot x\text{H}_2\text{O}$	3.085
Sb	0.017	Sb_2O_3	0.041
Sm	0.342	$\text{Sm}(\text{NO}_3)_3 \cdot 6\text{H}_2\text{O}$	1.010
Sr	0.146	$\text{Sr}(\text{NO}_3)_2$	0.352
Te	0.160	$\text{H}_6\text{O}_6\text{Te}$	0.564
Zr	0.900	$\text{Zr}(\text{NO}_3)_4 \cdot x\text{H}_2\text{O}$	2.479
Fe	0.084	$\text{Fe}(\text{NO}_3)_3 \cdot 9\text{H}_2\text{O}$	0.610
Cr	0.011	$\text{Cr}(\text{NO}_3)_3 \cdot 9\text{H}_2\text{O}$	0.085
Ni	0.026	$\text{Ni}(\text{NO}_3)_2 \cdot 6\text{H}_2\text{O}$	0.126
Ca	0.637	$\text{Ca}(\text{NO}_3)_2$	2.608
Al	0.062	$\text{Al}(\text{NO}_3)_3 \cdot 9\text{H}_2\text{O}$	0.862

*Ag is used as mediated redox catalyst for the electro-oxidative dissolution of Pu rich oxide fuel

** 8 g/L of Nd in excess was added to simulate trans-uranic elements (Np, Am and Cm)

During the extraction of U and Pu from the aqueous solution in 4 M nitric acid using 30 % tributyl phosphate in n- dodecane (TBP-DD), the solubility of TBP represents a balance between the highly polar oxygen atoms which favour miscibility with aqueous phase. Owing to its mutual solubility with nitric acid, the aqueous stream leaving the extraction cycle contains a small amount of TBP. The aqueous solubility of TBP in HLLW in 4 M HNO_3 is around 220 ppm. Hence, to simulate the exact plant condition, denitration was also carried out with simulated waste solution in 4 M HNO_3 containing 220 ppm dissolved TBP at the optimized feed flow conditions.

5.4.3. Estimation of HNO₃, HCOOH and HCHO

5.4.3.1. Analysis of a mixture of nitric and formic acids

A mixture of two acids can be estimated with a precision of a few parts per thousand, provided the dissociation constants of the two acids differ by at least 3 to 4 orders of magnitude. The K_a (HNO₃) is $10^{1.3}$ and that of HCOOH is $10^{-3.75}$; they differ by more than 10^4 . The total acidity (HNO₃ + HCOOH) was estimated by acid-base titration against standardised NaOH solution using a Metrohm auto titroprocessor and the individual acidity of HNO₃ and HCOOH (one of the reaction intermediates) was estimated by exploiting the variation in the pH of strong and weak acids at the neutralization point.

5.4.3.2. Analysis of formaldehyde

A potentiometric titration based analytical method using hydrazine was developed to determine the concentration of unreacted formaldehyde present in the reaction mixture during denitration. 20 ml of 0.4 M hydrazine hydrate solution was taken in a dry beaker whose pH was ~ 9.5 and the pH was adjusted to 5.6 (as reference) using a combined glass electrode in an auto titroprocessor by the addition of dilute nitric acid(0.025M). The corresponding volume added (V_1) was recorded. 0.2 ml of the aliquot containing the intermediate products was added. Hydrazine forms strong complex with formaldehyde as well as nitric acid. Owing to the presence of acid as well as formaldehyde in the aliquot, the concentration of free hydrazine decreases which has to be titrated against dilute nitric acid. Finally the pH was brought back to 5.6 by the addition of dilute nitric acid. The titre value (V_2) was recorded. From the difference in titre values ($V_1 - V_2$), the strength of was estimated. The free acidity measured is subtracted from the total concentrations of (HNO₃ + HCHO) to give individual HCHO concentration. The error involved in determining the residual HCHO and HCOOH in the product solution was estimated to be $\pm 3\%$.

5.4.4. Optimization of Feed Rate of HCHO

Continuous denitration experiments were conducted initially using the apparatus shown in Fig. V.1 with different feed rates of HCHO starting from 0.06 to 0.3 L/h for the constant flow of 1.2 L/h of 4 M nitric acid. The results are tabulated in Tables V.3 to V.7.

Table V.3. Process conditions and concentrations of acid and HCHO in the product solution during and after terminating a denitration experiment, Feed rates of (a) HCHO: 0.06 L/h and (b) HNO₃: 1.2 L/h

Time/h	Temperature/(°C)	[HCHO]/M	[HCOOH]/M	[HNO ₃]/M	Total acidity/M
0	98	13.10	0	4.01	4.01
1	98	0.38	0.16	3.62	3.78
2	98	0.27	0.15	2.85	3.00
3	98	0.25	0.16	2.36	2.52
4	98	0.27	0.09	2.12	2.21
24	32	0.19	0.06	1.82	1.88

When the total acidity of the product solution reaches about 2 M, the concentration of formic acid, which is an intermediate in the oxidation of HCHO, starts to build up. Formic acid being corrosive in nature will attack the stainless steel reactor vessel in the plant. Hence, the reaction was stopped when the total acidity of the product was approaching 2 M. Since the reaction of formic acid with nitric acid is rather slow, traces of residual HCHO and HCOOH will be present in the product. For the purpose of eliminating these, the reaction mixture was refluxed at the temperature of reaction for about 2 h. The product was analysed after one day to estimate the amount of HCHO and HCOOH for the purpose of ascertaining that no reaction will initiate on its own, while the denitrated waste solution is stored in waste vault tanks.

Table V.4. Concentrations of acid and HCHO in the product solution during and after terminating a denitration experiment; Feed rates of (a) HCHO: 0.12 L/h and (b) HNO₃: 1.2 L/h

Time/h	Temperature/(°C)	[HCHO]/M	[HCOOH]/M	[HNO ₃]/M	Total acidity/M
0	98	13.10	0	4.01	4.01
1	98	1.21	0.30	2.01	2.31
2	98	0.87	0.27	1.82	2.09
3	98	0.91	0.26	1.69	1.95
4	98	0.92	0.27	1.58	1.85
24	32	0.41	0.21	1.22	1.43

During the above experiment, as the flow rate of the reductant (HCHO) was slightly higher, the denitration could be achieved at a faster rate; but the accumulation of the residual formaldehyde went on increasing, which should be eliminated completely, for the process to be safe in the plant.

Table V.5. Results of the denitration experiment with feed rates of (a) HCHO: 0.18 L/h and (b) HNO₃: 1.2 L/h

Time/h	Temperature/(°C)	[HCHO]/M	[HCOOH]/M	[HNO ₃]/M	Total acidity/M
0	98	13.10	0	4.01	4.01
1	98	0.79	0.33	1.83	2.16
2	98	0.67	0.29	1.58	1.87
3	98	0.69	0.30	1.39	1.69
4	98	0.73	0.28	1.32	1.50
24	31	0.26	0.16	0.96	1.12

As per literature, when the concentration of nitric acid is 4 M, denitration occurs according to Eq. (2), which corresponds to destruction of 4 mole of HNO₃ by 3 mole of formaldehyde. This ratio of 4:3 has been validated in the present work by varying the feed rate of HCHO for a constant volume of HNO₃ in the denitration by batch mode, as discussed in Section 4.a. Hence, further experiments were carried out with the feed rates of HCHO and HNO₃ as 0.24 and 0.30

L/h respectively (corresponding to 3: 4 mole ratio). Nevertheless, the trend followed in all the experiments was more or less identical and the rate of denitration did not vary much.

Table V.6. Process conditions and analytical results from the product solution during and after terminating a denitration experiment; Feed rates of (a) HCHO: 0.24 L/h and (b) HNO₃: 1.2 L/h

Time/h	Temperature/(°C)	[HCHO]/M	[HCOOH]/M	[HNO ₃]/M	Total acidity/M
0	98	13.10	0	4.01	4.01
1	98	0.43	0.31	1.66	1.97
2	98	0.31	0.28	1.27	1.55
3	98	0.41	0.29	1.15	1.44
4	98	0.40	0.31	1.12	1.43
24	32	0.03	0.16	0.77	0.93

Table V.7. Results of acid killing experiment with the feed rates as (a) HCHO: 0.30 L/h and (b) HNO₃: 1.2 L/h.

Time/h	Temperature/(°C)	[HCHO]/M	[HCOOH]/M	[HNO ₃]/M	Total acidity/M
0	98	13.10	0	4.01	4.01
1	98	0.57	0.56	1.69	2.25
2	98	0.60	0.37	1.26	1.63
3	98	0.63	0.40	1.18	1.58
4	98	0.64	0.46	1.17	1.63
24	30	0.23	0.32	0.74	1.06

The results given in Tables V. 3 -7 indicate that the destruction rate not only depends on the feed rates, but also on capacity of the reactor and on the residence time of the reactants in the vessel, since at lower feed rates the reduction rates were less due to insufficient quantity of the reductant and at very high feed rates the reaction rates decreased apparently owing to insufficient residence time of the reactants in the vessel. These results also reveal that the destruction of nitric acid is very rapid initially and slows down when the total acidity reaches to about 2 M because of the accumulation of formic acid in the solution. This is due to the low oxidation efficiency of 2 M

nitric acid as compared to the rate of oxidation of HCHO by 4 M nitric acid. Hence, the rate of accumulation of formic acid was higher than the rate of its consumption, resulting in the higher total acidity of the product solution. It is also evident from the results that the total acidity attains the steady state value at about 1.5 M. Kim et al. [1] could accelerate denitration and destroy the residual acid to about 0.4 M by electrolytic trimming. It could be observed in the present study that slow reduction of nitric acid occurs in the receiver tank also, even at ambient temperature until all residual formaldehyde is consumed, which is evident from the concentration of the reactants and products after a day (listed in Tables V. 3-7). Refluxing the solution in the reactor vessel for about 2 h at the reaction temperature of 98°C, after stopping the feeds also enables to destroy the residual HCHO and HCOOH.

5.4.5. Effect of Refluxing on the Destruction of Residual HCHO

Since the reduction rate of nitric acid was slow below 2 M due to the accumulation of HCOOH, the feed flow to the reactor vessel was stopped after attaining a total acidity of 2 M in a denitration experiment and the contents in the reactor were subjected to refluxing for 5 h. The concentrations of residual formic acid as well as formaldehyde were estimated and the results are also tabulated in Table V.8.

Table V.8. Concentrations of HNO₃, HCHO and HCOOH in the product solution during refluxing

Reflux Time/h	Temperature/ (°C)	[HCHO]/M	[HCOOH]/M	[HNO ₃]/M
0	99	0.43	0.31	1.66
1	99	0.21	0.14	1.33
2	99	0.11	0.08	1.18
3	99	0.06	0.07	1.16
4	99	0.02	0.08	1.16
5	99	0.02	0.07	1.17

It is observed that refluxing is effective in oxidising the residual formaldehyde and formic acid within the time period of about 2-3 h. Subsequently, the residual formaldehyde and formic acid

in the reactor vessel were destroyed by refluxing the product solution for 3 h after stopping the feed solutions, at the total acidity of about 2 M.

5.4.6. Denitration of Simulated Waste, With and Without Dissolved Organics

Destruction of 4 M nitric acid from a simulated waste solution was carried out at the optimum flow rates of HNO_3 and HCHO as 1.2 and 0.24 L/h respectively, at 98°C . Though the temperature of the heating mantle was kept constant throughout the experiment, the temperature of the solution in the vessel was found to increase by 3-4 degree in the presence of metal ions and organics, when the reaction was initiating due to the exothermicity of the denitration reaction. Figure V.3 shows the increase in temperature of the process as a function of time for initial period of 10 min., beyond which temperature is almost constant.

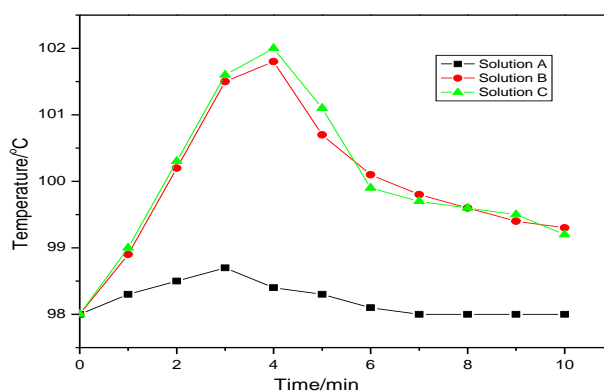


Fig. V.3. Variation of reaction temperature with time for initial 10 min. during denitration of Solution-A: pure 4 M HNO_3 ; Solution-B: Simulated HLLW and Solution-C: Simulated HLLW with organics (Feed rate of formaldehyde: 0.24 L/h; Feed rate of nitric acid: 1.2 L/h)

The variation in temperature was negligible for Solution-A after 5 minutes of denitration, but in the presence of heavy metal ions, the temperature of Solution-B shot up to 99°C when the reaction started and it gradually increased to 101.7°C within 5 minutes, which could be due to the contribution by the enthalpy of formation of metal formates by the metal ions in HLLW and subsequently, temperature stabilized at 99.2°C . In the denitration reaction with Solution-C, the

effect of organics in raising the temperature of the reaction mixture was not observed and the temperature increase was comparable to that of Solution-B. In case of simulated HLLW (with or without dissolved organics), the reaction started in a controlled manner, but within 1 minute vigorous reaction could be observed associated with heavy frothing. The results of the two experiments (Solutions B and C) are tabulated in the Tables V.9 and 10 respectively.

Table V.9. Results of denitration experiment using simulated HLLW solution in 4 M HNO₃; Feed rates of (a) HCHO: 0.24 L/h and (b) HNO₃: 1.2 L/h

Time/h	Temperature/(°C)	[HCHO]/M	[HCOOH]/M	[HNO ₃]/M	Total acidity/M
0	98.0	13.10	0	4.01	4.01
1	99.1	0.48	0.41	2.56	3.04
2	99.1	0.39	0.34	1.96	2.35
3	99.0	0.44	0.29	1.52	1.96
4	99.1	0.42	0.31	1.44	1.86
24	99.1	0.35	0.13	1.38	1.73

Table V.10. Concentrations of acid and HCHO in the product solution during denitration of a simulated HLLW solution with dissolved TBP; Feed rates of (a) HCHO: 0.24 L/h and (b) HNO₃: 1.2 L/h

Time/h	Temperature/(°C)	[HCHO]/M	[HCOOH]/M	[HNO ₃]/M	Total acidity/M
0	98.0	13.10	0	4.01	4.01
1	99.2	0.56	0.36	2.86	3.22
2	99.1	0.46	0.34	2.34	2.68
3	99.1	0.48	0.37	1.88	2.25
4	99.0	0.49	0.42	1.56	1.98
24	99.0	0.38	0.27	1.54	1.81

A marginal decrease in the reduction rate was noticed for the simulated waste nitrate solution with and without dissolved organics, which is attributed to the formation of heavy foaming of the reaction mixture, as well as due to the formation of metal formates with HCOOH.

Assuming denitration with HCHO to be apparent third-order reaction [4], the rate of destruction of nitric acid was computed by solving the following mass balance equations (8) and (9) numerically for different feed rates of HCHO and HNO₃.

$$\frac{dc_A}{dt} = \left(\frac{F_A}{V}\right)C_{Ai} - \left(\frac{F_A + F_B}{V}\right)C_A - kC_A^3C_B^{14} \quad (8)$$

$$\frac{dc_B}{dt} = \left(\frac{F_B}{V}\right)C_{Bi} - \left(\frac{F_A + F_B}{V}\right)C_B - kC_A^3C_B^{14} \quad (9)$$

where, subscripts A and B represent nitric acid and formaldehyde respectively. F, V and k are volumetric flow rate, volume of the reactor vessel and rate constant [4] and subscript 'i' refers to the inlet condition. The computed data have been plotted along with the experimental results for the reaction with the feed rates of HCHO and HNO₃ as 0.18 and 1.2 L/h respectively, in Fig V.4.

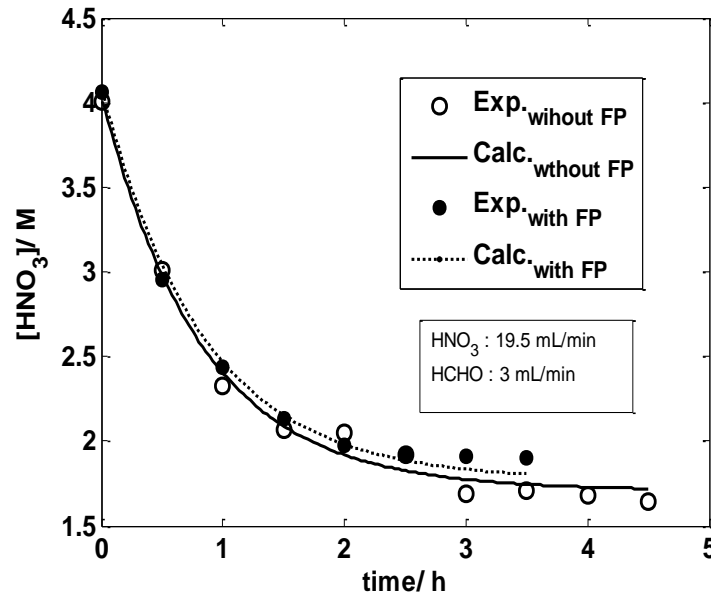


Fig. V.4. Vessel outlet concentration of HNO₃ with time (data points: experimental results; lines: computed results)

The agreement between the two sets of data is reasonable as could be seen from the figure. The results pertaining to an experiment conducted for a solution simulated with fission products have

also been shown in the same figure.

To investigate the effect of organics and metal ions on frothing observed during denitration of simulated HLLW and simulated HLLW with dissolved TBP, continuous denitration experiments were conducted with these solutions. Controlled frothing was observed even in the presence of dissolved organics. Experiments carried out at a higher concentration of TBP (1000 ppm) showed no difference in rate of reduction of acid and the extent of frothing. The results are tabulated in Table V.11.

Table V.11. Comparison of concentrations of HNO₃, HCHO and HCOOH in the product solution with different stock solutions

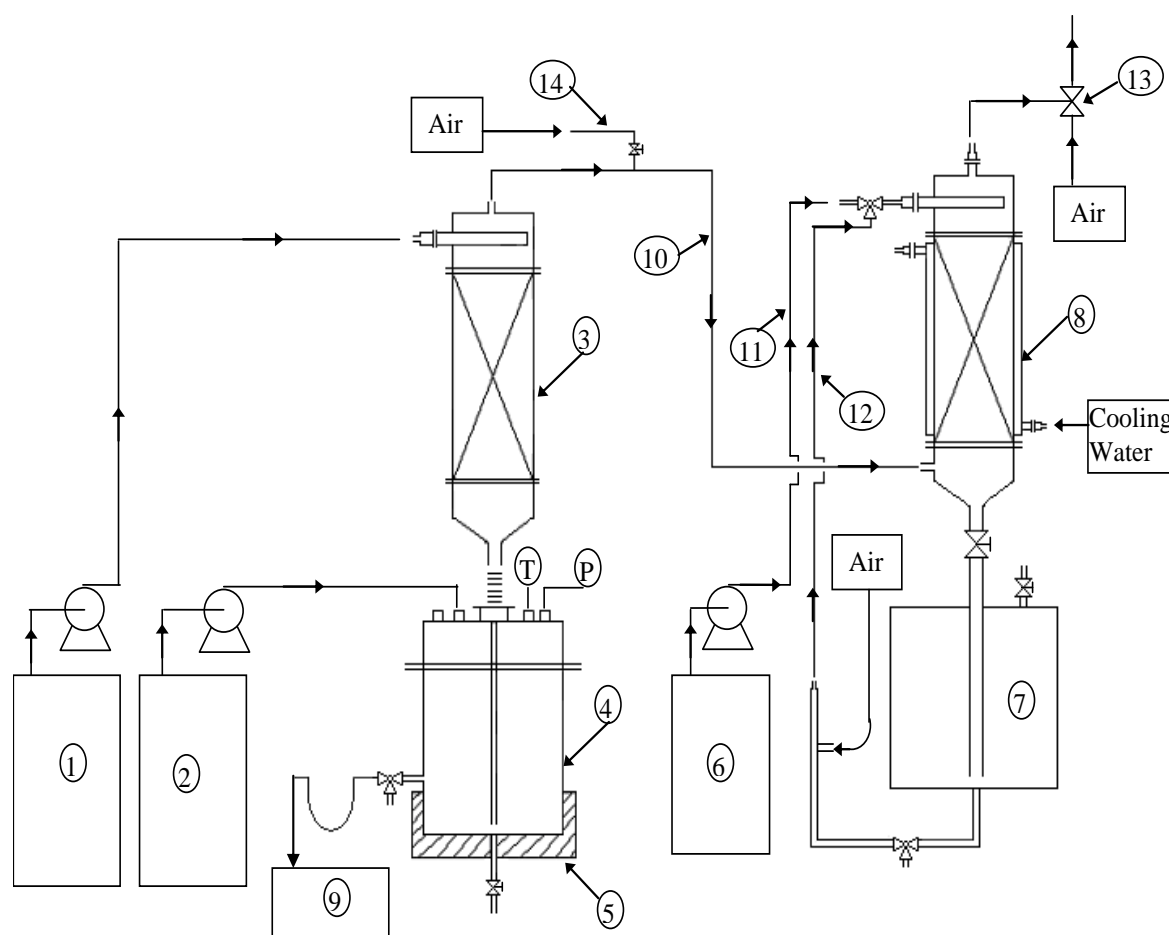
Time / h	Solution A			Solution B			Solution C		
	[HNO ₃]	[HCOOH]	[HCHO]	[HNO ₃]	[HCOOH]	[HCHO]	[HNO ₃]	[HCOOH]	[HCHO]
0	4.03	0	12.5	4.07	0.100	12.5	4.06	0	12.5
0.25	3.1	0.245	0.082	3.60	0.110	0.096	2.95	0.265	0.226
0.50	2.3	0.229	0.258	2.96	0.083	0.031	2.65	0.235	0.254
0.75	1.9	0.253	0.226	2.05	0.009	0.119	2.10	0.200	0.140
Reflux time: 2 h	---	---		1.54	0.050	BDL	1.70	0.009	0.047

Solution A: 4 M HNO₃; Solution B: Simulated HLLW with 220 ppm TBP; Solution C: Simulated HLLW with 1000 ppm TBP

The results of the lab scale continuous denitration experiments reveal that vigorous reaction with frothing results during the denitration of HLLW in the presence of dissolved organics and the frothing is mainly due to the metal ions rather than the organics. It was also found that frothing can be controlled by adding suitable anti-foaming agents to the reaction mixture.

5.5. Pilot plant scale denitration studies.

Based on the laboratory generated data and on the description of the apparatus reported in literature [8], an optimum design was made for pilot plant scale experiments and is shown in Fig. V.5. The reactor, which was a borosilicate glass vessel fitted with ports on the lid for temperature sensor, pressure gauge and for admitting formaldehyde, was placed on an electric heating mantle fitted with a PID temperature controller. Controlled flow of 4 M nitric acid was pumped into the vessel through a packed tower mounted above the reactor. HCHO was discharged directly into the acid feed in the vessel with the aid of a metering pump. The packed tower was filled with 12 mm glass rings. The products of the reaction, NO_x , CO_2 and H_2O vapour were made to travel upward through the packed tower, blended with air to oxidize NO to NO_2 and routed into the bottom portion of another packed column provided with a downward flow of reflux water. NO_2 was absorbed by the reflux water and the recovered acid was recirculated through the absorber for improved scrubbing and was collected in the receiver tank. The product solution was continuously vented out into the collection tank from the reactor with the aid of a 3 port 2 way valve. Care was taken to maintain the temperature of the reactor vessel above 98°C during the entire operating period. Throughout the experiments negative pressure was maintained in the apparatus. The optimum air flow needed for oxidation of NO was determined to be 20 to 30 L/h and the optimum reflux water flow required for acid absorption was 10 L/h. Samples from the vent port and collection tank were analysed periodically for free acidity, unreacted formaldehyde and the intermediate compound, formic acid. Complete destruction of residual HCHO and HCOOH in the product solution was ascertained either by refluxing the contents in the reactor for 2-3 h at the reaction temperature after stopping the addition of acid and the reductant or by allowing the product solution to reside in the collection tank for 24 h at ambient temperature.



1. Nitric acid feed
 2. Formaldehyde feed
 3. 4"/1000 mm packed column
 4. 6"/500mm Reaction vessel
 5. Heating mantle
 6. Water for absorption
 7. Recovered acid tank
 8. Packed column with cooling jacket
 9. Collection tank
 10. Vapour line
 11. Water line for absorption
 12. Air lift line
 13. Ejector
 14. Air line for bleeding
- T – Thermocouple
P – Pressure indicator

Fig. V.5. Borosilicate apparatus for pilot plant scale denitration and NO_x absorption

5.5.1. Results of Experiments with 3 and 6 L/h as the Feed Rates of Acid

Starting with 3 L/h of 4 M nitric acid, denitration was carried out up to the feed rate of 6 L/h in continuous mode. Accordingly, the feed rates of HCHO used were from 0.7 to 1.5 l/h, maintaining the mole ratio of HCHO to HNO₃ as 3:4. For full-scale plant capacity, the throughput of acid required is 6 L/h. Hence, experiments were also carried out using this feed rate with Solution-A (pure 4 M HNO₃), Solution-B (a synthetic solution simulated with fission and corrosion product elements (listed in Table V.2) dissolved in 4 M nitric acid) and Solution-C (the aqueous solution after equilibrating Solution-B with 40 ml of 100 % commercial TBP for 24 h; addition of TBP was warranted as the actual waste solution contains about 200 ppm of organics). The results are tabulated in Table V.12 - V.15.

Table V.12. Concentrations of intermediate products during and after denitration experiment with feed rates of (a) HCHO: 0.72 L/h and (b) HNO₃: 3 L/h

Time/h	Temp/(°C)	[HCHO]/M	[HCOOH]/M	[HNO ₃]/M	Total acidity/M
0	98	13.10	0	4.01	4.01
0.5	96.3	0.39	0.86	1.82	2.68
1.0	96.2	0.31	0.69	1.26	2.27
1.5	96.1	0.21	0.45	1.65	2.10
24	31	0.12	0.22	1.23	1.45

Table V.13. Results of denitration experiment with feed rates of (a) HCHO: 1.12 L/h and (b) HNO₃: 4.5 L/h

Time/h	Temp/(°C)	[HCHO]/M	[HCOOH]/M	[HNO ₃]/M	Total acidity/M
0	98.2	13.10	0	4.01	4.01
0.5	96.5	0.85	0.86	1.58	2.44
1.0	96.4	0.71	0.77	1.36	2.13
1.5	96.4	0.52	0.74	1.18	1.92
24	32	0.47	0.26	0.55	0.81

Table V.14. Denitration experiment with feed rates of (a) HCHO: 1.5 L/h and (b) HNO₃: 6.0 L/h

Time/h	Temp/(°C)	[HCHO]/M	[HCOOH]/M	[HNO ₃]/M	Total acidity/M
0	98	13.10	0	4.01	4.01
0.5	96.7	1.46	0.84	1.51	2.34
1.0	96.3	1.24	0.90	1.20	2.10
1.5	95.8	1.62	1.05	1.03	2.08
24	32.6	0.27	0.22	0.51	0.76

The steady state concentrations of formaldehyde, formic acid, nitric acid and the total acidity determined for the experiment with feed rates of HCHO and HNO₃ as 1.5 and 6 L/h respectively (Plant condition), have been plotted as a function of time in Fig. V.6.

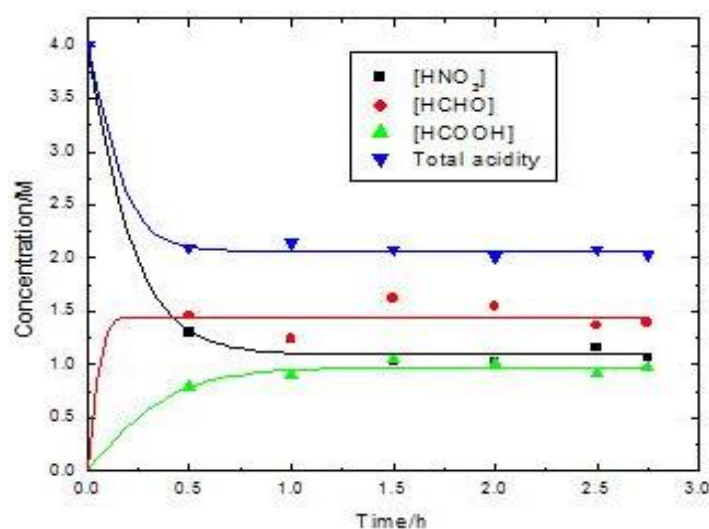


Fig. V.6. Continuous destruction of 4 M nitric acid in pilot plant scale set up; Feed rates of HNO₃ and HCHO: 6 and 1.5 L/h respectively

For high feed rates, maximum destruction occurred within 0.5 h of the commencement of the reaction and the concentrations of unreacted HCHO and HCOOH in the product solution were

found to be significantly high, resulting in the total acidity value as high as 2 M, though the concentration of nitric acid alone was found to be only about 1 M. However, leaving the product solution overnight in the collection tank at ambient temperature could lead to appreciable reduction of the total acidity. Hence, better denitration yields can be obtained even without any external agency.

Table V.15. Results of the denitration experiment with simulated HLLW; feed rates of (a) HCHO: 1.5 L/h and (b) HNO₃: 6.0 L/h

Time/h	Temp/(°C)	[HCHO]/M	[HCOOH]/M	[HNO ₃]/M	Total acidity/M
0	98.2	13.10	0	4.01	4.01
0.5	97.8	1.35	0.91	1.93	2.84
1.0	97.5	0.52	0.86	1.38	2.24
1.5	97.0	0.54	0.58	0.97	1.55
2.5	96.6	0.58	0.45	0.64	1.09
24	31.4	0.32	0.29	0.61	0.90

In all these experiments, the initiation of the reaction was observed to be within 1 to 2 minutes when the temperature of the reactor was above 98°C. However, the temperature dropped during the course of the reaction owing to the large volume of the reactants fed into the reactor at ambient temperature. The reaction proceeded in a controlled manner in the case of destruction of pure 4 M HNO₃. Foaming could be seen in the reactor as soon as the reaction started with simulated HLLW solution in the presence or absence of dissolved organics. However, no antifoaming agent was added to control foaming, though foaming reached up to the top of packed tower in the experiment with Solutions B and C, which are shown in Fig. V.7.



Fig. V.7. Picture showing frothing in the denitration experiment conducted with Solution B

Table V.16. Concentration of intermediate products in the denitration experiment with simulated HLLW containing dissolved TBP; Feed rates of HCHO: 1.5 L/h and (b) HNO₃: 6.0 L/h

Time/h	Temp/(°C)	[HCHO]/M	[HCOOH]/M	[HNO ₃]/M	Total acidity/M
0	98.1	13.10	0	4.01	4.01
0.5	96.2	0.62	0.40	1.38	1.78
1.0	95.9	0.74	0.57	1.14	1.71
1.5	95.8	0.81	0.67	0.82	1.49
24	30.9	0.22	0.21	0.67	0.88

The results obtained with pilot plant as well as full-scale plant capacity feed rates are summarised in Table V.17. The data given in Table V.17 are the concentrations estimated for the

solutions in the collection tank after terminating the experiments.

Table V.17. Concentrations of HNO₃, HCHO and HCOOH in the collection tank after terminating the addition of reactants in pilot plant as well as full-scale capacity experiments

Sl. No.	Feed rates of HCHO and HNO ₃ (L/h)	Concentration (M)			Denitration efficiency (%)
		HNO ₃	HCHO	HCOOH	
1	0.7 ; 3.0	1.65	0.14	*ND	69
2	1.1 ; 4.5	0.64	0.58	0.45	70
3	1.5 ; 6.0 (Solution A)	0.71	0.45	0.37	77
4	1.5 ; 6.0 (Solution B)	0.64	0.58	0.45	77
5	1.5 ; 6.0 (Solution C)	0.81	0.81	0.67	75

*Not detected

The first three experiments listed in Table V.17 were performed with pure 4 M nitric acid (Solution A). The fourth and fifth experiments were with synthetic solutions B and C. The denitration efficiency of HCHO was calculated based on the results of lab scale experiments that 3 mole of HCHO were consumed by 4 mole of acid. It could be seen from Table V.17 that for full-scale plant capacity (experiments: 3 to 5), the denitration efficiency remained more or less same and it was better than the efficiency calculated for pilot plant scale runs. It is apparent that the efficiency in the case of Solution C (experiment 5) was marginally lower than those values for other experiments due to severe foaming of the reaction mixture. The influence of metal ions in increasing the rate of reduction was not noticed as these ions are known to bind the formate ions and decrease the concentration of free formic acid available for denitration reaction. Analysis of the samples in the collection tank after 24 h revealed that sizeable amount of the residual acid was destroyed by HCHO and HCOOH in the tank also, as the concentration of the acid and the reductants in the collection tank were about 50 to 60 % lower than the steady state concentrations. Volume reduction of about 10 % could be achieved in the overall denitration reaction.

5.5.2. Recovery of Nitric Acid

The recovered nitric acid by absorption of NO_2 in water in the receiver tank was estimated to be only 6-14 % of the acid which was destroyed. This inefficient recovery was due to the insufficient capacity of the NO_x absorption tower. Hence, modification of the scrubbing column will be required in the equipment for the plant in order to improve the recoverability of nitric acid.

5.6. Conclusions

Continuous acid destruction of pure nitric acid and synthetic waste solutions (to simulate HLLW) with formaldehyde was investigated in pilot plant scale equipment. The reaction proceeded in a safe and controlled manner at temperatures above 98°C with an induction period of 1 to 2 minutes. About 4 mole of acid was destroyed by 3 mole of HCHO and the reaction efficiency was computed to be in the range 70-80 %. Denitration was demonstrated for full-scale plant processing rates in the same equipment. Destruction was successfully carried out without antifoaming agents though severe foaming could be observed in the synthetic solution containing degraded organics and fission product metal ions. Refluxing the contents of the reactor after terminating the experiment for an hour or allowing the product solution to reside in the collection tank for a day could result in the completion of denitration reaction and bringing down the residual acidity to more than 50 % of the steady state concentration, without any external agency. Volume reduction of about 10 % could be achieved in the overall denitration reaction. Absorption of NO_2 in water in the receiver tank yielded only 6-14 % of the acid which was destroyed. Hence, scrubbing column needs sizing for effective recovery of the acid in addition to determining quantitatively the influence of metal ions in foaming of the reactants prior to implementing the present design in the plant.

References

1. Kim, K.W., Kim, S.H., Lee, E.H., *J. Radioanal. Nucl. Chem.*, **260** (2004) 99
2. Bray, L.A., (1963) Report HW-76973
3. Evans, T.F., (1959) Report HW-58587
4. Healy, T.V., *J. Appl. Chem.*, **8** (1958) 553
5. Satyabrata, M., Falix, L., Sreenivasan, R., Pandey, N. K., Mallika, C., Koganti, S.B., Kamachi Mudali, U., *J. Radioanal. Nucl. Chem.*, **285** (2010) 687
6. Kumar, S.V., Nadkarni, M.N., Mayankutty, P.C., Pillai, N.S., Shinde, S.S., (1974) Report BARC-781
7. Jeffries, S.B., (1973) US Patent 3715320
8. Forsman, R.C., Oberg, G.C., (1963) Report HW-79622
9. Kondo, Y., Kubota, M., *J. Nucl. Sci. Technol.*, **29** (1992) 140
10. Lee, E.H., Whang, D.S., Kim, K.W., Kwon, S.G., Yoo, J.H., *J. Korean Ind. Eng. Chem.*, **8** (1997) 132
11. Kim, K.W., Kim, S.H., Lee, E.H., *J. Nucl. Sci. Technol.*, **41** (2004) 473
12. Drobnik, S., (1972) US Patent 3673086
13. Drobnik, S., Hild, W., Kaufmann, F., Koschorke, H., (1979) US Patent 4144186

EVOLUTION OF PHYSIOCHEMICAL PROPERTIES AND METAL RETENTION BEHAVIOUR OF THERMALLY AND RADIOLYTICALLY DEGRADED TBP-DD/NPH SYSTEMS IN NITRIC ACID MEDIUM

6.1. Introduction

Liquid-liquid extraction based PUREX process is the most widely adopted process for the reprocessing of spent nuclear fuel. Solvent extraction uses 30 % Tri-n-Butyl Phosphate (TBP, solvent) in Normal Paraffin Hydrocarbon (NPH) or Dodecane (DD) (Diluents) as the extractant for the separation of plutonium and uranium from nitric acid solution containing a large number of fission products. During the extraction stage, nitric acid also gets extracted to the solvent [1]. Owing to high dose of radiation encountered during extraction stage, the solvent as well as the diluent employed in the extraction process undergo chemical, thermal and especially radiolytic degradation resulting in a number of degradation products with varying physiochemical properties. The accumulation of the degradation products in the solvent can lead to different types of damage that disrupt the PUREX process, such as a decrease in the decontamination performance of uranium and plutonium for fission products (mainly ruthenium, zirconium, cerium, and niobium) [2, 3], an increase of product loss, namely, uranium and plutonium in aqueous raffinates [4], formation of emulsions, suspensions and cruds at the liquid-liquid interfaces which disturb the continuous extraction process [5] and the evolution of physiochemical properties of the phases, mainly viscosity and the interfacial tension, etc. [6]. To identify suitable radiation resistant solvent and diluents for liquid-liquid extraction process in the nuclear industry, it is imperative to consider the stability of the molecules proposed and to integrate the data generated from systematic degradation studies in order to check the robustness

of the solvent subjected to radiolysis or hydrolysis, particularly in terms of efficiency and of selectivity.

6.2. Scope of the work

Hydrolytic and radiolytic degradation of TBP diluted in Dodecane or NPH in the presence/absence of nitric acid have been investigated. Physicochemical properties such as density, viscosity, surface tension and phase disengagement time (PDT) were measured for undegraded as well as degraded solutions. The extent of damage caused by thermal and radiation induced reactions in TBP-DD/NPH-HNO₃ systems has been assessed by the measurement of zirconium retention in the organic phase. The results are compared with those of undegraded or raw systems. The effectiveness of sodium carbonate washing of the degraded organic phase for restoring the original quality of the solvent has been evaluated. The IR spectra of the raw samples and the degraded samples before and after solvent wash were recorded to find out the functional groups generated/removed.

6.3. Experimental details

6.3.1. Thermal Degradation

Thermal degradation of different sets of solutions consisting of pure TBP, TBP + 4 M HNO₃ (v/v), 30 % TBP-DD, 30 % TBP-DD + 4 M HNO₃ (v/v), DD + 4 M HNO₃ (v/v), NPH + 4 M HNO₃ (v/v), 30 % TBP-NPH and 30 % TBP-NPH + 4 M HNO₃ (v/v) at 40°C for 800 h and at 60°C for 400 h respectively, were carried out. The solutions were mixed continuously during degradation at the speed of 400 rpm using an incubator shaker. Samples were analyzed at intervals of every 200 h for degraded samples at 40°C and after every 100 h for degraded samples at 60°C to evaluate the changes in physicochemical properties and metal retention behaviour. The thermal degradation as a function of aqueous phase acidity (2, 6 and 8 M HNO₃) at the above two temperatures were also carried out to investigate the alteration in

physiochemical properties. All the properties were measured for the organic phases only after their separation from aqueous phase.

6.3.2. Radiolytic Degradation

Radiolytic degradation of various sets of samples such as TBP + 4 M HNO₃ (v/v), 30 % TBP-DD, 30 % TBP-DD + 4 M HNO₃ (v/v), DD + 4 M HNO₃ (v/v), NPH + 4 M HNO₃ (v/v), 30 % TBP-NPH and 30 % TBP-NPH + 4 M HNO₃ (v/v) were carried out using ⁶⁰Co gamma source up to 20 MRad absorbed doses. Samples were taken out from the chamber after regular intervals of 5 MRad for the measurement of physiochemical properties and metal retention behaviour. All radiolytic degradation experiments were carried out under static condition. Another set of samples 30 % TBP-DD, 30 % TBP-DD + 4 M HNO₃ (v/v), 30 % TBP-NPH and 30 % TBP-NPH + 4 M HNO₃ (v/v) were irradiated to a very high dose of 100 MRad to accelerate the formation of large amount of degraded products to facilitate their characterization.

6.3.3. Viscosity, Density and Surface Tension Measurements

Anton Paar DMA-4500 digital densitometer was used to measure the density of pure as well as the degraded samples generated during thermal and radiolytic degradation of the solvent-diluent systems. The instrument is temperature programmable to measure the density as a function of temperature to an accuracy of $5 \times 10^{-6} \text{ g/cm}^3$ and a repeatability of $1 \times 10^{-6} \text{ g/cm}^3$. Similarly, Anton Paar Lovis-2000 ME digital viscometer was used to measure the viscosity of the samples. Here, three measurements were taken and the average time was converted into a final viscosity value in centipoise. SEO (Surface Electro Optics) make DST-60 Surface Tension Analyzer was employed for the measurement of surface tension of various liquid samples based on Du Nouy ring method.

6.3.4. Phase Disengagement Time

The phase disengagement time (PDT) is the time taken for the disappearance of all the dispersed droplets at the interface formed after a vigorous shaking of the organic and the aqueous phases. During the experiment, 3 mL of the organic phase was shaken vigorously with 3 mL of 3 M nitric acid solution in a 10 mm inner-diameter, 15 mL stoppered test tube. The two phases were allowed to separate by holding the tube in vertical position. The time required for the disengagement was measured using a stop-watch of least count, 0.01 s. The measured PDT values are the average of two independent experiments.

6.3.5. Estimation of Zr in the Aqueous Phase by Spectrophotometry Using Arsenazo(III)

The method for the estimation of Zr by spectrophotometry in aqueous nitric acid solution using Arsenazo(III) as chromogenic reagent was standardized. A stock solution containing 100 ppm Zr was prepared by taking desired amount of $Zr(NO_3)_4 \cdot 5H_2O$ in milli pore water and was analyzed by ICP-OES technique.

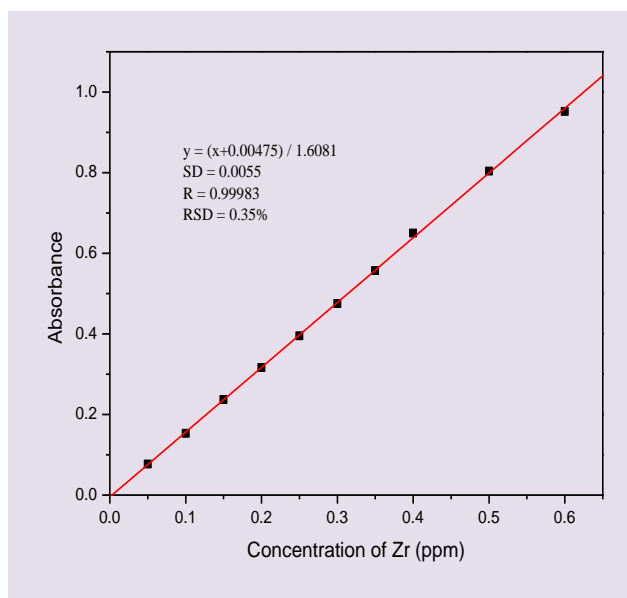


Fig. VI.1. Calibration graph for Zr estimation in aqueous phase

Solutions of different concentrations of Zr ranging from 0.05 to 0.6 ppm were prepared from the above stock solution after suitable dilution. The calibration graph for the above range is shown in Fig.VI.1. For spectrophotometric analysis, to a suitable aliquot, 5 ml of 10 M HNO₃ was added followed by 0.5 ml of 10 % sulfamic acid to destroy the nitrous acid. 0.5 ml of Arsenazo(III) prepared in dilute alkali was added to the above solution as chromogenic reagent and the solution was kept for 45 min. for the formation of a stable coloured complex of Zr with arsenazo. The absorbance of the above solution was recorded at 665 nm.

For the concentration range from 0.05 to 0.6 ppm, this method has a standard deviation (SD) of 0.0055 and RSD 0.35 %. The results obtained using spectrophotometry for unknown samples were compared with that obtained using ICP-OES, which has an error of ± 5 ppm.

6.3.6. Zirconium Retention Test

Plutonium/Zirconium retention behaviour of the degraded solvent with respect to the undegraded pure solvent is a measure of the extent of degradation. For the estimation of zirconium retention by degraded samples, equal volumes of degraded organic and Zr stock solution were equilibrated for 45 min using a test tube rotator. Zirconium concentration in the aqueous solution was measured using UV-Visible spectrophotometry after recording the absorbance at 665 nm. Subsequently, the loaded organic was stripped using 0.01 M HNO₃ for effective stripping of Zr from organic to aqueous phase. The Zr concentration in the stripped aqueous solution was measured. The difference gives the retention. For solvent wash, equal volumes of degraded organic and 0.5 M Na₂CO₃ were equilibrated for 45 min. Zr retention by the organic phase after solvent wash was measured in the same manner as discussed above. The Zr retention of the raw samples as well as the degraded samples before and after solvent wash was measured.

6.4. Results of thermal degradation studies

6.4.1. Variation in Physical Properties (Density, Viscosity and Surface Tension)

Viscosity and density of the extractant are two important process parameters that dictate the hydrodynamics of the extractant during the solvent extraction process. It is essential that the viscosity of the organic phase be sufficiently low to permit the ready flow of solutions in low-power agitators for phase dispersion and efficient phase separation [7]. Change in densities of thermally degraded solvent phases (organic) as a function of time at 40 and 60°C are compared with those of fresh samples in Tables VI.1. and VI.2.

Table VI.1. Densities (g/cc, at 25°C) of different systems thermally degraded at 40°C

Description of sample	Raw sample	200 h at 40°C	400 h at 40°C	600 h at 40°C	800 h at 40°C
Pure TBP	0.97248	0.97247	0.97251	0.97248	0.97247
Pure TBP + 4 M HNO ₃ (Org)	1.01486	1.01489	1.01503	1.01501	1.01523
30 % TBP-DD	0.81096	0.81116	0.81096	0.81116	0.81201
30 % TBP-DD + 4 M HNO ₃ (Org)	0.83242	0.83237	0.83282	0.83297	0.83365
DD + 4 M HNO ₃ (Org)	0.74486	0.74516	0.74520	0.74523	0.74531
NPH + 4 M HNO ₃ (Org)	0.75795	0.76340	0.76334	0.76341	0.763343
30 % TBP-NPH	0.82032	0.82142	0.82113	0.82099	0.82085
30 % TBP-NPH + 4 M HNO ₃ (Org)	0.83147	0.83449	0.83469	0.83486	0.83501

Marginal decrease or insignificant change in the densities was observed for samples thermally degraded in the absence of aqueous nitric acid phase at 40°C. On the contrary, for all other systems degraded in the presence of aqueous nitric acid, though the change in density was low, an increasing trend was observed for TBP-DD as well as TBP-NPH systems, which could be attributed to the extraction of nitric acid and water molecules from aqueous to organic phases.

Table VI.2. Densities at 25°C (g/cc) for various systems thermally degraded at 60°C

Sample Description	Raw sample	100 h at 60°C	200 h at 60°C	300 h at 60°C	400 h at 60°C
Pure TBP	0.97248	0.97257	0.97267	0.97255	0.97255
Pure TBP + 4 M HNO ₃ (Org)	1.01486	1.01737	1.01650	1.01808	1.01819
30 % TBP-DD	0.81096	0.81301	0.81184	0.81386	0.81597
30 % TBP-DD + 4 M HNO ₃ (Org)	0.83242	0.83387	0.83365	0.83416	0.83435
DD + 4 M HNO ₃ (Org)	0.74486	0.7452	0.74521	0.74578	0.74589
NPH + 4 M HNO ₃ (Org)	0.75795	0.7637	0.76388	0.76517	0.76723
30 % TBP-NPH	0.82032	0.81973	0.81940	0.81951	0.81993
30 % TBP-NPH + 4 M HNO ₃ (Org)	0.83147	0.83574	0.83588	0.83589	0.83599

Thermal degradation of the same set of samples at 60°C up to 400 h resulted in the marginal increase in density of all samples irrespective of the presence of aqueous nitric acid phase or not, which might be due to the formation of interacting molecules such as acidic degradation products in the organic phase as a result of the thermal treatment.

Thermal degradation of 30 % TBP in DD and 30 % TBP in NPH equilibrated with nitric acid of different acidities (2, 4, 6 and 8 M) at 40 and 60°C for 400 h was carried out to study the effect of aqueous nitric acid phase in altering the densities of the organic phases. The results are tabulated in Tables VI.3 and VI.4 respectively.

Table VI.3. Densities (g/cc) at 25°C, for thermally degraded systems w.r.to aqueous phase acidity at 40°C

Description of sample	Raw sample	100 h at 40°C	200 h at 40°C	300 h at 40°C	400 h at 40°C
30 % TBP-DD + 2 M HNO ₃ (v/v)-Org	0.82387	0.82387	0.82401	0.82413	0.82440
30 % TBP-DD + 4 M HNO ₃ (v/v)-Org	0.83243	0.83241	0.83237	0.83281	0.83289
30 % TBP-DD + 6 M HNO ₃ (v/v)-Org	0.83807	0.83813	0.83838	0.83863	0.83891
30 % TBP-DD + 8 M HNO ₃ (v/v)-Org	0.84068	0.84041	0.84124	0.84137	0.84214
30 % TBP-NPH + 2 M HNO ₃ (v/v)-Org	0.82084	0.83423	0.83418	0.83435	0.83525
30 % TBP-NPH + 4 M HNO ₃ (v/v)-Org	0.82968	0.84425	0.84446	0.84463	0.84471
30 % TBP-NPH + 6 M HNO ₃ (v/v)-Org	0.83493	0.85081	0.85100	0.84986	0.85076
30% TBP-NPH + 8 M HNO ₃ (v/v)-Org	0.84447	0.85405	0.85403	0.85311	0.85391

Table VI.4. Densities (g/cc) at 25°C, for various systems thermally degraded w.r.to aqueous phase acidity at 60°C

Sample Description	Raw sample	100 h at 60°C	200 h at 60°C	300 h at 60°C	400 h at 60°C
30 % TBP-DD + 2 M HNO ₃ (v/v)-Org	0.8238	0.82363	0.82323	0.82472	0.82481
30 % TBP-DD + 4 M HNO ₃ (v/v)-Org	0.83243	0.83381	0.83371	0.83419	0.83435
30 % TBP-DD + 6 M HNO ₃ (v/v)-Org	0.83807	0.83830	0.83860	0.83871	0.83897
30 % TBP-DD + 8 M HNO ₃ (v/v)-Org	0.84068	0.84099	0.84157	0.84183	0.84212
30 % TBP-NPH + 2 M HNO ₃ (v/v)-Org	0.82084	0.82070	0.82035	0.82137	0.82166
30 % TBP-NPH + 4 M HNO ₃ (v/v)-Org	0.82968	0.82979	0.83012	0.83024	0.83043
30 % TBP-NPH + 6 M HNO ₃ (v/v)-Org	0.83493	0.83626	0.84132	0.84693	0.84737
30 % TBP-NPH + 8 M HNO ₃ (v/v)-Org	0.84447	0.84057	0.85728	0.85793	0.85831

Tables VI.1 to VI.4 reveal that for both TBP-DD and TBP-NPH systems, the density of organic phases increased w.r.to the acidity of the aqueous phase due to the extraction of acid as well as water molecules to the organic phases. Similar trend was observed when the samples were thermally degraded as a function of acidity as well as time. However, the changes in densities are minimal. The results also indicate that even though the aqueous phase acidity increased from 2 to 8 M, the densities of the organic phases did not vary much during thermal degradation at 60°C in both systems.

The variation in the viscosity of the organic phases during thermal degradation at 40 and 60°C as a function of time and aqueous phase acidity are tabulated in Tables VI.5–VI.8.

Table VI.5. Viscosity (mPa.S) at 25°C, for various systems thermally degraded at 40°C

Description of sample	Raw sample	200 h at 40°C	400 h at 40°C	600 h at 40°C	800 h at 40°C
Pure TBP	3.345	3.349	3.360	3.361	3.355
Pure TBP + 4 M HNO ₃ (Org)	5.979	5.981	5.980	5.986	6.012
30 % TBP-DD	1.637	1.631	1.629	1.645	1.644
30 % TBP-DD + 4 M HNO ₃ (Org)	1.845	1.822	1.835	1.874	1.857
DD + 4 M HNO ₃ (Org)	1.360	1.359	1.352	1.378	1.405
NPH + 4 M HNO ₃ (Org)	1.283	1.303	1.312	1.319	1.332
30 % TBP-NPH	1.618	1.633	1.621	1.623	1.621
30 % TBP-NPH + 4 M HNO ₃ (Org)	1.889	1.848	1.852	1.878	1.891

Table VI.6. Viscosity (mPa.S) of different systems at 25°C, after thermal degradation at 60°C

Sample Description	Raw sample	100 h at 60°C	200 h at 60°C	300 h at 60°C	400 h at 60°C
Pure TBP	3.345	3.385	3.364	3.360	3.361
Pure TBP + 4 M HNO ₃ (Org)	5.979	5.916	5.852	5.832	6.033
30 % TBP-DD	1.637	1.646	1.847	1.798	1.727
30 % TBP-DD + 4 M HNO ₃ (Org)	1.845	1.847	1.841	1.855	1.873
DD + 4 M HNO ₃ (Org)	1.360	1.344	1.343	1.361	1.366
NPH + 4 M HNO ₃ (Org)	1.283	1.291	1.297	1.302	1.326
30 % TBP-NPH	1.618	1.615	1.607	1.601	1.635
30 % TBP-NPH + 4 M HNO ₃ (Org)	1.889	1.849	1.842	1.869	1.880

Table VI.7. Viscosity (mPa.S) for various systems thermally degraded w.r.to aqueous phase acidity at 40°C

Description of sample	Raw sample	100 h at 40°C	200 h at 40°C	300 h at 40°C	400 h at 40°C
30 % TBP-DD + 2 M HNO ₃ (v/v)-Org	1.862	1.846	1.855	1.862	1.840
30 % TBP-DD + 4 M HNO ₃ (v/v)-Org	1.845	1.848	1.825	1.853	1.837
30 % TBP-DD + 6 M HNO ₃ (v/v)-Org	1.812	1.796	1.800	1.804	1.812
30 % TBP-DD + 8 M HNO ₃ (v/v)-Org	1.782	1.770	1.782	1.787	1.793
30 % TBP-NPH + 2 M HNO ₃ (v/v)-Org	1.717	1.861	1.850	1.881	1.911
30 % TBP-NPH + 4 M HNO ₃ (v/v)-Org	1.889	1.867	1.856	1.865	1.862
30 % TBP-NPH + 6 M HNO ₃ (v/v)-Org	1.653	1.806	1.813	1.822	1.828
30% TBP-NPH + 8 M HNO ₃ (v/v)-Org	1.631	1.772	1.775	1.779	1.783

Table VI.8 Viscosity (mPa.S) at 25°C, for various systems thermally degraded w.r.to aqueous phase acidity at 60°C

Sample Description	Raw sample	100 h at 60°C	200 h at 60°C	300 h at 60°C	400 h at 60°C
30 % TBP-DD + 2 M HNO ₃ (v/v)-Org	1.862	1.877	1.829	1.887	1.894
30 % TBP-DD + 4 M HNO ₃ (v/v)-Org	1.845	1.862	1.839	1.846	1.878
30 % TBP-DD + 6 M HNO ₃ (v/v)-Org	1.812	1.817	1.794	1.819	1.816
30 % TBP-DD + 8 M HNO ₃ (v/v)-Org	1.782	1.783	1.777	1.788	1.792
30 % TBP-NPH + 2 M HNO ₃ (v/v)-Org	1.717	1.697	1.686	1.713	1.711
30 % TBP-NPH + 4 M HNO ₃ (v/v)-Org	1.889	1.839	1.841	1.872	1.881
30 % TBP-NPH + 6 M HNO ₃ (v/v)-Org	1.653	1.671	1.722	1.821	1.886
30 % TBP-NPH + 8 M HNO ₃ (v/v)-Org	1.631	1.671	1.773	1.828	1.891

Similar to the density values, the change in viscosity of TBP-DD and TBP-NPH systems were insignificant during the thermal degradation at 40 or 60°C. Also, variation in the aqueous phase acidity from 2 to 8 M did not alter the viscosity of the organic phases.

Interfacial tension or surface tension, which is the driving force during phase separation, is a direct measure of the extent of degradation of the organic phase. The higher the interfacial or surface tension, rapid is the coalescence rate and hence, smaller will be the phase separation time. The surface tension values measured for thermally degraded TBP-DD and TBP-NPH systems at 40 and 60°C as a function of aqueous phase acidity and time are tabulated in Tables VI.9 and VI.10.

Table VI.9. Surface tension (dyne/cm) at 25°C, for various systems thermally degraded w.r.to aqueous phase acidity at 40°C

Description of sample	Raw sample	100 h at 40°C	200 h at 40°C	300 h at 40°C	400 h at 40°C
30 % TBP-DD + 2 M HNO ₃ (v/v)-Org	23.32	22.32	23.29	23.24	23.19
30 % TBP-DD + 4 M HNO ₃ (v/v)-Org	23.54	23.46	23.38	23.34	23.12
30 % TBP-DD + 6 M HNO ₃ (v/v)-Org	22.46	22.49	22.41	22.31	22.32
30 % TBP-DD + 8 M HNO ₃ (v/v)-Org	22.45	23.02	23.06	23.53	23.76
30 % TBP-NPH + 2 M HNO ₃ (v/v)-Org	22.02	22.92	23.30	23.31	23.30
30 % TBP-NPH + 4 M HNO ₃ (v/v)-Org	22.06	23.37	23.29	23.29	23.45
30 % TBP-NPH + 6 M HNO ₃ (v/v)-Org	22.15	23.36	23.36	23.28	23.51
30% TBP-NPH + 8 M HNO ₃ (v/v)-Org	22.23	23.43	23.36	23.35	23.43

Table VI.10. Surface tension (dyne/cm) at 25°C, for thermally degraded systems w.r.to aqueous phase acidity at 60°C

Sample Description	Raw sample	100 h at 60°C	200 h at 60°C	300 h at 60°C	400 h at 60°C
30 % TBP-DD + 2 M HNO ₃ (v/v)-Org	23.32	23.55	23.40	23.39	23.23
30 % TBP-DD + 4 M HNO ₃ (v/v)-Org	23.54	23.69	23.62	23.38	23.23
30 % TBP-DD + 6 M HNO ₃ (v/v)-Org	22.46	23.76	23.76	23.57	23.41
30 % TBP-DD + 8 M HNO ₃ (v/v)-Org	22.45	23.60	23.68	23.13	22.66
30 % TBP-NPH + 2 M HNO ₃ (v/v)-Org	22.02	22.60	23.32	22.97	22.41
30 % TBP-NPH + 4 M HNO ₃ (v/v)-Org	22.06	22.85	23.31	23.08	22.81
30 % TBP-NPH + 6 M HNO ₃ (v/v)-Org	22.15	22.84	23.37	23.29	22.74
30 % TBP-NPH + 8 M HNO ₃ (v/v)-Org	22.23	22.84	22.58	22.64	22.44

The surface tension values of the degraded organic phases did not change significantly and no particular trend was followed with increasing temperature or nitric acid concentration. Since the instrument itself has the reproducibility in the range ± 1 dyne/cm for standard samples, the variation in surface tension observed in degraded samples may be due to instrumental error.

A minimum phase separation time is warranted after solvent extraction to avoid the degradation of the solvent system due to the presence of highly active aqueous phase. The phase separation time (PDT) of thermally degraded TBP-DD and TBP-NPH systems w.r.to 3 M nitric acid aqueous phase is given in Tables VI.11 and VI.12.

Table VI.11. PDT (s) of various systems thermally degraded at 40°C

Description of sample	Raw sample	200 h at 40°C	400 h at 40°C	600 h at 40°C	800 h at 40°C
30 % TBP-DD	35	38	42	50	54
30 % TBP-DD + 4 M HNO ₃ (Org)	35	38	40	47	50
30 % TBP-NPH	36	43	47	52	60
30 % TBP-NPH + 4 M HNO ₃ (Org)	35	44	45	49	56

Table VI.12. PDT (s) of various systems thermally degraded at 60°C

Sample Description	Raw sample	100 h at 60°C	200 h at 60°C	300 h at 60°C	400 h at 60°C
30 % TBP-DD	35	40	45	53	70
30 % TBP-DD + 4 M HNO ₃ (Org)	35	40	45	52	65
30 % TBP-NPH	36	45	49	54	63
30 % TBP-NPH + 4 M HNO ₃ (Org)	35	45	48	52	58

As the extent of thermal degradation increases, the PDT of the organic phases increased for TBP-DD as well as TBP-NPH systems, possibly indicating the formation of large amount of interacting molecules like acidic and nitration products.

6.4.2. Zirconium Retention

Zirconium retention tests for the organic phases were performed to assess the extent of damage caused by thermal degradation. In these experiments, 1170 ppm of Zr in 4 M HNO₃ was loaded into the organic phase and subsequently stripped with 0.01 M nitric acid. The amount of zirconium retained by the organic phase was monitored and compared with that of the undegraded solvent. The effectiveness of sodium carbonate (0.5 M) washing of the degraded organic phase for restoring the original quality of the solvent has been evaluated. The results are listed in Tables VI.13-VI.19.

Table VI.13. Zirconium retention (ppm) by raw samples; stock Zr: 1170 ppm

System	Extraction	Stripping	Retention	Retention after solvent wash
TBP	412.3	411.9	0.4	Nil
30 % TBP-DD	133.9	133.6	0.3	Nil
30 % TBP-NPH	184.5	184.1	0.4	Nil
(30 % TBP-DD) + 4 M H ⁺	304.8	304.1	0.7	Nil
(30 % TBP-NPH) + 4 M H ⁺	311.1	310.5	0.6	Nil

The results given in Table VI.13 indicate that less than 1 ppm of Zr was retained by the organic phases, with or without nitric acid, which could be due to the presence of acidic impurities in TBP itself. Since the acidic impurities were removed by alkali wash completely, no retention of Zr by the same set of solutions was observed after sodium carbonate wash.

Table VI.14. Zirconium retention (ppm) by thermally degraded samples at 40°C for 200 h; stock Zr: 1170 ppm

System	Before solvent wash			After solvent wash		
	Ext	Strip	Ret	Ext	Strip	Ret
TBP	456.5	447.4	9.1	409.5	409.9	Nil
30 % TBP (d)-DD*	140.0	138.7	1.3	131.4	130.7	0.7
30 % TBP-DD	151.4	149.1	2.3	147.4	146.3	1.1
(30 % TBP-DD) + 4 M H ⁺	475.2	393.7	81.5	134.3	132.9	1.8
30 % TBP-(DD + 4 M H ⁺)	196.6	188.2	8.4	178.8	179.2	Nil
30 % TBP-(NPH + 4 M H ⁺)	203.0	190.7	12.3	180.3	180.0	0.3
30 % TBP-NPH	195.6	192.7	2.9	188.8	187.3	1.5
(30 % TBP-NPH) + 4 M H ⁺	532.4	430.8	101.6	172.2	170.5	1.7

*30%TBP (d)-DD: degraded TBP made to 30% using DD; Ext: Extraction; Strip: Stripping; Ret: Retention

Table VI.15. Zirconium retention (ppm) by thermally degraded samples at 40°C for 400 h; stock Zr: 1170 ppm

System	Before solvent wash			After solvent wash		
	Ext	Strip	Ret	Ext	Strip	Ret
TBP	481.4	460.2	21.2	436.9	433.4	3.5
30 % TBP (d)-DD	196.6	194.5	2.1	142.7	142.1	0.6
30 % TBP-DD	186.8	183.7	3.1	158.4	156.8	1.6
(30 % TBP-DD) + 4 M H ⁺	776.0	545.3	230.7	139.5	136.9	2.6
30 % TBP-(DD + 4 M H ⁺)	267.2	247.4	19.8	239.9	236.1	3.8
30 % TBP-(NPH + 4 M H ⁺)	274.8	245.2	29.6	243.8	240.1	3.7
30 % TBP-NPH	236.9	233.7	3.2	187.1	185.7	1.4
(30 % TBP-NPH) + 4 M H ⁺	873.2	601.7	271.5	224.7	222.1	2.6

The results discussed above reveal that thermal degradation of TBP-DD and TBP-NPH systems up to 200 h at 40°C would not be an issue as the solvent can be recycled easily by one time solvent wash. However, degradation does occur at this temperature, which is obvious from the Zr extraction values before wash and this is attributed to the formation of DBP in the respective samples. It was observed that the Zr extraction by TBP-NPH system at 40°C after 100 and 200 h was higher than the TBP-DD system, with and without aqueous nitric acid phase.

Table VI.16. Zirconium retention (ppm) by thermally degraded samples at 40°C for 600 h; stock Zr: 1170 ppm

System	Before solvent wash			After solvent wash		
	Ext	Strip	Ret	Ext	Strip	Ret
TBP	694.8	653.5	41.3	619.5	615.8	3.7
30 % TBP (d)-DD	353.9	351.0	2.9	342.6	343.1	Nil
30 % TBP-DD	388.7	369.5	19.2	381.8	376.2	5.6
(30 % TBP-DD) + 4 M H ⁺	881.7	513.4	368.3	427.8	402.2	25.6
30 % TBP-(DD + 4 M H ⁺)	397.9	378.1	19.8	347.6	339.8	7.8
30 % TBP-(NPH + 4 M H ⁺)	417.3	403.0	14.3	382.2	364.2	18.0
30 % TBP-NPH	480.2	441.4	38.8	421.7	309.1	12.6
(30 % TBP-NPH) + 4 M H ⁺	917.8	519.3	398.5	516.4	477.5	38.9

Table VI.17. Zirconium retention (ppm) by thermally degraded samples at 40°C for 800 h; stock Zr: 1170 ppm

System	Before solvent wash			After solvent wash		
	Ext	Strip	Ret	Ext	Strip	Ret
TBP	850.6	793.8	56.8	777.3	773.2	4.1
30 % TBP (d)-DD	406.6	401.2	5.4	396.9	394.8	1.8
30 % TBP-DD	439.0	423.7	16.7	414.4	402.5	11.9
(30 % TBP-DD) + 4 M H ⁺	974.3	421.8	552.5	607.8	576.6	31.2
30 % TBP-(DD + 4 M H ⁺)	456.4	443.6	12.8	432.0	412.6	19.4
30 % TBP-(NPH + 4 M H ⁺)	491.2	479.6	11.6	472.2	449.9	22.3
30 % TBP-NPH	533.0	490.6	42.4	410.3	384.2	26.1
(30 % TBP-NPH) + 4 M H ⁺	1008.2	373.7	634.5	822.0	754.1	67.9

Beyond 200 h, one time washing of the degraded solvent will not be sufficient to remove all the acidic degradation products, which is obvious from the results tabulated above. Even with samples degraded in the absence of nitric acid, significant amount of Zr gets retained by the organic phases. In all the cases, Zr retention by thermally degraded TBP-NPH system after solvent wash was found to be higher than that of TBP-DD system.

Table VI.18. Zirconium retention (ppm) by thermally degraded samples at 60°C for 100 h; stock Zr: 1170 ppm

System	Before solvent wash			After solvent wash		
	Ext	Strip	Ret	Ext	Strip	Ret
TBP	458.7	443.4	15.3	405.2	404.9	0.3
30 % TBP (d)-DD	237.2	231.6	5.6	181.3	180.9	0.4
30 % TBP-DD	253.6	245.5	8.1	188.6	183.0	5.6
(30 % TBP-DD) + 4 M H ⁺	499.4	20.83	216.5	354.3	258.3	96
30 % TBP-(DD + 4 M H ⁺)	198.5	189.8	8.7	172.8	169.6	3.2
30 % TBP-(NPH + 4 M H ⁺)	205.8	193.5	12.3	167.6	163.5	4.1
30 % TBP-NPH	287.2	277.6	9.6	188.8	187.3	9.8
(30 % TBP-NPH) + 4 M H ⁺	541.65	13.4	266.5	397.4	261.2	136.2

Table VI.19. Zirconium retention (ppm) by thermally degraded samples at 60°C for 200 h; stock Zr: 1170 ppm

System	Before solvent wash			After solvent wash		
	Ext	Strip	Ret	Ext	Strip	Ret
TBP	567.6	553.5	23.1	529.0	525.3	3.7
30 % TBP (d)-DD	409.5	397.5	12.0	392.1	390.2	1.9
30 % TBP-DD	482.5	469.1	13.4	462.7	452.1	10.6
(30 % TBP-DD) + 4 M H ⁺	1053.4	212.9	840.5	783.5	545.5	238
30 % TBP-(DD + 4 M H ⁺)	407.9	394.1	13.8	378.2	365.7	12.5
30 % TBP-(NPH + 4 M H ⁺)	516.1	529.7	17.5	479.9	460.6	19.3
30 % TBP-NPH	547.2	527.3	19.9	496.3	472.9	23.4
(30 % TBP-NPH) + 4 M H ⁺	1133.0	172.7	960.3	1106.8	840.4	266.4

The Zr retention (which is assumed to be mainly due to DBP formation in TBP based compounds) by the thermally degraded samples at 60°C for 100 h, was found to be higher than

the values estimated for degraded samples at 40°C for 800 h; this is due to the fast kinetics for TBP degradation at elevated temperatures. There could be the formation of some interacting molecules also as shown in Fig VI.2. The degraded compound formed (based on Blake's hypothesis) has a greater tendency to bind Zr.

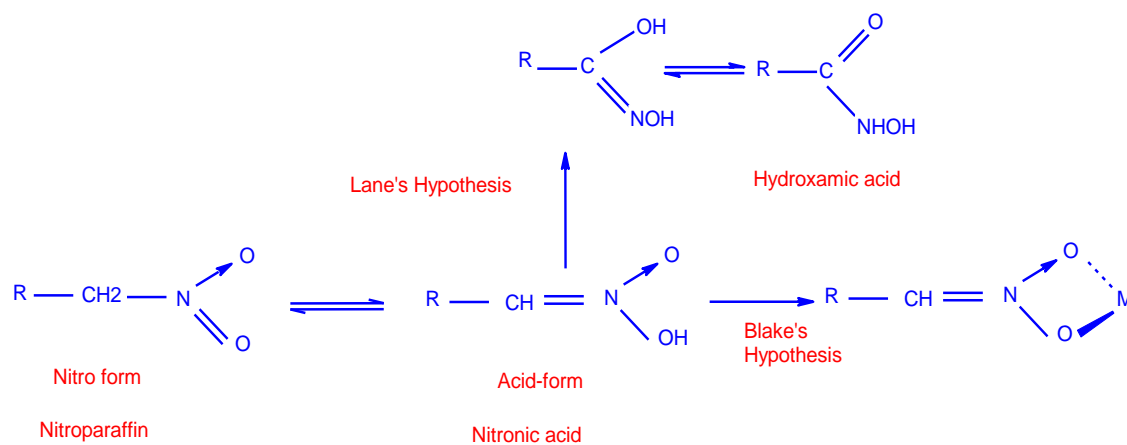


Fig. VI.2. Mechanism for the formation of interacting molecules

6.4.3. IR Analysis of the Thermally Degraded Samples

The FT-IR spectra of the thermally degraded samples were recorded to find out if any new class of compounds was formed. The IR spectra recorded for degraded TBB-DD and TBP-NPH systems at different temperatures w.r.to time are shown in Figs. VI.3–VI.8.

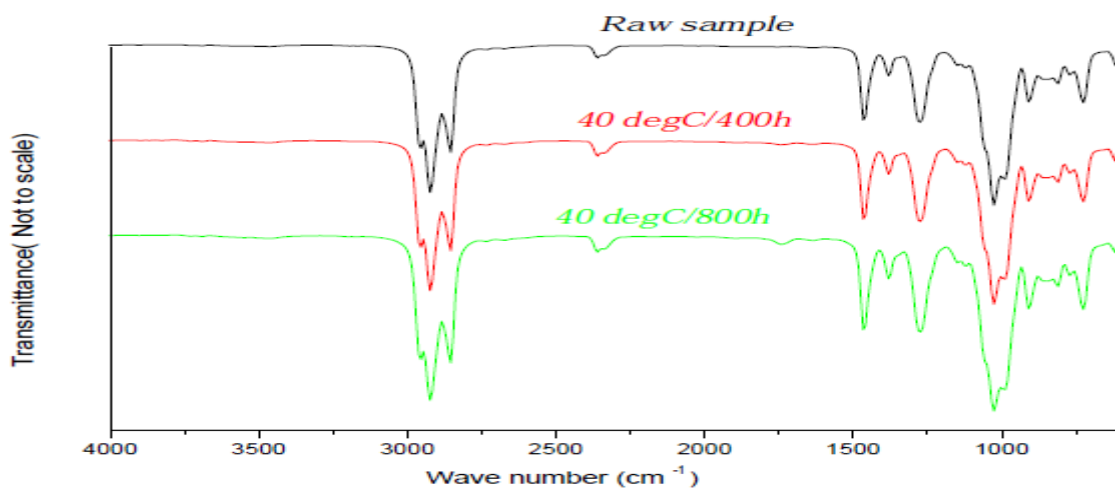


Fig. VI.3. Comparison of IR spectra of thermally degraded 30 % TBP-DD system at 40°C

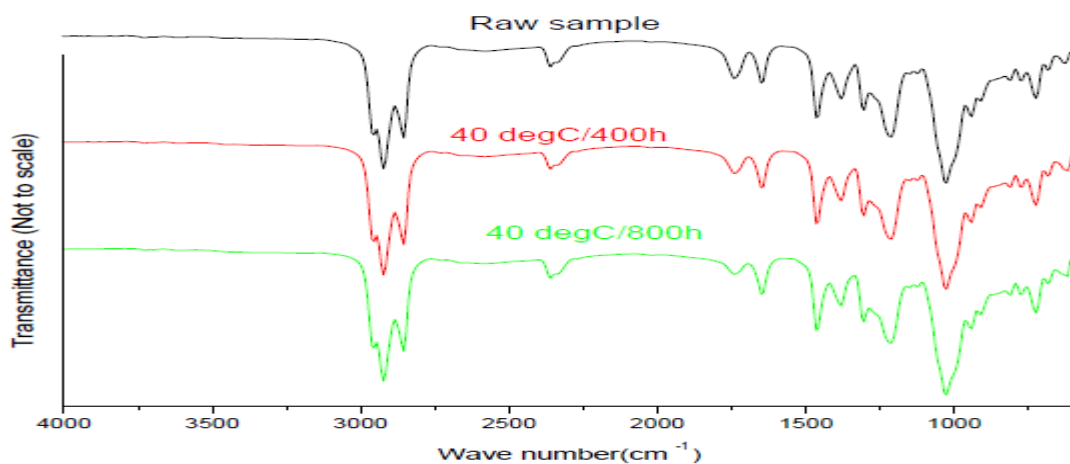


Fig. VI.4. Comparison of IR spectra of thermally degraded 30 % TBP-DD-HNO₃ system at 40°C

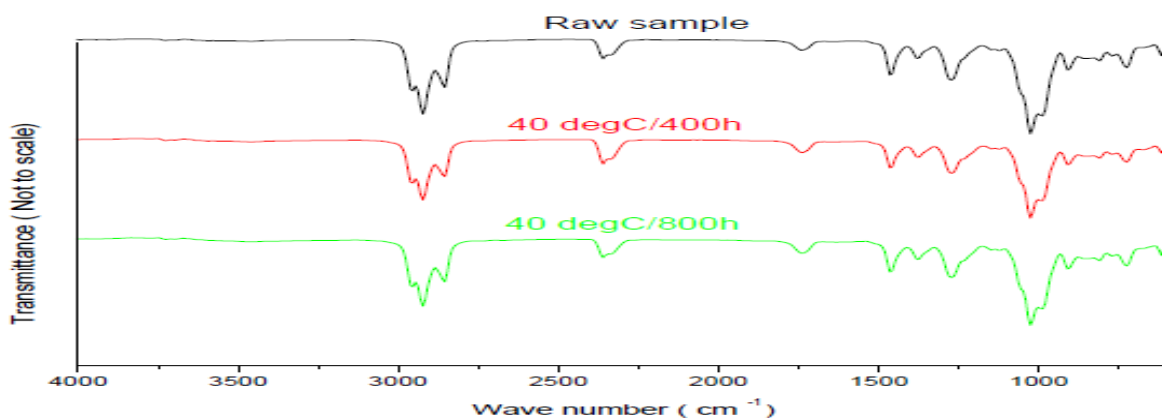


Fig. VI.5. Comparison of IR spectra of thermally degraded 30 % TBP-NPH system at 40°C

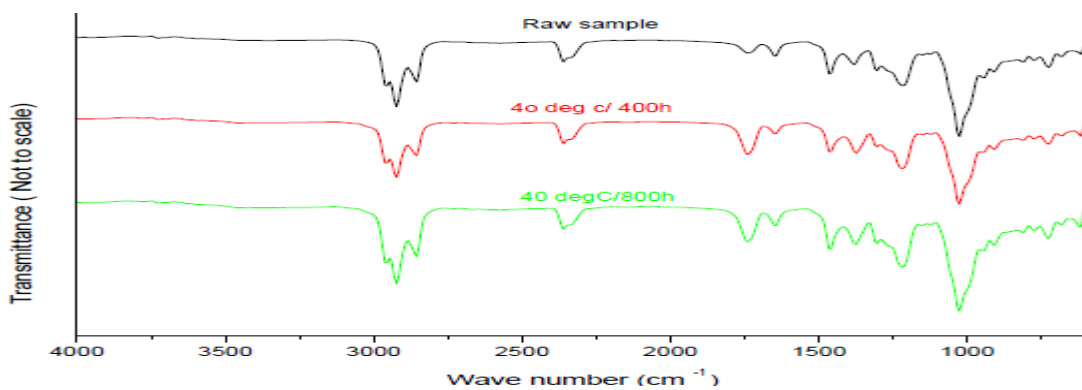


Fig. VI.6. Comparison of IR spectra of thermally degraded 30 % TBP-NPH-HNO₃ system at 40°C

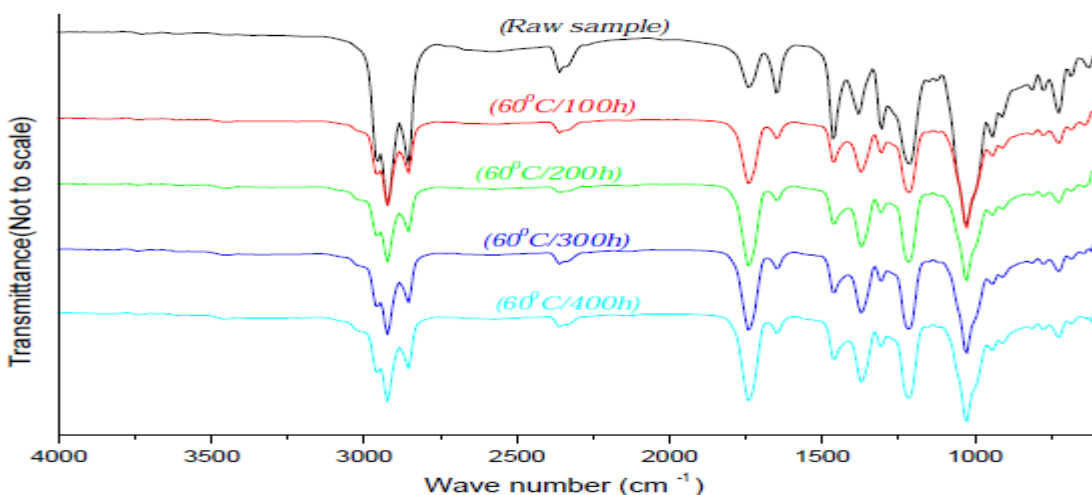


Fig. VI.7. Comparison of IR spectra of thermally degraded 30 % TBP-DD-HNO₃ system at 60°C

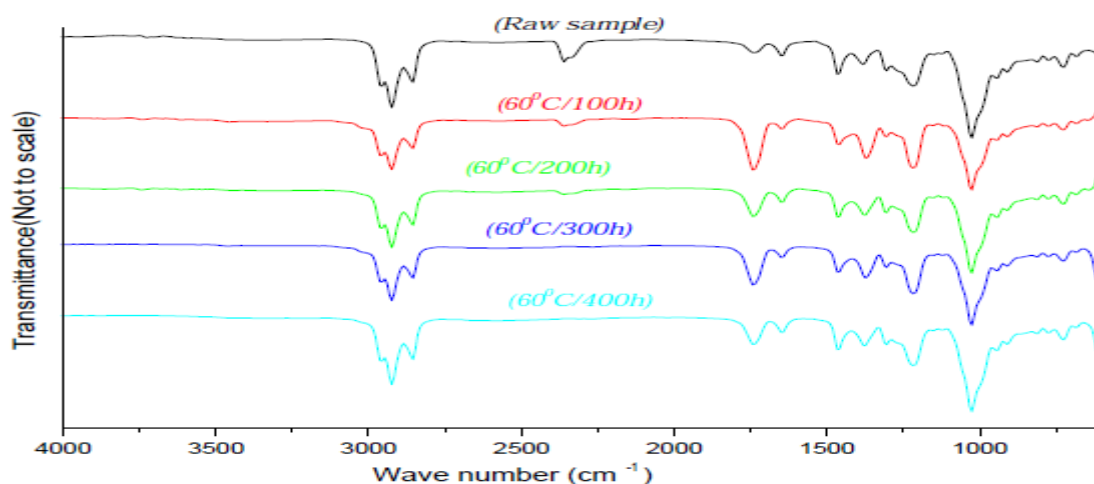


Fig. VI.8. IR spectra of thermally degraded 30% TBP-NPH-HNO₃ system at 60°C

The IR spectra recorded for both TBP-DD and TBP-NPH systems were almost identical and new peaks corresponding to the formation of different classes of compounds did not appear. Shift in peak frequencies was also not observed for the different systems at 40 and 60°C. These observations imply that the Zr retention estimated for various samples may be due to the formation of DBP only, which is the primary degradation product of TBP and it has high affinity to bind Zr.

6.5. Results of radiolytic degradation studies

6.5.1. Variation in Physical Properties (Density, Viscosity and Surface Tension)

Change in the density and viscosity of radiolytically degraded solvent (organic) with and without 4 M HNO₃ as the aqueous phase, as a function of absorbed dose was compared with those values measured for fresh samples in Table VI.20 and VI.21.

Table VI.20. Densities (g/cc) at 25°C, for the radiolytically degraded systems as a function of absorbed dose

Sample description	Density (g/cc)				
	Raw sample	5 MRad	10 Mrad	15 MRad	20 MRad
Pure TBP + 4 M HNO ₃ (Org)	1.01486	1.00848	1.01406	1.01421	1.01488
30 % TBP-DD	0.81096	0.81167	0.81215	0.81236	0.81274
30 % TBP-DD + 4 M HNO ₃ (Org)	0.83242	0.83359	0.83424	0.83499	0.83588
DD + 4 M HNO ₃ (Org)	0.74486	0.74565	0.74586	0.74592	0.74611
NPH + 4 M HNO ₃ (Org)	0.75795	0.74164	0.75801	0.75826	0.75841
30 % TBP-NPH	0.82032	0.82031	0.82076	0.82141	0.82166
30 % TBP-NPH + 4 M HNO ₃ (Org)	0.83147	0.83055	0.83134	0.83202	0.83294

A very marginal increase in density at the highest absorbed dose of 20 MRad was observed in the radiolytically degraded samples; this trend is similar to that observed with thermally degraded samples.

Table VI.21. Viscosity (mPa.s) at 25°C, for various radiolytically degraded systems as a function of absorbed dose

Sample Description	Viscosity (mPa.S)				
	Raw sample	5 MRad	10 Mrad	15 MRad	20 MRad
Pure TBP + 4 M HNO ₃ (Org)	5.865	5.876	5.882	5.910	5.952
30 % TBP-DD	1.637	1.623	1.667	1.692	1.718
30 % TBP-DD + 4 M HNO ₃ (Org)	1.845	1.867	1.887	1.906	1.932
DD + 4 M HNO ₃ (Org)	1.360	1.347	1.456	1.489	1.504
NPH + 4 M HNO ₃ (Org)	1.283	1.206	1.413	1.465	1.487
30 % TBP-NPH	1.618	1.488	1.546	1.661	1.682
30 % TBP-NPH + 4 M HNO ₃ (Org)	1.889	1.704	1.737	1.886	1.896

In TBP-NPH system the viscosity decreased initially and beyond 10 MRad, an increasing trend was observed.

The surface tension and phase disengagement times measured for the radiolytically degraded TBP-DD and TBP-NPH systems are given in Tables VI.12 and VI.13 respectively.

Table VI.22. Surface tension (dyne/cm) at 25°C, for various radiolytically degraded systems as function of absorbed dose

System	Surface Tension (dyne/cm)				
	Raw	5 MRad	10 MRad	15 MRad	20 MRad
30 % TBP-DD	23.26	23.33	23.41	23.33	23.21
30 % TBP-DD + 4 M HNO ₃ (v/v)-Org	23.54	23.53	23.61	23.53	23.41
30 % TBP-NPH	22.16	23.03	23.18	23.03	22.81
30 % TBP-NPH + 4 M HNO ₃ (v/v)-Org	22.06	23.16	23.23	23.15	22.87
TBP + 4 M HNO ₃ (v/v)-Org	26.13	26.54	26.63	26.47	26.22
DD + 4 M HNO ₃ (v/v)-Org	22.84	22.96	23.20	22.78	22.63
NPH + 4 M HNO ₃ (v/v)-Org	22.49	22.58	22.79	22.36	22.38

The surface tension values did not change appreciably in all the samples up to the absorbed dose of 20 MRad and the variation was within ± 1 dyne/cm, as observed during thermal degradation.

Table VI.23. Phase Disengagement Time (s) of various radiolytically degraded systems as a function of absorbed dose

Description of sample	Raw sample	5 MRad	10 MRad	15 MRad	20 MRad
30 % TBP-DD	35	35	38	40	45
30 % TBP-DD + 4 M HNO ₃ (Org)	35	37	38	40	42
30 % TBP-NPH	36	45	49	54	63
30 % TBP-NPH + 4 M HNO ₃ (Org)	35	45	48	52	58

The PDT values gradually increased with absorbed dose. The increase was more in the case of samples which were radiolyzed without aqueous nitric acid. Further, the increase for TBP-NPH system was more than that of TBP-DD system.

6.5.2. Zirconium Retention

For Zr retention experiments, 1490 ppm of Zr in 4 M HNO₃ was loaded into the radiolysed organic phase and the loaded organic was stripped with 0.01 M nitric acid. The amount of zirconium retained by the organic phase was estimated. The effectiveness of sodium carbonate (0.5 M) washing of the degraded organic phase for restoring the original quality of the solvent has been evaluated. The results are listed in Tables VI.24 to VI.28.

Table VI.24. Zirconium retention (ppm) by radiolytically degraded samples after the absorbed dose of 5 MRad; Stock Zr: 1490 ppm

System	Before solvent wash			After solvent wash	
	Ext	Strip	Ret	Ext	Ret
30 % TBP-DD	639.9	260.5	379.4	220.1	Nil
(30 % TBP-DD) + 4 M H ⁺	739.4	307.8	431.6	234.9	Nil
30 % TBP-NPH	570.2	235.7	334.5	232.5	Nil
(30 % TBP-NPH) + 4 M H ⁺	744.4	297.8	446.6	237.4	Nil

Table VI.25. Zirconium retention (ppm) by radiolytically degraded samples after 10MRad;

Stock Zr: 1490 ppm

System	Before solvent wash			After solvent wash	
	Ext	Strip	Ret	Ext	Ret
30 % TBP-DD	911.1	185.9	725.2	242.4	14.3
(30 % TBP-DD) + 4 M H ⁺	923.5	280.4	643.1	247.4	18.7
30 % TBP-NPH	819.0	195.8	623.2	252.4	13.6
(30 % TBP-NPH) + 4 M H ⁺	925.9	258.1	667.8	247.4	16.4

Table VI.26. Zirconium retention (ppm) by radiolytically degraded samples after 15 MRad;

stock Zr: 1490 ppm

System	Before solvent wash			After solvent wash	
	Ext	Strip	Ret	Ext	Ret
30 % TBP-DD	1147.4	166.0	981.4	289.7	33.4
(30 % TBP-DD) + 4 M H ⁺	1152.3	190.9	961.4	267.5	41.5
30 % TBP-NPH	1065.3	141.2	924.1	274.78	31.5
(30 % TBP-NPH) + 4 M H ⁺	1152.4	193.4	959.0	269.5	44.6

Table VI.27. Zirconium retention (ppm) by radiolytically degraded samples after 20MRad, stock Zr: 1490 ppm

System	Before solvent wash			After solvent wash	
	Ext	Strip	Ret	Ext	Ret
30% TBP-DD	1319.0	91.4	1227.6	344.4	86.5
(30% TBP-DD)+4M H ⁺	1323.9	90.4	1233.5	361.5	97.8
30% TBP-NPH	1314.0	98.8	1215.2	319.5	89.7
(30% TBP-NPH)+4M H ⁺	1336.4	101.3	1235.1	347.4	101.3

The above results revealed that after radiolysis up to 5 MRad, though significant amount of Zr gets retained by organic phase, a single wash using 0.5 M Na₂CO₃ was effective in removing the retained Zr. The Zr retention of the sample at the absorbed dose of 10 MRad was almost comparable to the Zr retention values observed with thermally degraded samples at 40°C for 800 h. So beyond the absorbed dose of 5 MRad, one time washing with carbonate solution will not be effective in removing all the acidic degradation products. It is also probable that there might be the generation of some complex forming compounds which bind Zr, but hydrophobic in nature. It was observed that the Zr retention by radiolyzed TBP-NPH system was marginally higher than that by TBP-DD system.

6.5.3. IR analysis of the radiolytically degraded samples

The FT-IR spectra of the radiolyzed samples (only organic phases) were recorded over the wave number range 4000-500 cm⁻¹ in order to identify new functional groups generated if any, during radiolysis. The IR spectra of the irradiated samples have been compared with that of unirradiated one in Figs. VI.9 to VI.12.

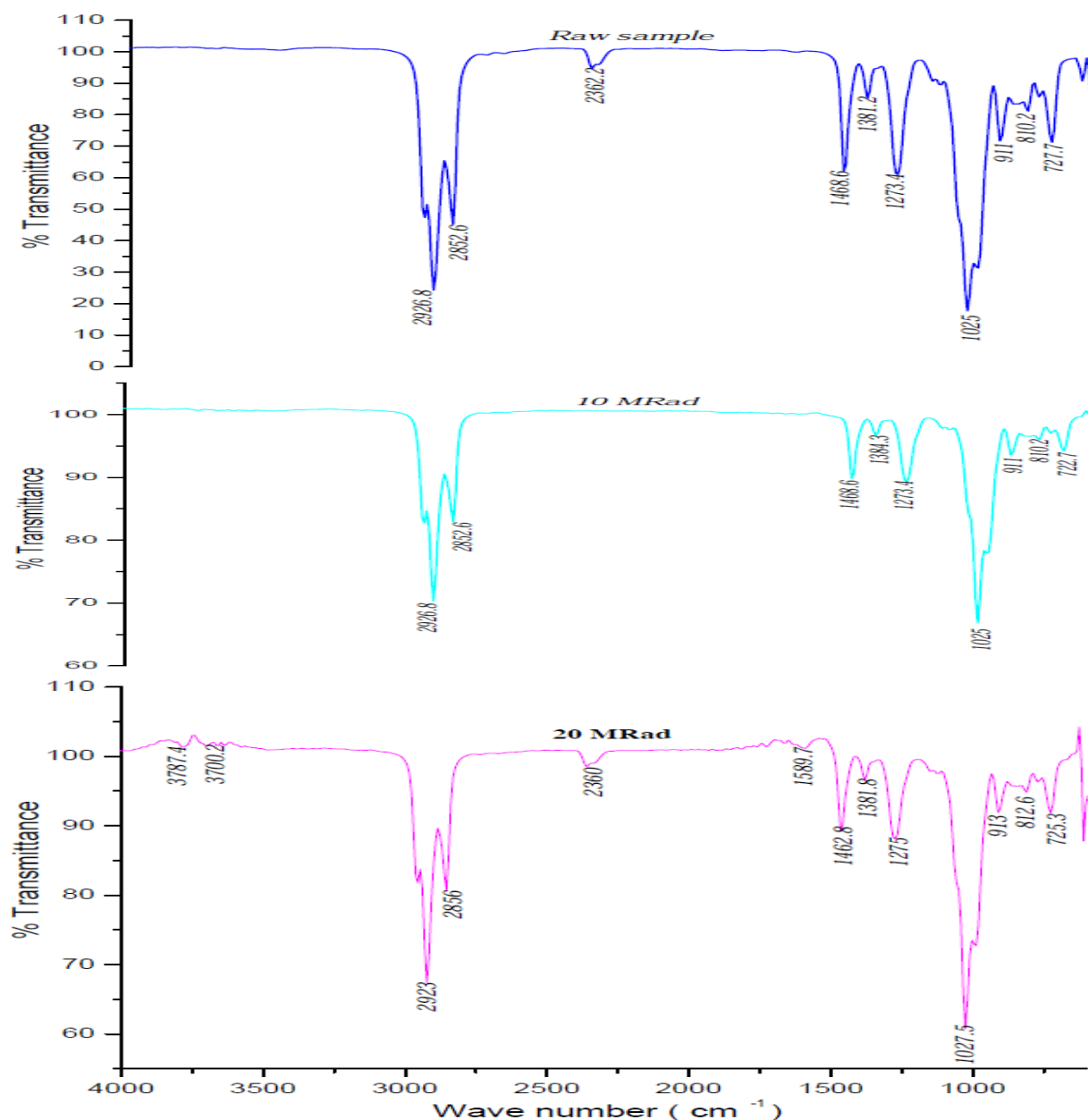


Fig. VI.9. Comparison of IR spectra of radiolytically degraded 30 % TBP-DD w.r. to absorbed dose

Up to 10 MRad, the IR spectra of raw and radiolysed samples were identical; but at 20 MRad, three additional peaks at 1589.7, 3700.2 and 3787.4 cm^{-1} could be observed. While the former one can be attributed to C=C stretching in aromatic compounds, the latter two peaks are attributed to O-H stretching frequencies in alcohols, which could have formed from TBP radiolysis i.e. butanol.

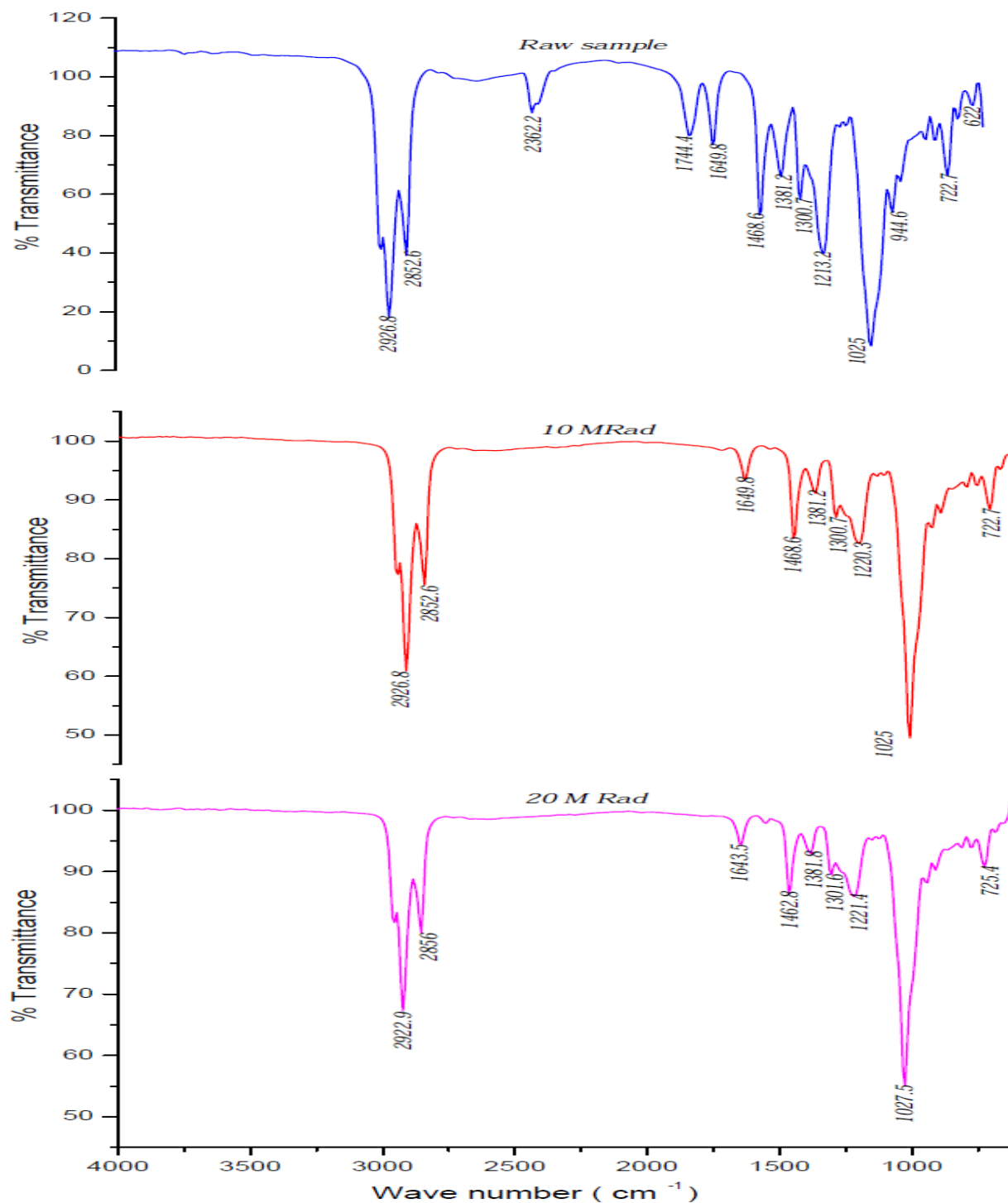


Fig. VI.10. Comparison of IR spectra of radiolytically degraded 30 % TBP-DD-HNO₃ system w.r.to absorbed dose

In these samples, no new peaks were observed even up to 20 MRad, other than a marginal shift in frequencies.

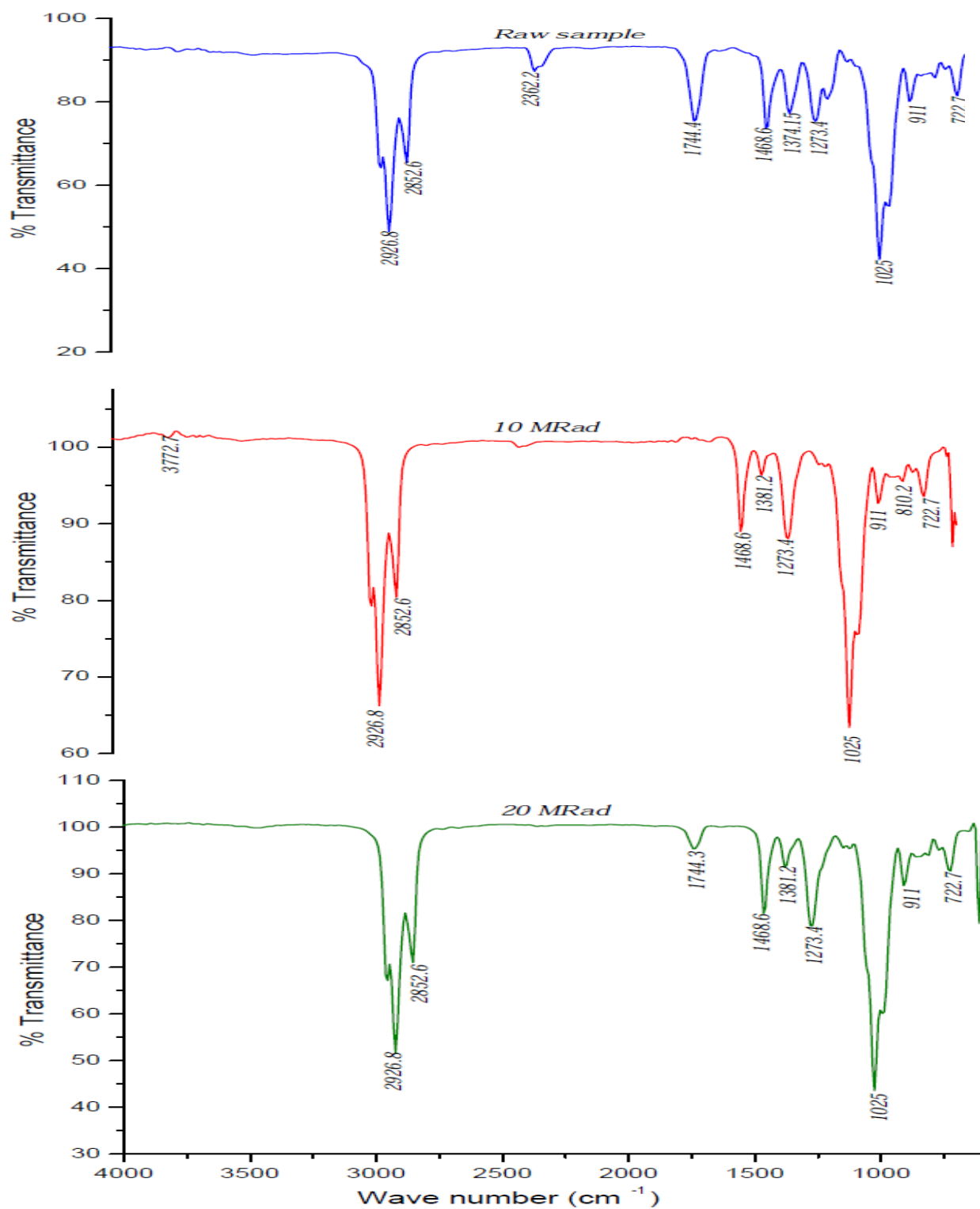


Fig. VI.11. Comparison of IR spectra of radiolytically degraded 30 % TBP-NPH w.r.to absorbed dose

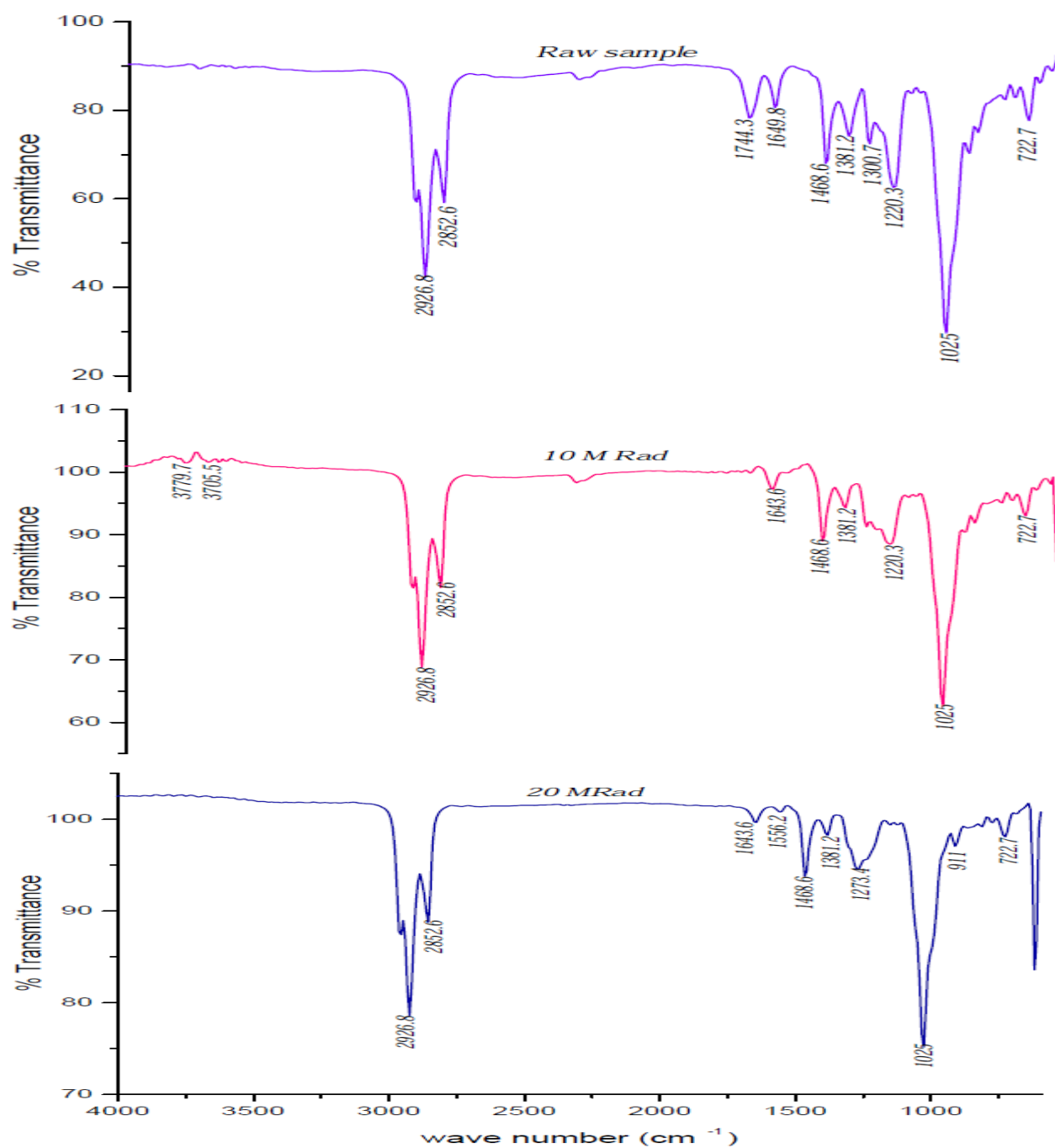


Fig. VI.12. Comparison of IR spectra of radiolytically degraded 30 % TBP-NPH-HNO₃ w.r.t absorbed dose

The IR spectra were identical except two additional peaks at 3705 and 3779 cm⁻¹ at 10 MRad.

Fig. IV.13 presents the IR spectra of 30 % TBP-DD equilibrated with 4 M HNO₃ (organic phase) and degraded to a higher absorbed dose of 100 MRad.

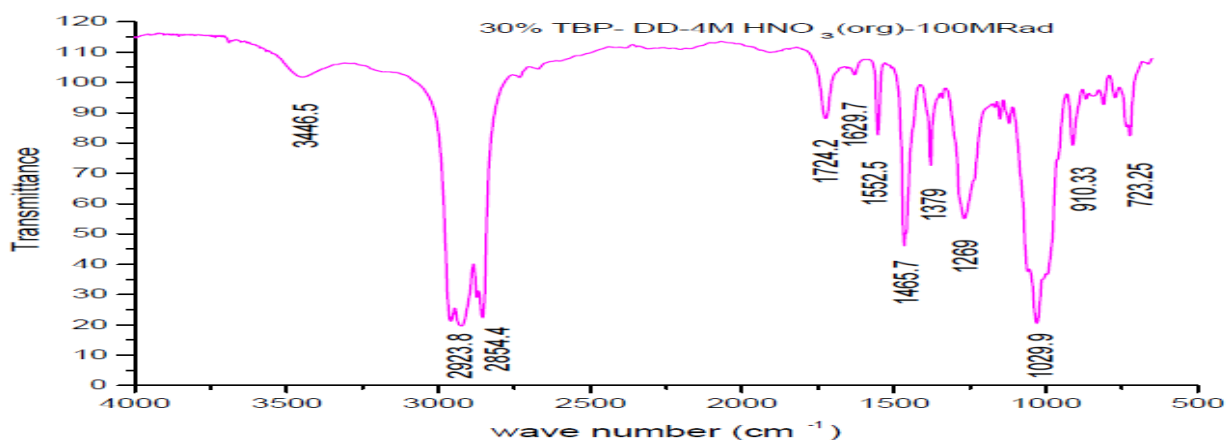


Fig. VI.13. IR spectra of radiolytically degraded 30 % TBP-DD-HNO₃ after irradiating to 100 MRad

Extra two well defined peaks observed at 1724.2 and 3446.5 cm⁻¹ in Fig. VI.13 while compared to that of the raw sample indicates the formation of carbonyl and amine based compounds at higher dose. The radiolyzed sample at 100 MRad was fractionally distilled at 2 mbar pressure to characterize the fractions collected. The IR spectra of the fractions collected at different temperatures are shown in Fig. IV.14.

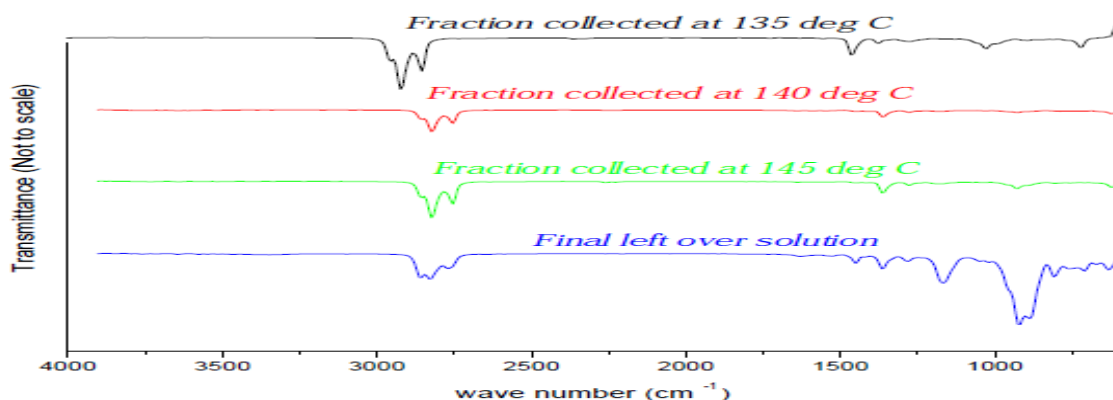


Fig. VI.14. IR spectra of the fractions collected during the distillation of radiolytically degraded 30 % TBP-DD-HNO₃ system after 100 MRad

This figure indicates that the fractions collected at 135, 140 and 145°C are due to pure dodecane whereas, the left over fraction consisted of higher molecular weight TBP based compounds.

6.6. Conclusion

Thermal degradation behavior of TBP diluted with Dodecane or NPH in the presence/absence of nitric acid has been investigated. Thermal degradation at 40°C for 800 h or at 60°C for 400 h did not alter significantly the physiochemical properties such as density, viscosity and surface tension. But metal retention was observed to be significant. When the duration of degradation at high temperature increases, one time solvent wash is not effective in restoring the quality of solvent. Radiolysis up to 20 MRad brought marginal change in density, viscosity and PDT; however, the surface tension remained more or less the same. Beyond 10 MRad, solvent washing will not be effective to remove the degraded products, as significant amount Zr gets retained by organic phases. Irradiation to a higher dose of 100 MRad indicated the formation of new classes of compounds. Irrespective of the nature of degradation (either radiolytic or thermal), TBP-DD systems were observed to have better stability than the TBP-NPH system, based on metal retention behaviour.

References

1. Hesford, E.; Mc Kay, H.A.C., *J. Inorg. Nucl. Chem.* **13** (1960) 156
2. Nowak, Z., Nowak, M., Seydel, A., *Radiochem. Radioanal. Lett.* **38** (1979) 343
3. Neace, J.C., *Sep. Sci. Technol.* **18** (1983) 1581
4. Hardy, C.J., Scargill, D., *J. Inorg. Nucl. Chem.* **17** (1961) 337
5. Smith D.N., Edwards H.G., Hugues M.A., Courtney, B., *Sep. Sci. Technol.* **32** (1997) 2821
6. Tripathi, S.C., Ramanujam, A., *Sep. Sci. Technol.* **38** (2003) 2307
7. Venkatesan, K.A., Robert Selvan, B., Antony, M.P., Srinivasan, T.G., Vasudeva Rao, P.R., *Sol. Extr. Ion. Exch.*, **24** (2006) 747

EFFECT OF TEMPERATURE, ACIDITY AND ELECTROLYTES ON THE SOLUBILITY OF TBP IN AQUEOUS PHASE

7.1. Introduction

Tri-n-butyl phosphate (TBP) diluted with hydrocarbon diluents is widely used for the extractive reprocessing of spent nuclear fuels [1]. During extraction, the solubility of TBP represents a balance between the highly polar oxygen atoms which favor miscibility with aqueous phase and the alkyl groups due to the hydrophobic nature and hence, affinity towards organic phase [2]. Owing to its mutual solubility, trace amount of TBP is left out in the aqueous solution after the extraction step. As it is potentially hydrolyzable in non-volatile species which have adverse effects on process operation, the amount that is carried with the various aqueous streams in an extraction process has greater importance. Thus, when the aqueous solutions are concentrated at high temperatures in evaporators, exothermic reactions due to the decomposition of TBP compounds take place. Several accidents occurring during the heating of nitric acid solutions containing TBP have been reported in literature [3-5]. The solubility of pure TBP in water is about 0.4 g/L at 25°C [2] and in aqueous solution of 3 M HNO₃, it is around 270 mg/L [6]. When TBP is diluted with an inert substance which is insoluble in water, the solubility of TBP decreases. Baldwin et al. [7] have measured the solubility of TBP in water at temperatures from 3.4 to 50°C and reported that on molar basis the solubility of TBP in water drops from 0.004 M at 3.4°C to 0.0011 at 50°C, with a value of 0.0016 M at 25°C. Presence of salts in the aqueous phase decreases the solubility markedly. Solubility of TBP and its decomposition products in HNO₃ system containing uranyl nitrate in the concentration range 200-1200 g/L at 25-128°C has been studied by Usachev et al. [8]. The solubility of TBP in aqueous solutions of plutonium

nitrate and in highly radioactive liquid waste (HRLW) generated from the aqueous reprocessing of spent nuclear fuels was investigated by Kuno et al. [9] and an empirical formulation was derived for the solubility of TBP in plutonium nitrate in the range of 0 ~ 0.1 M Pu and 1 ~ 8 M HNO₃ concentrations. Velavendan et al. [10] have investigated the effect of uranium and different fission product metal ion concentrations on the solubility of TBP in various nitric acid concentrations (0–15.7 M) at room temperature.

Though enough data on the solubility of pure TBP or TBP/diluents in aqueous medium have been reported in the literature, information on TBP solubility in the presence of electrolytes in various nitric acid concentrations over a range of temperatures is incomplete and sometimes contradictory also. Hence, it is essential to generate solubility data for pure TBP in different concentrations of nitric acid in the presence of electrolytes, as a function of temperature.

7.2. Scope of the work

The solubility of TBP in nitric acid (0–14 M) was determined in the temperature range 25–60°C, for the purpose of understanding the distribution equilibrium of TBP between aqueous and organic phases as well as to provide input for designing a suitable contactor in order to remove the dissolved TBP from aqueous streams in the PUREX process. The present work also describes the individual as well as the combined effect of electrolytes such as Zr(NO₃)₄, Ru(NO₃)₃NO and UO₂(NO₃)₂ on the solubility of TBP in aqueous phase over a range of temperature. The concentrations of TBP dissolved in aqueous phase, both free and bound to the acid due to the formation of TBP complexes with nitric acid have been calculated. A classical thermodynamic approach has been used to determine the formation constants of TBP-nitric acid complexes.

7.3. Solubility measurements

Analysis of TBP was performed using Shimadzu gas chromatograph (Model 14 B) equipped with flame ionization detector (FID). SE-30 stainless steel packed column (4 m long x 1/8" ID) was used for separation. Nitrogen was used as the carrier gas with a flow rate of 30 mL/min. The column oven, injector and detector temperatures were maintained at 230, 260 and 260°C respectively. Hydrogen gas was used as fuel and zero air was used as supporting gas with the flow rate of 30 and 300 mL/min respectively. IC net 2.3 Metrohm software was used for data acquisition.

7.3.1. Calibration Procedure

A stock solution of TBP was prepared by diluting a known weight of TBP with n-dodecane. All standard solutions of TBP (2 to 200 ppm) were prepared by appropriate dilution of the stock solution. The calibration graph obtained is shown in Fig. VII.1. The graph was linear with the R^2 value of 0.995. The relative standard deviation was 5 % at 2 ppm and 2 % at 200 ppm.

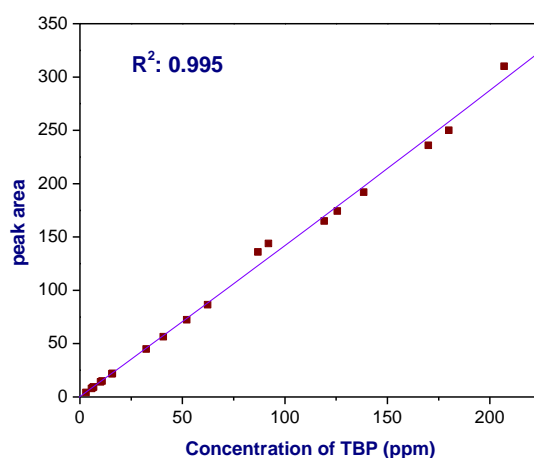


Fig. VII.1. Calibration graph for dissolved TBP (2 to 200 ppm)

7.3.2. Equilibration with Aqueous Phase

To determine the solubility of TBP in nitric acid as a function of temperature, experiments were performed in test tubes with ground stoppers by shaking equal volume of the aqueous and organic phases for 45 min. using an incubator shaker at the desired temperature. The phases were brought into contact and then allowed to separate in a water bath which controlled the temperature within $\pm 0.5^\circ\text{C}$. After phase separation, the aqueous phase was analysed for acid and TBP.

7.3.3. Estimation of TBP in Aqueous Phase

A known volume of the resulted aqueous phase was mixed with fresh n-dodecane, using vortex mixer and then centrifuged. 5 μL of the resulting organic phase was injected into the gas chromatograph using 10 μL Hamilton microliter syringe. Solubility data were generated at various temperatures in the range 25-80 $^\circ\text{C}$. Solubility of TBP in the presence of individual metal ions (U, Ru and Zr) as well as U, Ru and Zr together, at various concentrations of nitric acid as a function of temperature was determined. The instrumental conditions described above were used for all the determinations. Uranium in the stock solution was determined by Davis and Gray method and the concentrations of Zr and Ru were determined using ICP-OES technique. The acid concentration in all the solutions was estimated by titrating against standardised alkali.

7.4. Influence of temperature, acid concentration and metal ions on the solubility of tbp.

7.4.1. Effect of Temperature and Nitric Acid Concentration

Variation of aqueous solubility of TBP with nitric acid concentration and temperature is plotted in Fig. VII.2. It was observed that with increase in acidity, solubility of TBP decreased gradually; passing through a minimum at about 8 M and then increased with acidity. The initial decrease in solubility of TBP with increasing acidity is probably due to the fact that dissolution

occurs mainly as a result of the transition of free TBP molecules into the aqueous solution at lower acid concentrations. The formation of compounds by the acid and TBP makes a small contribution to the solubility in this range. Further increase in solubility of TBP in the aqueous phase with acidity is due to the formation of 1:1 complex of TBP with HNO_3 up to 8 M and beyond which various higher TBP-nitric acid complexes, such as $\text{TBP} \cdot 2\text{HNO}_3$ formation are expected.

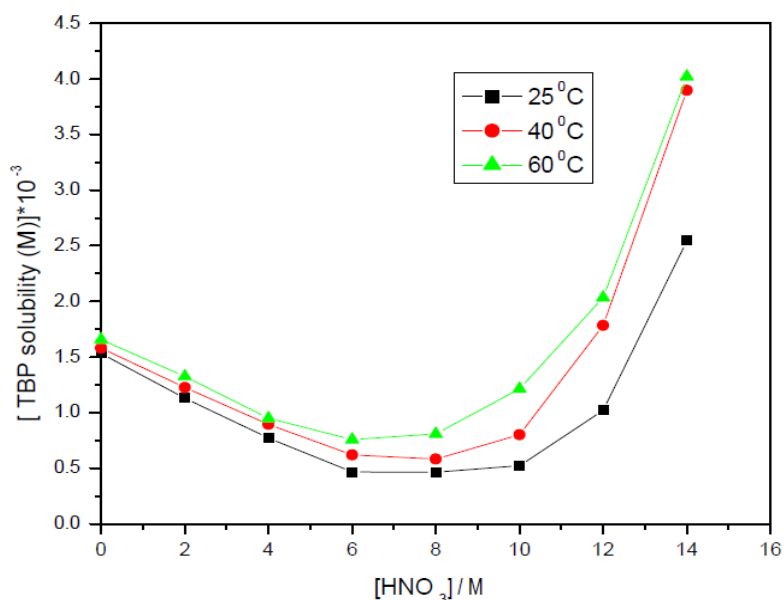


Fig. VII. 2. Solubility of pure TBP in aqueous phase as a function of temperature and acidity

Solubility of TBP in water at room temperature was found to be 0.407 g/L which is in agreement with the reported value of 0.402 ± 0.03 g/L (1.54 mmol/L). With increase in temperature, the solubility of TBP in aqueous phase was found to increase. There are discrepancies in the literature on the dependence of solubility data with temperature. Higgins et al. [7] reported that the solubility of TBP in the aqueous phase decreased with temperature. Other investigators [8, 9] observed that increase in temperature increases the solubility of TBP. The results obtained in the present work are in accordance with the data reported in the latter literature [8, 9].

7.4.2. Effect of Individual Metal Ions as a Function of Acidity and Temperature

Figures VII.3-5 show the solubility of pure TBP in various nitric acid concentrations (0-14 M) at three different temperatures 25, 40 and 60°C in the presence of troublesome fission product metal ions Zr and Ru separately and also in the presence of the heavy metal atom U respectively. In the stock solutions containing Zr and Ru, the concentrations of metal ions were fixed as 1 g/L and that of U was fixed as 40 g/L at all acidities.

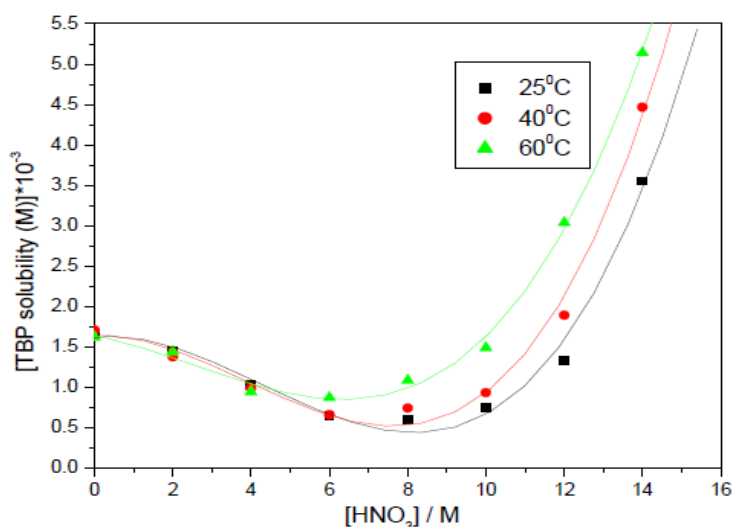


Fig. VII.3. Solubility of pure TBP in aqueous phase as a function of temperature and acidity in the presence of Ru

Presence of salts in the aqueous phase decreases the solubility of TBP. However, in the presence of Ru significant increase in the solubility of TBP was observed at all acidities when compared to that in the absence of any metal ions. The solubility curve followed the same trend of decreasing gradually with increase in acidity, attaining a minimum and again increasing with increase in nitric acid concentration. Up to 4 M acid in the presence of Ru, increase in temperature resulted in decreasing the solubility beyond which solubility increased with temperature. Figures VII.3 and 4 reveal that beyond 10 M acidity, Zr suppresses the solubility of TBP in nitric acid, whereas Ru significantly increases the solubility. In solutions containing Zr

at higher acidity, the solubility could not be measured at 60°C due to the split in peak observed in the GC spectrum. The solubility curves in the presence of metal ions were found to follow the same trend as that for pure TBP. Nevertheless, higher concentration of U (40 g/L) drastically decreased the solubility of TBP, which did not show significant increase even at acidities above 8 M. In this case also, increase in temperature resulted in increasing the solubility of TBP in the aqueous phase.

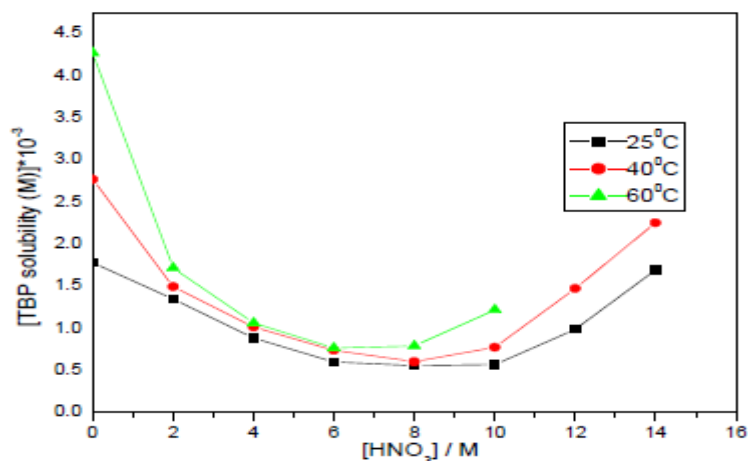


Fig. VII.4. Solubility of TBP in aqueous phase as a function of temperature and acidity in the presence of Zr

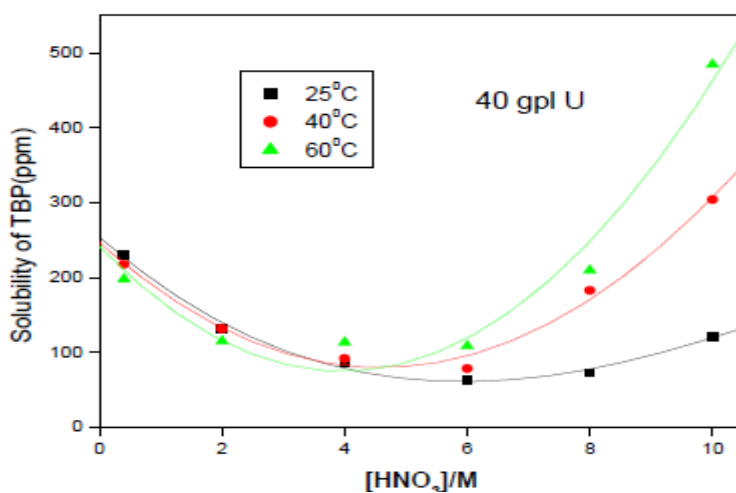


Fig. VII.5. Solubility of pure TBP in aqueous phase in the presence of U

7.4.3. Effect of Metal Ions Together as a Function of Acidity and Temperature

To investigate the combined effect of the interfering fission product metal ions and heavy metal, temperature and acidity, stock solutions of acidity 0.7 to 10 M were prepared with 1 g/L each of Ru and Zr and 40 g/L of U. Measurements were carried out at 25, 40 and 60°C. The results are plotted in Fig. VII.6. It could be seen from the figure that the individual effect of Ru and Zr on the solubility of TBP in aqueous phase was suppressed by uranium ion. At all temperatures, minimum solubility was observed at 6 M acidity. Increase in temperature resulted in increasing the solubility.

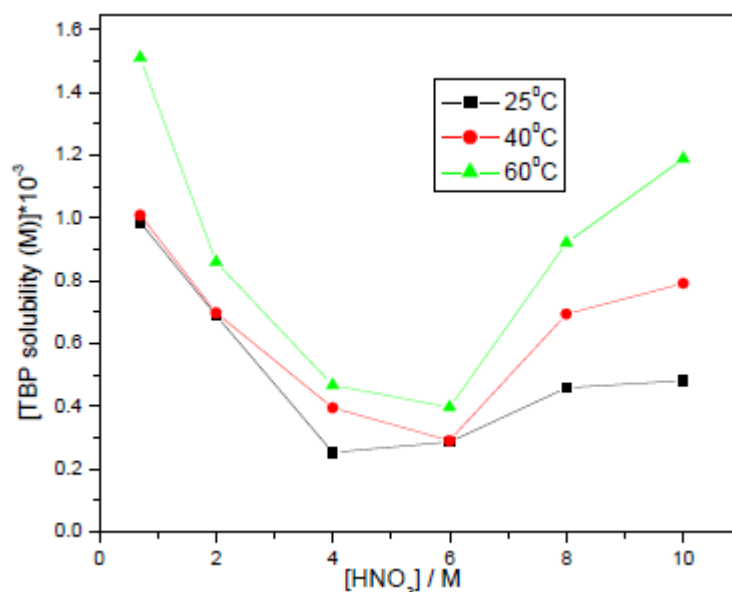


Fig. VII.6. Solubility of TBP in aqueous phase as a function of temperature and acidity in the presence of U, Ru and Zr

7.5. Thermodynamic modeling of the experimental data

The solubility of non-electrolytes in aqueous electrolyte solutions has traditionally been modeled by using Setschenow equation for salt effect [15]. Use of Setschenow equation for aqueous solubility of TBP under limited conditions has been reported in the literature. Shekhar Kumar and Koganti [12] have proposed an empirical relation based on an extended salt effect model to

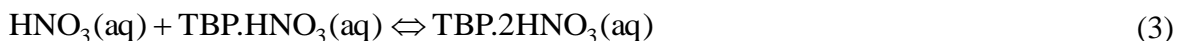
predict the aqueous solubility of TBP in 5 to 100 % TBP/*n*-dodecane-nitric acid-water biphasic system at 298.15 K. However, empirical correlations often used for this purpose cannot be considered reliable under conditions that are outside the experimental data base used to validate the model. There is no generalized model available to account for the presence of the diluent and for multicomponent electrolyte solutions in which only some electrolytes are solvated and extracted by TBP.

In aqueous solutions of electrolyte, virtually non-extractable by TBP (such as NaNO₃, NaCl, KCl etc.), solubility of the extractant decreases with increase in electrolyte concentration [13, 14]. The TBP which is soluble in the aqueous phase will be only in the form of TBP molecules and are not combined with the electrolytes. Its solubility in such electrolyte solutions obeys the Setschenow equation [15] which is given by,

$$\log C_{TBP}^e = \log[TBP]_w - k_s C_{el}^e \quad (1)$$

where, C_{TBP}^e is the analytical concentration of TBP in the electrolyte solution, $[TBP]_w$ is the analytical concentration of TBP in water, C_{el}^e is the equilibrium concentration of the electrolyte in aqueous phase and k_s is the salting out coefficient or Setschenow coefficient. On the other hand, in solutions of electrolytes which are extracted by TBP more complex situation exists. In the case of TBP-nitric system, TBP dissolves in the aqueous phase not only as a result of the transition of its molecules into aqueous phase but also as a result of formation of complexes by the acid with TBP. Since Eq. (1) presupposes the absence of chemical reaction between the organic solvent and the electrolyte, it is invalid in the above form for the electrolytes extractable by TBP. In this case Setschenow equation can be applied only to free TBP i.e. not bound to the acid.

The complexation of nitric acid by TBP can be described on the basis of the following reaction equilibria:



Equation (2) is accounted for the extraction of nitric acid by TBP at higher acidities. The extraction data of Davis [16] however, suggest that the 1:2 complex does not become the major TBP species until the aqueous HNO_3 concentration reaches 8 to 10 M. The equilibrium constants for Eqs. (2) and (3) in terms of activities are

$$K_1 = \frac{a_{\text{TBP.HNO}_3}}{a_{\text{TBP}} \cdot a_{\text{HNO}_3}} \quad (4)$$

$$K_2 = \frac{a_{\text{TBP.2HNO}_3}}{a_{\text{TBP.HNO}_3} \cdot a_{\text{HNO}_3}} = \frac{a_{\text{TBP.2HNO}_3}}{K_1 a_{\text{TBP}} a_{\text{HNO}_3}^2} \quad (5)$$

Representing the organic phase activity in terms of product's concentration and activity coefficient and separating the organic phase activity coefficient from the right side of Eqs. (4) and (5) gives,

$$K_1^* = K_1 \frac{\gamma_{\text{TBP}}}{\gamma_{\text{TBP.HNO}_3}} = \frac{[\text{TBP.HNO}_3]}{[\text{TBP}_f^e] \cdot a_{\text{HNO}_3}} \quad (6)$$

and

$$K_2^* = K_1 K_2 \frac{\gamma_{\text{TBP}}}{\gamma_{\text{TBP.2HNO}_3}} = \frac{[\text{TBP.2HNO}_3]}{[\text{TBP}_f^e] \cdot a_{\text{HNO}_3}^2} \quad (7)$$

where $[\text{TBP}_f^e]$ is the equilibrium concentration of free TBP dissolved in the aqueous phase.

Based on the extraction equilibria in Eqs. (2) and (3), the total aqueous concentration of TBP bound to acid is given by

$$[\text{TBP}]_{\text{bound}}^{\text{e}} = [\text{TBP.HNO}_3] + [\text{TBP.2HNO}_3] \quad (8)$$

or,

$$[\text{TBP}]_{\text{bound}}^{\text{e}} = K_1^* [\text{TBP}_f^{\text{e}}] \cdot a_{\text{HNO}_3} + K_1^* \cdot K_2^* [\text{TBP}_f^{\text{e}}] \cdot a_{\text{HNO}_3}^2 \quad (9)$$

On dissolution of the tri-butyl phosphate not bound to the acid in the aqueous phase, the Setschenow equation holds the form,

$$\log[\text{TBP}_f^{\text{e}}] = \log[\text{TBP}]_{\text{w}} - k_s C_{\text{HNO}_3}^{\text{e}} \quad (10)$$

Then, mass balance equation for TBP in the aqueous phase can be written as,

$$[\text{TBP}]_{\text{bound}}^{\text{e}} = C_{\text{TBP}}^{\text{e}} - [\text{TBP}_f^{\text{e}}] \quad (11)$$

Estimation of equilibrium constants of Eqs. (6) and (7) requires values of activity of un-dissociated nitric acid, which are obtained from the data reported by Davis and Bruin [17] by correlating their results as functions of the stoichiometric aqueous nitric acid concentration.

The degree of dissociation of nitric acid estimated by Davis and Bruin was correlated using the stoichiometric nitric concentrations in the aqueous phase as follows:

$$\ln(\alpha) = -3 \times 10^{-5} C_{\text{HNO}_3}^4 + 7 \times 10^{-4} C_{\text{HNO}_3}^3 - 0.0105 C_{\text{HNO}_3}^2 - 3.7 \times 10^{-3} C_{\text{HNO}_3} - 0.0039 \quad (12)$$

The activity of un-dissociated nitric acid was calculated from

$$a_{\text{HNO}_3} = \gamma_u C_u = \gamma_u (1 - \alpha) C_{\text{HNO}_3} \quad (13)$$

Similarly, the activity coefficient of un-dissociated nitric acid was determined by least-square fitting using the experimental results of Davis and Bruin and is expressed as follows:

$$\ln(\gamma_u) = -0.0019688 C_{\text{HNO}_3}^2 + 0.31034 C_{\text{HNO}_3} - 0.001482 \quad (14)$$

$$0.05 \leq C_{\text{HNO}_3} \leq 14\text{M}$$

Equilibrium constants and salting out coefficient were determined by non-linear regression analysis of experimental data using Eqs. (10 – 14) and values are listed in Table VII.1. The solubility of TBP in various concentrations of nitric acid (0 to 14 M) at different temperatures from 25 to 60°C in the presence of ruthenium and zirconium was computed. Figures VII.7-9 show the comparison between experimental and calculated values of aqueous solubility of TBP and reasonably good agreement was found.

Table. VII.1. Equilibrium constants and salting out coefficient values at 25°C

Parameter	K_1^*	K_2^*	K_s
No metal ion	0.0092	0.0042	0.0765
In the presence of zirconium	0.0047	0.006	0.0641
In the presence of ruthenium	0.0040	0.0104	0.0621

7.5.1. Effect of Nitric Acid Concentration

Variation of aqueous solubility of TBP with nitric acid concentration is shown in Fig. VII.7 at 25°C. It was observed that with increase in acidity solubility of TBP decreases slowly passes through a minimum at about 8 M and then increases with acidity.

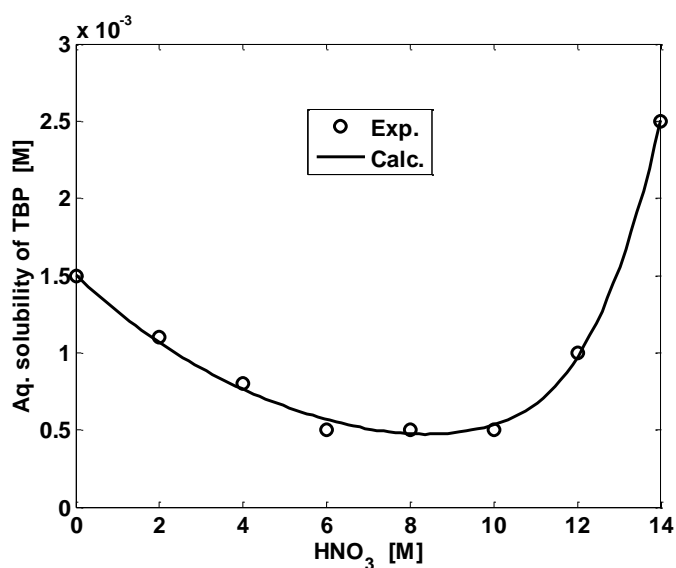


Fig. VII.7. Aqueous solubility of TBP as a function of nitric acid concentration at 25°C

With increase in acidity, the concentration of various TBP-nitric complex rises (as shown in Fig. VII.8 (a) & (b)) and the solubility of TBP in the aqueous phase increases.

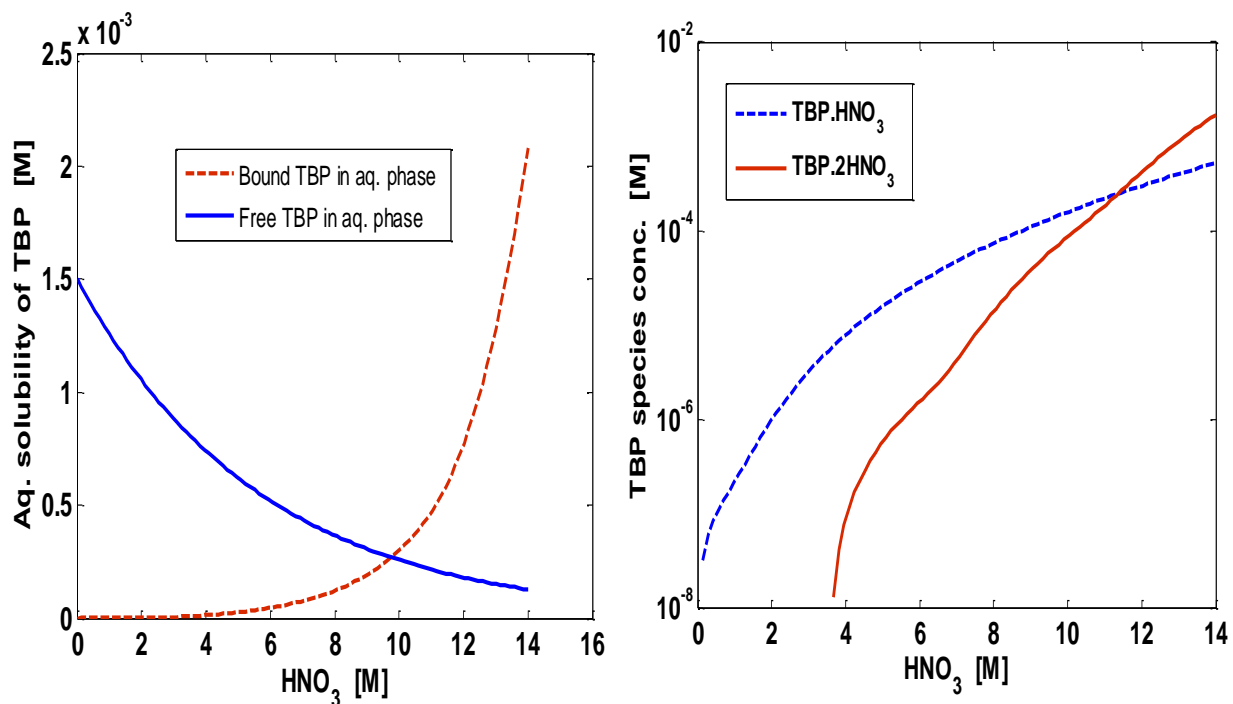


Fig. VII.8. (a) Concentration of bound TBP and free TBP vs acidity; (b) Concentration of different species of TBP vs acidity

7.5.2. Effect of Temperature

Figure VII.9 shows a comparison between experimental and calculated values of aqueous phase solubility of 100 % TBP at different temperatures and acidities. It was observed that with increase in temperature the solubility of TBP in aqueous phase increases.

There are discrepancies in the literature on the solubility data as a function of temperature. Two studies report that the solubility of TBP in the aqueous phase decreases with temperature [7, 13]

but others declare that with increase in temperature the solubility of TBP increases [8, 9]. The results of the present study are in accordance with the data reported in Ref. [8 and 9].

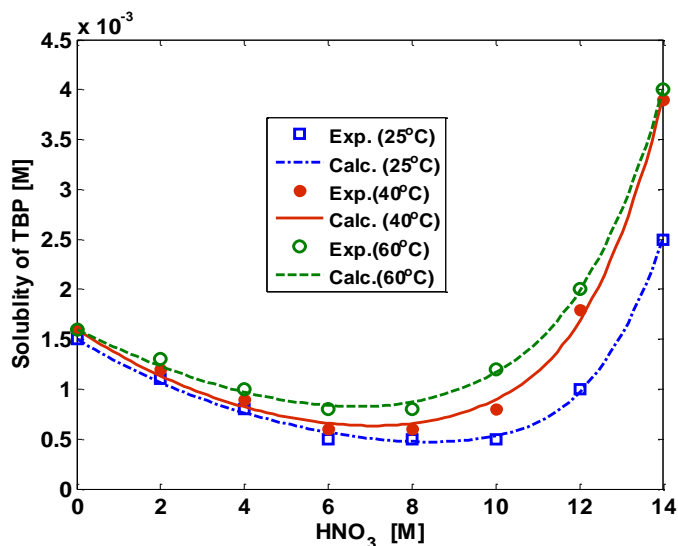


Fig. VII.9. Solubility of pure TBP in aqueous phase as a function of temperature and acidity

The temperature dependence of the equilibrium constant of the reversible reaction is given by Van't Hoff's relationship as,

$$\frac{d(\ln K)}{dT} = \frac{\Delta H}{RT^2} \quad (15)$$

If the enthalpy change of the reaction, ΔH is assumed to be constant over the temperature range then, Eq. (15) can be easily integrated to give

$$\ln \frac{K}{K_1} = -\frac{\Delta H}{R} \left(\frac{1}{T} - \frac{1}{T_1} \right) \quad (16)$$

Figure VII.10 (a and b) show the plots of natural logarithm of equilibrium constants vs reciprocal of temperature and they are linear in agreement with Eq. (16). The values of ΔH obtained from the slope of these plots using least-square fitting are given in Table VII.2. The values of free energy and entropy changes were calculated using the following equations:

$$\Delta G = -RT \ln K \quad (17)$$

$$\Delta G = \Delta H - T\Delta S \quad (18)$$

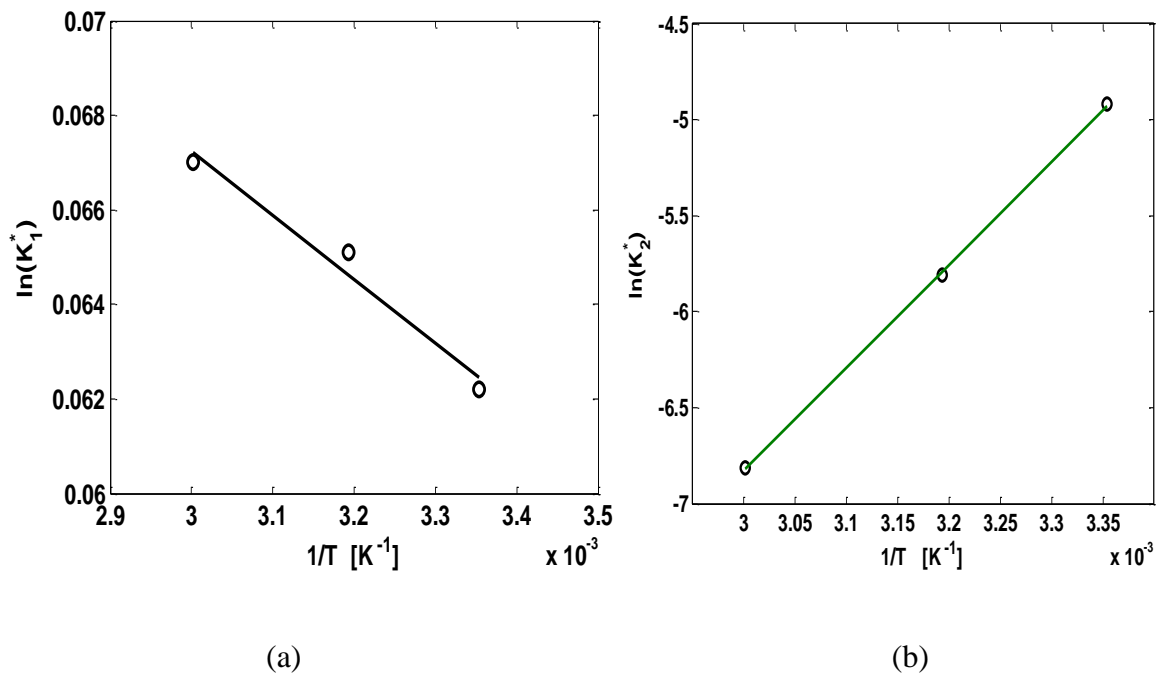


Fig. VII.10. Effect of temperature on equilibrium constants

Table VII. 2. Values of thermodynamic parameters

Parameter	ΔH (kcal/mol)	ΔG (kcal/mol)	ΔS cal/(mol.K)
For Eq. (2)	12.96	3.3	32.4
For Eq. (3)	-18.78	2.8	-72.5
For physical solubility	-0.42	1.8	-4.8

7.5.3. Effect of Individual Metal Ions

Solubility of TBP in nitric acid solutions was calculated in the presence of Zr and Ru with concentration of about 1 g/L separately and the comparison of experimental and calculated values is shown in Fig. VII.11.

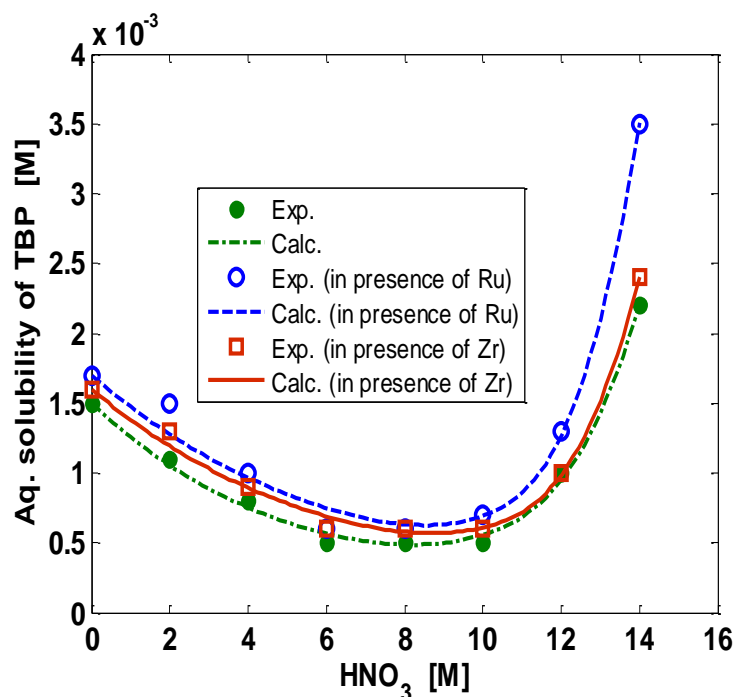


Fig. VII.11. Effect of Zr and Ru ions on the solubility of TBP at different nitric acid concentrations

It is observed that the presence of these metals in aqueous solutions of nitric acid increases the solubility of TBP. In the presence of ruthenium ions, there was a significant increase in the solubility of TBP (as observed from Fig VII.11) as compared to that of zirconium nitrate ions.

7.5.4. Effect of TBP Concentration

Figure VII.12 shows the comparison between the experimental and calculated values of the aqueous solubility of TBP at different volume percentages of TBP as a function of nitric acid concentration. It was observed that the solubility of TBP in aqueous nitric acid solutions decreases with the volume percent of TBP. This may be due to the fact that the dissolution of TBP in the aqueous phase is affected by the presence of a diluent. The values of equilibrium constants and salting-out coefficients are also affected by the presence of a diluent, just as in the case of the extraction of uranium and plutonium, where the distribution coefficients of these elements are functions of TBP concentrations.

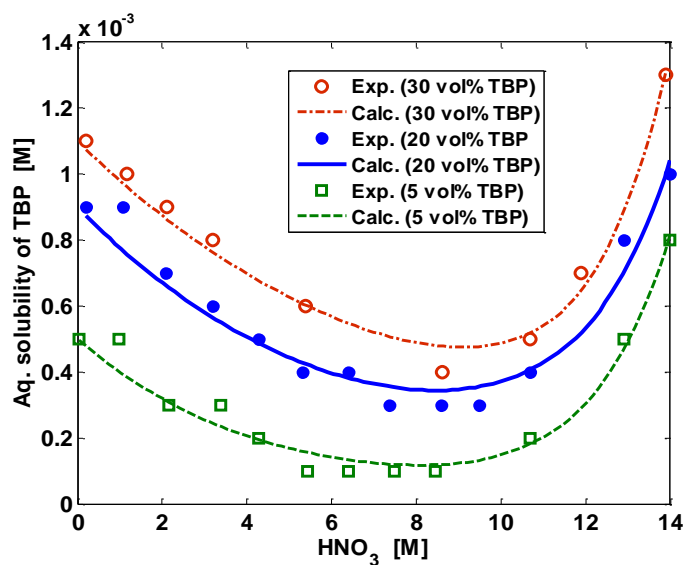


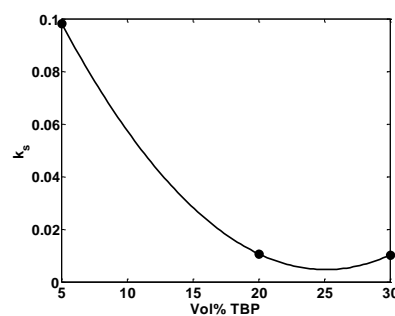
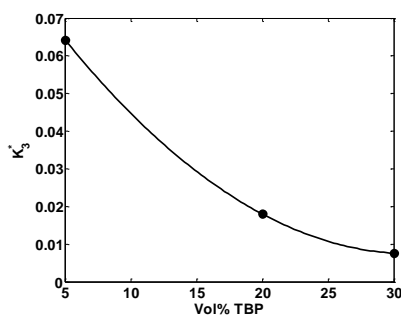
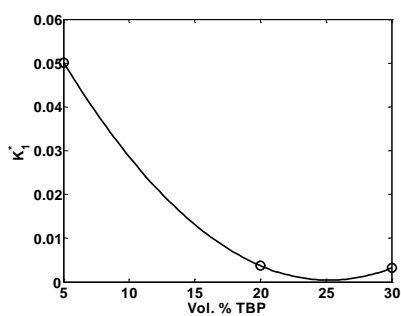
Fig. VII.12. Effect of volume percent of TBP on its solubility at different nitric acid concentrations

Figures VII.13 (a-c) show the variation of equilibrium constants and salting out coefficient values with TBP concentrations. The equilibrium constants and salting out coefficient are related to TBP concentration as follows:, F is the volume fraction of TBP

$$K_1^* = 0.6402F^{-1.624} \quad (19)$$

$$K_2^* = 0.41062F^{-1.121} \quad (20)$$

$$k_s = 0.80912F^{-1.35} \quad (21)$$



(a) (b) (c)

Fig.VII.13. Variation of equilibrium constants and salting out coefficient with TBP concentration

7.6. Conclusion

The solubility of TBP in nitric acid solutions (0 – 14 M) was measured in the temperature range 25 to 60°C. The effect of temperature and presence of the extractable metal ions ruthenium, zirconium and uranium on the solubility of TBP was investigated. With increase in temperature solubility increased and in the presence of extractable salts the solubility of TBP did not show a systematic trend. Fission product metal ions (Zr and Ru) increased the solubility of TBP in aqueous phase whereas the heavy metal atom (U) decreased its solubility. When present together, the individual effect of fission product metal ions was suppressed by that of heavy metal ions. Irrespective of the metal ions present, increase in temperature resulted in increasing the solubility of TBP in aqueous phase. The solubility data have been correlated to equilibrium constants and salting out coefficient using classical thermodynamic approach. The effect of temperature and presence of extractable salts like ruthenium and zirconium nitrate on the solubility of TBP have been analysed using the model equations. The agreement between experimental and calculated results is reasonably good. Thermodynamic parameters such as heat of reaction, Gibb's free energy change and entropy change have also been estimated by analyzing the experimental data.

References

1. Schulz, W.W., Navratil, J.D., (1984) Science and technology of tributyl phosphate, vol 1, Chapter 7, CRS Press Inc., Boca Raton
2. Burger, L.L., Forsman, R.C., (1951) Report HW 20936
3. Sege, G., (1953) Report HW-28690
4. Biplab, D., Mandal, P., Kumar Shekhar, *J. Radioanal. Nucl. Chem.*, **288** (2011) 641
5. Dicholkar, D.D., Patil, L.K., Gaikar, V.G., Kumar Shekhar, Kamachi Mudali, U., Natarajan, R., *J. Radioanal. Nucl. Chem.*, **289** (2011) 545
6. Leroy, (1967) ORNL-TR-4344
7. Higgins, C.E., Baldwin, W.H., Soldano, B.A., *J. Phys. Chem.*, **63** (1959) 113
8. Usachev, V.N., Markov, G.S., *Radiokhimiya*, **46** (2004) 436
9. Kuno, Y., Hina, T. Akiyama, T., Matsui, J., *J. Nucl. Sci. Tech.*, **30** (1993) 567
10. Velavendan, P., Ganesh, S., Pandey, N.K., Geetha, R., Ahmed, M.K., Kamachi Mudali, U., Natarajan, R., *J. Radioanal. Nucl. Chem.*, DOI 10.1007/s10967-012-1945-1 (2012)
11. Alcock, K., Grimley, S.S., Healy, T.V., Kennedy, J., McKay, H.A.C., *Trans. Faraday Soc.*, **52** (1956) 39
12. Sekhar, K., Koganti, S.B., *Nucl. Technol.*, **129** (2000) 279
13. Belousov, E.A., Zakharova, L.Yu., *J. Phys. Chem.*, **49** (1975) 1695
14. Gordon, J.E., "The Organic chemistry of Electrolytic Solutions", John Wiley & Sons, New York, (1975)
15. Setschenow, Z., *Z. Chem. Physik*, **4** (1899) 117
16. Davis, W. Jr., *Nucl. Sci. Engg.*, **14** (1962) 159
17. Davis, W. Jr., Bruin, H.J.De., *J. Inorg. Nucl. Chem.*, **26** (1964) 1069

SUMMARY AND SCOPE FOR FUTURE WORK

8.1. SUMMARY

8.1.1. Parametric Studies on the Electrochemical Destruction of Nitric Acid

This study was undertaken to address some of the issues like effect of surface area of counter electrode (anode) during electrochemical destruction of nitric acid, optimum current density value required for obtaining better reduction efficiency and identifying suitable corrosion resistant diaphragm material and its characterisation, which details are essential to implement the process of electrochemical destruction of waste nitric acid in the plant. The main findings of the study are summarized below.

- ✚ Cyclic voltammetric studies revealed the reduction of nitric acid to be a quasi-reversible process and hence, it is under kinetic and mass transfer control.
- ✚ Electrochemical reduction of 4 M nitric acid conducted under constant potential as well as current conditions indicated that the overall reaction follows zero order kinetics.
- ✚ Comparison of the performance of anodes of different surface area in the reduction process suggested that anode with higher surface area will significantly reduce the temperature of the cell thereby avoiding the evaporation loss and improving energy efficiency.
- ✚ Failure of platinum electroplated titanium anodes after 450 h of functioning implies that plated anodes should be used in electrochemical cells only at low anodic current density in order to extend the life of the electrode.
- ✚ Reaction bonded silicon nitride tube fabricated indigenously possessed superior properties and it performed better than the imported commercial tube as diaphragm in electrolytic cells.

8.1.2. Development of a Continuous Homogeneous Process for denitration by Treatment with Formaldehyde

Though electrochemical method for denitration offers safety and is a kinetically controlled process, it is not energy efficient in addition to the task of fabricating costly noble metal, corrosion resistant electrodes such as Pt-Ir anode, because Pt electroplated anodes could not withstand high anodic current density (which is desirable for good conversion efficiency) in corrosive environment in the plant. Hence, denitration by a chemical method which provides very fast kinetics for the reduction reaction was investigated in detail. This process can be directly adopted in the plant, following stringent safety measures.

The summary of this study is listed below.

- ✚ Continuous destruction of pure nitric acid and synthetic waste solutions (to simulate HLLW) with formaldehyde was demonstrated for plant capacity.
- ✚ The reaction proceeds in a safe and controlled manner at temperatures above 98°C with an induction period of about a minute and the reduction efficiency was computed to be in the range 70-80 %.
- ✚ Destruction was successfully carried out without antifoaming agents though severe foaming was observed in the synthetic solution comprising degraded organics and fission product metal ions.
- ✚ Refluxing the contents of the reactor after terminating the experiment for an hour or allowing the product solution to reside in the collection tank for a day could result in the completion of denitration reaction and bringing down the residual acidity and unreacted reductants to more than 50 % of the steady state concentration, without any external agency.
- ✚ Volume reduction of about 10 % could be achieved in the overall denitration reaction.

8.1.3. A Study on the Evolution of Physiochemical Properties and Metal Retention Behaviour of Thermally and Radiolytically Degraded TBP-DD/NPH Systems in Nitric Acid Medium

A simulated and systematic study was undertaken to evaluate the degradation behaviour of the solvent (30% TBP) under accelerated thermal and irradiation conditions in order to assess the extent of damage caused on the solvent in the plant and to take remedial action for the removal of degraded products for the purpose of recycling of the used solvent. The main features of this study are as follows:

- ✚ Thermal degradation at 40°C for 800 h or at 60°C for 400 h did not alter the physiochemical properties namely density, viscosity and, surface tension to a significant range but metal retention was significant.
- ✚ Once the duration of degradation at high temperature increases, one time solvent wash is not effective in restoring the quality of solvent.
- ✚ Radiolysis up to 20 MRad produced a minor change in density, viscosity and PDT, but the surface tension was not affected.
- ✚ Beyond 10 MRad, cleaning the solvent by washing with Na₂CO₃ is not effective, as significant amount of Zr gets retained by organic phases.
- ✚ Irradiation to a higher dose of 100 MRad, indicated the formation of new classes of compounds.
- ✚ Metal retention behaviour implies that irrespective of the nature of degradation (either radiolytic or thermal), TBP-DD system possesses better stability than TBP-NPH system.

8.1.4. Effect of Temperature, Acidity and Electrolytes on the Solubility of TBP in Aqueous Phase

For the purpose of understanding the distribution equilibrium of TBP between aqueous and organic phases as well as to provide input for designing a suitable contactor, this study was taken

up to determine the solubility of TBP in nitric acid (0 – 14 M) at different temperatures. The effect of fission product metal ions Ru and Zr and the heavy metal U on the aqueous solubility of TBP was evaluated. The conclusions of this study are as follows:

- ✚ With increase in temperature, solubility of TBP in aqueous phase increased and in the presence of extractable salts the solubility of TBP did not show a systematic trend.
- ✚ Fission product metal ions (Zr and Ru) increased the solubility of TBP in aqueous phase whereas the heavy metal atom (U) decreased its solubility.
- ✚ When present together, the individual effect of the fission product metal ions was suppressed by that of the heavy metal ion.
- ✚ Irrespective of the metal ions present, increase in temperature resulted in increasing the solubility of TBP in aqueous phase.
- ✚ The solubility data have been correlated with equilibrium constants and salting out coefficient using a classical thermodynamic approach.
- ✚ The effect of temperature and extractable salts like ruthenium and zirconium nitrates on the solubility of TBP were analysed using model equations.
- ✚ Thermodynamic parameters such as enthalpy of reaction, Gibb's free energy change and entropy change have also been estimated by analysing the experimental data.

8.2. SCOPE FOR FUTURE WORK

- ✚ Identifying individual metal ions and their concentrations responsible for frothing during denitration of simulated HLLW and attempting to separate them from plant waste solution.
- ✚ Comparing the efficiency of various anti foaming agents and optimizing their concentrations for suppressing the frothing of reaction mixture during denitration with formaldehyde.

- ✚ Complete characterization of the products formed during thermal and radiolytic degradation using advanced analytical techniques.
- ✚ Measurement of plutonium retention by the degraded samples.
- ✚ Identifying alternate cleaning agents for effective washing of degraded solvents.
- ✚ Selection of alternate solvent-diluent system which offers resistance to radiolysis and evaluating their performance.
- ✚ Measurement of solubility of TBP in aqueous solution in the presence of other fission product metal ions as well as in actual plant solutions.

JOURNAL PUBLICATIONS AND CONFERENCE PROCEEDINGS**Journals**

1. "Development of a continuous homogeneous process for denitration by treatment with formaldehyde" **Satyabrata Mishra**, Falix Lawrence, R. Srinivasan, N.K. Pandey, C. Mallika, S.B. Koganti and U. KamachiMudali, *J. Radioanal. Nucl.Chem.* 2010, 285, 687- 695.
2. "Development and characterization of porous silicon nitride tubes" **Satyabrata Mishra**, C. Mallika, P.K. Das, U. KamachiMudali and R. Natarajan, *Trans.Ind.Ceram. Soc.* **2013**, 72, 52-55.
3. "Thermodynamics of solubility of tri-n-butyl phosphate in nitric acid solutions" **Satyabrata Mishra**, S. Ganesh, P. Velavendan, N.K. Pandey, C. Mallika, U.K. Mudali and R. Natarajan, *Adv. Chem.Engg.Research*, **2013**, 2, 55-60.
4. "Effect of temperature, concentration of acid and metal ions on the solubility of TBP in aqueous phase" **Satyabrata Mishra**, S. Ganesh, P. Velavendan, N.K. Pandey, C. Mallika, U.K. Mudali and R. Natarajan, *J. Radioanal. Nucl. Chem.* (Communicated).
5. "Effect of metal ions and organics on chemical denitration of HLLW" SanatKarmakar, **Satyabrata Mishra**, C. Mallika, U. KamachiMudali and R. Natarajan, *J. Chem. Engg. Sci.* (Communicated).
6. "Electrochemical divided cell design for radioactive environment" **Satyabrata Mishra**, Falix Lawrence, N.K. Pandey, C. Mallika, U. KamachiMudali and R. Natarajan, *J. Applied Electrochem.* (Manuscript under preparation).
7. "A comparative study on the evolution of physiochemical properties and metal retention behaviour of thermally degraded TBP-Dodecane-HNO₃/TBP-NPH-HNO₃ systems" **Satyabrata Mishra**, S.Joshi, N.K. Pandey, C. Mallika, U.K. Mudali and R. Natarajan, *Sep.Sci.Technol* (Manuscript under preparation).
8. "A systematic study on the effect of radiolysis in alteration of physiochemical and metal retention properties of TBP-Dodecane-HNO₃ and TBP-NPH-HNO₃ systems" **Satyabrata Mishra**, S.Joshi, N.K. Pandey, C. Mallika, U.K. Mudali and R. Natarajan, *Sep.Sci.Technol* (Manuscript under preparation).

Conferences

1. **Satyabrata Mishra**, Falix Lawrence, R. Srinivasan, N.K. Pandey, C. Mallika and S.B. Koganti, "Influence of surface area of anodes in electrochemical reduction processes and performance evaluation of an electroplated Ti anode", Proc. Discussion Meet on Electroanalytical Techniques and Their Applications (DM-ELANTE-2008), Munnar, Feb. 2008, Paper No. 15.
2. **Satyabrata Mishra**, Falix Lawrence, C. Mallika, S.B. Koganti and U. KamachiMudali, "Characterisation of reaction bonded silicon nitride tubes", 20th Annual Conf. of Indian Nuclear Society (INSAC – 2009), organized by INS, IGCAR and BHAVINI, Chennai, Jan. (2010), p. 124.
3. **Satyabrata Mishra**, Falix Lawrence, R. Srinivasan, N.K. Pandey, C. Mallika, U. KamachiMudali and S.B. Koganti, "Pilot plant scale denitration by treatment with formaldehyde", Proc. DAE-BRNS Biennial Internatl. Symp.on Emerging Trends in Separation Science and Technology (SESTEC-2010), Kalpakkam, March (2010), pp. 297, 298
4. **Satyabrata Mishra**, C. Mallika, U. Kamachi Mudali, R. Natarajan and P.K. Das, "Development and characterization of porous silicon nitride tubes" Natl. Symp. on 'Materials and Processing (MAP-2012)', BARC, Mumbai, Oct . (2012).
5. **Satyabrata Mishra**, S. Ganesh, P. Velavendan, N.K. Pandey, C. Mallika, U.K. Mudali and R. Natarajan, "Effect of temperature, acidity and metal ions on the solubility of TBP in aqueous phase", The Eleventh Biennial Symp. on 'Nuclear and Radiochemistry (NUCAR-2013)', Jabalpur, Feb. (2013).
6. **Satyabrata Mishra**, S. Joshi, C. Mallika, N.K. Pandey, U. Kamachi Mudali and R. Natarajan, "Physiochemical properties and metal retention behaviour of thermally degraded TBP-Dodecane-HNO₃ and TBP-NPH-HNO₃ systems", 66th Annual Session of IChE (CHEMCON 2013), ICT, Mumbai, Dec. (2013)
7. **Satyabrata Mishra**, C. Mallika, U. Kamachi Mudali and R. Natarajan, "A systematic study on the alteration in physiochemical and metal retention properties of radiolytically degraded TBP-Dodecane-HNO₃ and TBP-NPH-HNO₃ systems", The Sixth Biennial Symp. on "Emerging Trends in Separation Science and Technology (SESTEC-2014)", BARC, Feb (2014)